MATRIGEL ALTERS THE EXPRESSION OF GENES RELATED TO ADIPOGENESIS AND THE PRODUCTION OF EXTRACELLULAR MATRIX IN 3T3-L1 CELLS

By CHITMANDEEP JOSAN, B.Sc.

A Thesis Submitted to the School of Graduate Studies in Partial Fulfilment of the Requirements for the Degree Master of Science

McMaster University MASTER OF SCIENCE (2018) Hamilton, Ontario (Medical Sciences)

TITLE: Matrigel alters the expression of genes related to adipogenesis and the production of extracellular matrix in 3T3-L1 cells

AUTHOR: Chitmandeep Josan, B.Sc. (McMaster University)

SUPERVISOR: Dr. Sandeep Raha

SUPERVISORY COMMITTEE:

Dr. Bernardo Trigatti

Dr. P. Ravi Selvaganapathy

NUMBER OF PAGES: 141

ACKNOWLEDGEMENTS

Dr. Sandeep Raha

Dr. Bernardo Trigatti

Dr. P. Ravi Selvaganapathy

A Special Thanks to the Raha Lab Members:

Michael Wong

O'llenecia

Jodi Rabeneck

TABLE OF CONTENTS

ABSTRACT

Studying molecular mechanisms underlying adipocyte differentiation is imperative to understanding adipocyte function and its role in obesity. However, majority of the research exploring adipogenesis is conducted with cell lines cultured directly on tissue culture plastic. Culturing cells on plastic may result in altered proliferation and differentiation, and subsequent change in pharmacological response. The extracellular matrix (ECM) plays a critical role in adipocyte development and survival. It is suggested that cells *in vitro* express high levels of ECM proteins to compensate for lack of an ECM. Differentiating preadipocytes on a substrate representative of the mature adipocyte extracellular environment may provide a more physiological response to drugs and environmental chemicals. The purpose of this study was to investigate the impact of Matrigel on 3T3-L1 cell growth, differentiation, lipid accumulation and responsiveness to Rosiglitazone. Matrigel decreased 3T3-L1 cell proliferation, enhanced lipid accumulation, and increased expression of adipogenic and lipogenic markers, including PPARγ, C/EBPα, SREBP1c, FAS, LPL, FABP4 and PLIN1. This was accompanied by a decrease in gene expression of ECM proteins, including fibronectin, collagen 1, collagen 3, collagen 4, laminin and collagen 6 in 3T3-L1 cells on Matrigel. Finally, Matrigel enhanced the response of 3T3-L1 cells to Rosiglitazone, which is a known PPARγ agonist and significantly increases lipid accumulation in 3T3-L1 cells. Our results suggest that enhanced lipid accumulation in 3T3-L1 cells on Matrigel is associated with decreased expression of ECM genes. Future studies require investigation of the cell-to-ECM interaction to confirm these findings. This study proposes that the nature of the ECM for cultured adipocytes alters temporal lipid accumulation patterns and response to various drugs as compared to 3T3-L1 cells grown on tissue culture plastic.

LIST OF FIGURES

LIST OF SUPPLEMENTARY FIGURES

LIST OF TABLES

LIST OF ABBREVIATIONS

ACC	Acetyl CoA Carboxylase
ACLY	ATP Citrate-lyase
ADIPOQ	Adiponectin
ADRP	Adipose differentiation-related protein
AGPAT	1-acylglycerol-3-phosphate acyltransferase
ANOVA	Analysis of Variance
ATCC	American Type Culture Condition
ATGL	Adipose Triglyceride Lipase
BMI	Body Mass Index
C/EBP	CCAAT-enhancer binding protein
cDNA	complimentary Deoxyribonucleic acid (DNA)
Col	Collagen
Col 1	Collagen 1
Col 3	Collagen 3
Col 4	Collagen 4
Col 6	Collagen 6
Ct	comparative cycle times
DAPI	4’,6-diamidino-2-phenylindole
ddH2O	Double distilled water
DEX	Dexamethasone
DMSO	Dimethyl Sulfoxide
ECM	Extracellular Matrix
EHS	Engelbreth-Holm-Swarm
FABP4	Fatty acid binding protein 4
FAS	Fatty acid synthase
FBS	fetal bovine serum
FDA	Food and Drug Administration
FFA	Free Fatty Acids
GPAT	Glycerol-3-phosphate acyltransferase
HPRT	Hypoxanthine-guanine phosphoribosyltransferase
HSL	Hormone-sensitive lipase
HSPG2	Heparan Sulfate Proteoglycan 2
IBMX	3-isobutyl-1-methylxanthine
IF	Immunofluorescence
IL-6	Interleukin 6
L32	60S ribosomal protein L32
Lam	Laminin
Lep	Leptin
LPL	Lipoprotein Lipase
L-GLUT	L-glutamine
MCP-1	Monocyte Chemoattractant Protein-1
MGL	Monoglyceride Lipase

MMP2	Matrix Metalloprotease 2
mRNA	messenger ribonucleic acid
NEFA	Non-esterified fatty acids
PAI-1	Plasminogen activator inhibitor-1
PAP	Phosphatidic acid phosphatase
Pen-Strep	Penicillin Streptomycin
PLIN	Perilipin
PPAR	Peroxisome proliferator-activated receptor gamma
PREF-1	Preadipocyte factor 1
qPCR	quantitative polymerase chain reaction
RBP4	Retinol binding protein 4
RNA	Ribonucleic Acid
ROSI	Rosiglitazone
RT-qPCR	Reverse Transcription Quantitative Polymerase Chain Reaction
SAT	Subcutaneous Adipose Tissue
SREBP1c	Sterol Regulatory Element Binding Protein 1
SVF	Stromal Vascular Fraction
T2D	Type 2 Diabetes
TG	Triglyceride
TIP47	Tail-interacting protein of 47 kDa
TNFα	Tumor necrosis factor alpha
US	United States; short for United States of America (USA)
VAT	Visceral Adipose Tissue
WAT	White Adipose Tissue
WHO	World Health Organization

CHAPTER 1. INTRODUCTION

Overview

Obesity is an epidemic of the 21st century affecting individuals of all ages, socioeconomic backgrounds and geographic regions[1]. Obesity increases the risk of mortality and morbidity, and is particularly associated with development of type 2 diabetes (T2D), cardiovascular diseases, respiratory disorders, osteoarthritis, sleep apnea, and overall poor quality of life[2]. In 2012, 1 in 4 adults in Canada were reported to be obese[3], with 1.27 to 11 billion dollars attributed to associated health care costs[4]. In 2016, more than 1.9 billion adults (39%) were overweight and over 650 million were obese (13%) worldwide[5]. The global economic impact of obesity is estimated at $2 trillion (US)[6]. By 2030, 38% of the world's population is estimated to be overweight and 20% obese[7]. Rising prevalence and increasing costs demand rapid advancement in therapeutics, which requires deeper understanding of the disease mechanisms.

Obesity is characterized by abnormal or excessive accumulation of fat to the extent that it adversely affects health[1]. Until recently, the role of fat or the white adipose tissue (WAT) in the development of obesity was considered to be very passive[8]. However, with recent discoveries, it is now acknowledged that adipocytes (the predominant cell types of the WAT) contribute to maintaining overall systemic homeostasis largely through their endocrine functions[9]. The WAT is now referred to as a multifunctional organ responsible for regulating energy and glucose homeostasis, insulin sensitivity, satiety, blood pressure and immunity[9]. Abnormalities in its energy storage and endocrine function result in improper signaling that lead to metabolic dysregulation and associated diseases[10]. Furthermore, overweight and obesity directly contribute to the risk of comorbidities[11].

WAT is surrounded by an extracellular matrix (ECM), which is a network of collagen and proteoglycans[12]. The role of ECM has evolved from being known as physical scaffold for tissues to an initiator of crucial biochemical and biomechanical cues required for cellular growth, adhesion, differentiation and homeostasis[13]. Importance of the ECM in cellular function and survival was widely recognized upon the discovery of diseases developed due to genetic defects of the ECM[14]. One such example is Osteogenesis imperfecta, which is a disorder of bone formation caused by mutations in the Collagen1A1 and Collagen1A2 genes[15]. As such, the cell-to-ECM interactions are now studied for drug discovery purposes. The WAT ECM undergoes constant remodeling to accompany changes in WAT size and shape[16]. Abnormal accumulation of the ECM components in the WAT leads to obesity, obesity-associated insulin resistance and T2D[17]. ECM protein deposition results in a hypoxic environment in the WAT, which accelerates fibrosis, adipocyte death and inflammation[18]. Furthermore, excess ECM deposition limits the angiogenic response of the WAT; angiogenesis is essential for oxygen and nutrient supply during WAT expansion[19].

ECM remodeling during adipocyte differentiation is accompanied by changes in gene and protein expression of ECM components[20]. Understanding the molecular changes in ECM development during adipocyte expansion presents the potential for discovery of a key molecule or pathway that can be manipulated to decrease ECM accumulation in obesogenic adipose tissue. However, most *in vitro* studies are conducted with preadipocyte cell lines cultured and differentiated directly on tissue culture plastic[21]. *In vivo,* proteins of adipocyte ECM are partially synthesized and secreted by the adipocytes, but the cells of the stromal vascular fraction (SVF) within the WAT also contribute to the adipocyte ECM[22]. Since, ECM impacts adipocyte cell shape,

growth and differentiation, and its absence or altered composition may impact cellular responses to drugs and other exogeneous stressors[23]. O'Connor et al., reported that ECM substrate significantly impacts proliferation, cell spreading and lipid accumulation of stromal-vascular fraction of human adipose subjected to *in vitro* adipogenesis[24]. In another study, 3T3-F442A cells differentiated on Fibronectin demonstrated increased proliferation and cell spreading, along with significantly reduced levels of lipid accumulation and expression lipogenic enzymes such as fatty acid synthase (FAS)[25]. Additionally, it is speculated that expression of ECM proteins may be significantly higher *in vitro* relative to *in vivo,* as a result cells attempt to compensate for the lack of an appropriate extracellular environment[13]. Finally, in some diseases, such as cancer, while drugs tested in monolayer cultures show effectiveness *in vitro,* very weak or no efficacy is found in real patients with tumors[26]. However, MCF-7 breast cancer cell line grown on chitosan scaffold displayed 15% reduction in cell growth when exposed to tamoxifen (breast cancer preventing medication), compared to 50% reduction in cell growth on tissue culture plastic; indicating that cancer cells cultured on a scaffold as spheroids resemble tumorigenicity found *in vivo*[27]. Therefore, culturing and differentiating preadipocyte cells on an ECM, representative of the tissue microenvironment, may provide a better understanding of the cell-to-ECM interaction to treat ECM-related dysfunctions in obesity, as well as more physiological pharmacological responses to cellular signaling.

The purpose of this study is to explore the impact of Matrigel[28], a hydrogel constituting of proteins similar to adipocyte basement membrane, on 3T3-L1 cell growth, differentiation, lipid accumulation and responsiveness to rosiglitazone; a drug known to increase lipid accumulation

in adipocytes[29]. In order to understand the study in its entirety, we must familiarize ourselves with the adipose tissue anatomy, WAT structure, WAT function, and WAT ECM.

White Adipose Tissue Anatomy

The WAT is characterized as a connective tissue that is organized to form a large organ with discrete anatomy, vasculature, and high physiological plasticity[30]. The WAT is distributed throughout the body in distinct depots[30]. Each anatomical depot differs in metabolic and hormonal profile, which contributes to the heterogeneity of the WAT and depot specific susceptibility to obesity[31]. In humans, the three main anatomical fat depots are intra-abdominal (visceral), upper-body/abdominal subcutaneous and lower body subcutaneous[30]. Intra-abdominal or visceral adipose tissue (VAT) can be further classified as omental, mesenteric, retroperitoneal, gonadal, and pericardial[30]. The upper-body subcutaneous adipose tissue (SAT), located mainly in the abdomen, when below the fascia is known as the deep SAT compartment, and when located superficially to the fascia is known as the superficial SAT compartment[30]. The lower body SAT, also known as the gluteofemoral depot, is located mainly in the buttocks and thighs[30].

Fat distribution within the human body is a strong predictor of obesity and its comorbidities[30,31]. The subcutaneous WAT acts as a barrier against infection, an insulator, and a cushion for protection against mechanical stress[30,32]. Visceral WAT protects vital organs within the peritoneum and ribcage[31]. Increased VAT is associated with an augmented risk for metabolic dysfunction, insulin resistance, T2D, hypertension, dyslipidemia and mortality[31]. By contrast, SAT is associated with improved insulin sensitivity, and reduced risk of T2D and other metabolic abnormalities[31].

Rodents have two main subcutaneous fat pads, which are located anteriorly and posteriorly[30]. The anterior pad is located between the scapulae, descending from the neck to the axillae; and the posterior pad (also known as the inguinal pad) spreads from the dorsolumbar region to the gluteal region[30]. The inguinal fat pad in rodents is comparable to the large gluteofemoral subcutaneous depot in humans[30,33]. The visceral fat pads in rodents is divided into the epididymal fat (located in to perigonadal region), retroperitoneal and mesenteric fat pad[30]. The retroperitoneal fat pad located on the kidneys and the mesenteric at pad located alongside the intestinal tract[30].

There are various differences between the human adipose depots and the rodent fat pads. For example, the human SAT is continuous with the dermal adipose tissue, whereas the rodent SAT is separated from the dermal fat by a smooth layer[30]. In humans, the omental (visceral) fat cells are smaller in size than subcutaneous adipocytes, while in rats visceral adipocytes are larger than subcutaneous fat cells[34]. In rodents, the mesenteric fat pad is considered most analogous to the human VAT, due to its location and biology[30,33]. However, this depot is not studied well in rodents due to limitations in surgical removal[30]. The perigonadal (or epididymal) fat pads are the largest and most available to obtain from rodents[30]. The perigonadal fat is the most frequently used in rodent studies and reported in literature[30,33]. However, humans do not have a fat depot similar to the 'perigonadal fat pad in rodents', and therefore it is suggested that this fat pad in rodents must be considered 'visceral-like' rather than true VAT[30,33]. It is extremely important to understand the anatomical and physiological differences between the human and rodent WAT in order to accurately interpret results from rodent studies

White Adipose Tissue Structure

The WAT participates in an extremely complicated network of signaling to carry out its energy metabolism and endocrine functions[35]. In order to understand the biochemical pathways underlying its function, it is very important to study its general structure. The WAT is composed of lipid-filled adipocytes that are surrounded by a rich vasculature and an extracellular matrix (Figure 1)[34]. Adipocytes are specialized fat-storing cells that accumulate lipids in the form of triglycerides (TGs)[35]. Mature adipocytes are characterized by a single large lipid droplet, which occupies 90% of the cell volume, displacing the nucleus and other cellular components (including mitochondria, endoplasmic reticulum, etc.) to the periphery of the cell (Figure 1)[34].

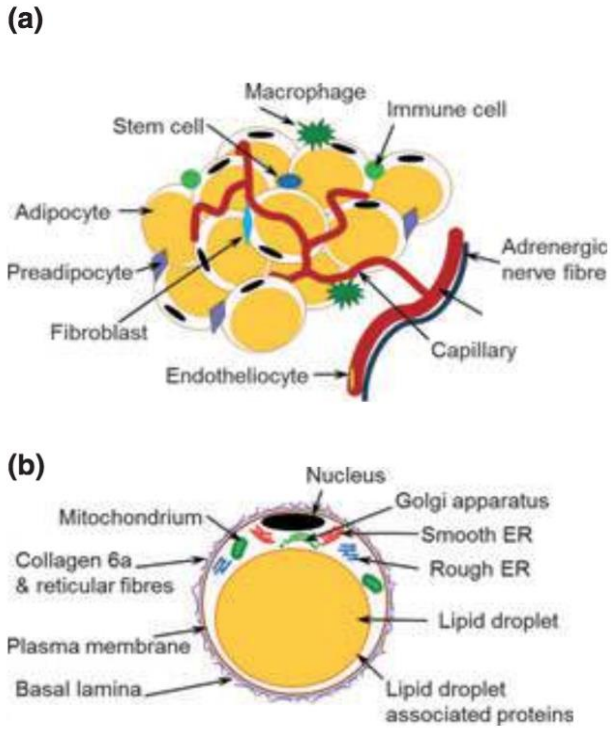

Figure 1. The White Adipose Tissue Structure. (a) Cell types present in the WAT. (b) Structure of an lipid filled mature adipocyte. Adapted from : Wronska & Kmiec (2012)[34].

The size of adipocytes varies in relation to the lipid content within the cell, and **c**hanges in size are correlated with changes in the cell function[34]**.** The phospholipid monolayer, which surrounds the lipid droplet, consists of structural proteins (e.g., perilipin), lipases, membrane-trafficking proteins, as well as receptors for hormones, neurotransmitters and cytokines[36]. A strong network of extracellular matrix proteins ensures integrity and survival of the adipocytes. Mature adipocytes are surrounded by a specialized ECM, known as the basement membrane, which is composed of collagen 4, laminin, entactin and other proteins that provide cells with support and input from the external environment to modulate function[37].

While adipocytes comprise 90% of the WAT mass in humans, they make up only 25%, or less, of the total cell population in the WAT[38]. This is due to the presence of a stromal vascular fraction (SVF) in the WAT. The SVF includes adipocyte precursor cells, mesenchymal stem cells, fibroblasts, endothelial progenitor cells and immune cells (i.e., T cells, B cells, mast cells and macrophages)[38–40]. The SVF is crucial for tissue regeneration, ECM remodeling, homeostasis, modulating tissue microenvironment, and providing the WAT with precursors for expansion[38]. The preadipocytes in the SVF contribute towards fibronectin and collagen 1 production, which are key proteins required for WAT ECM[12]. In addition, the basement membrane of mature adipocytes is produced through synthesis and secretin of ECM proteins by adipocytes, along with endothelial cells, monocytes/ macrophages and multipotent stem cells in the SVF[40].

The WAT is surrounded by a network of capillaries, which ensures delivery of nutrients and oxygen, sufficient routes for release of hormones and cytokines, and other factors that allow the WAT to efficiently carry out its function[34]. Maintenance of the blood supply is essential for WAT growth and expansion[41]. Remodeling of the vasculature alongside WAT expansion or

compression ensures supply of oxygen, nutrients and growth factors to prevent hypoxia and waste accumulation. In obesity, the visceral WAT becomes highly inflamed and induces vascular dysfunction as a consequence of the increased secretion of vasoconstrictive factors and pro-inflammatory adipokines[41]. This results in onset of vascular insulin resistance, endothelial dysfunction, and obesity-related metabolic and vascular complications[41].

White Adipose Tissue Development

Adipocytes originate from mesenchymal progenitor, multipotential stem cells, which form unipotential adipocyte precursor cells[38]. Commitment of unipotential adipocyte precursors to differentiation leads to the formation of preadipocytes[38]. Preadipocytes are cells that express early markers of adipocyte, but have not yet accumulated lipid[38]. Finally, preadipocytes differentiate into mature adipose cells, which express late markers of adipocytes and demonstrate triglyceride accumulation (Figure 2)[38].

Stage of adipogenesis[a]	Characteristics
Mesenchymal precursor	Proliferation Ability to differentiate into multiple lineages
Committed preadipocyte	Proliferation Commitment to differentiation along adipocyte lineage Fibroblast-like morphology
Growth-arrested preadipocyte	Lack of proliferation due to contact inhibition
Mitotic clonal expansion	Re-entry into the cell cycle induced by hormonal stimulation Several rounds of cell divisions (i.e. mitotic clonal expansion) Induction of C/EBPβ and C/EBPδ expression and activity
Terminal differentiation	Cell-cycle arrest Induction of PPARγ and C/EBPα expression Transcriptional activation of adipocyte genes (lipid and carbohydrate metabolism genes, adipokines)
Mature adipocyte	High expression of adipocyte genes Transcriptionally active PPARγ, C/EBPα and C/EBPβ Signet-ring morphology: large lipid droplet occupies majority of cell volume

Figure 2. Various stages of adipocyte differentiation. Summary of stages of adipogenesis from mesenchymal precursors to mature adipocytes. Adapted from Lefterova and Lazar (2009)[133].

In rodents (rats and mice), WAT is not detected macroscopically during embryonic life and at birth, whereas in pigs, rabbits and humans WAT is present at birth[38]. In the human embryo, fat

differentiation and proliferation occurs at the beginning of the third trimester of pregnancy[38]. It begins with aggregation of a dense mass of mesenchymal cells surrounded by small vessels, which then begin to form a rich capillary network around densely packed preadipocytes[38]. Fat cell density is found to be positively correlated with capillary density, with larger fat cells being closer to the large blood vessel openings[38]. The preadipocyte clusters are also surrounded by an extensive framework of extracellular matrix proteins[38]. During post-natal development, depending on body's energy status, storage needs, hormonal activity and transcription factors, preadipocytes are converted to mature lipid-containing adipocytes through a process known as adipogenesis[42].

To accumulate triglycerides within a single lipid droplet, preadipocytes within the WAT differentiate to mature adipocytes[35,34,43]. Adipocyte differentiation involves mesenchymal precursors that commit to preadipocytes, which then undergo growth-arrest and mitotic clonal expansion, followed by terminal differentiation and development of mature adipocytes (Figure 2)[42,44]. Majority of the current knowledge regarding adipocyte development is derived from cellular studies of adipocyte differentiation[45]. A variety of cell models are used to study the underlying molecular pathways of adipogenesis and adipocyte function *in vitro*, including pluripotent fibroblasts that can differentiate into several cell types or fibroblasts-like preadipocytes that are committed to adipocyte differentiation[46]. In addition, mature adipocytes, mesenchymal stem cells, and preadipocytes are also isolated from animal and human adipose tissue for primary cell culture. However, cell models allow for a homogenous population of cells and an increased number of passages relative to primary cells[46]. Therefore, cell lines of committed fibroblast-like preadipocytes, including the 3T3-L1 and 3T3-F442A cell lines, which are

murine swiss 3T3 cells disaggregated from embryos; C3H10T1/2 (mouse embryonic pluripotent stem cells), MEFs (mouse embryonic fibroblasts), and OP9 (mouse stromal cells) among others, are most frequently used to study adipogenesis *in vitro* (Figure 3)[46].

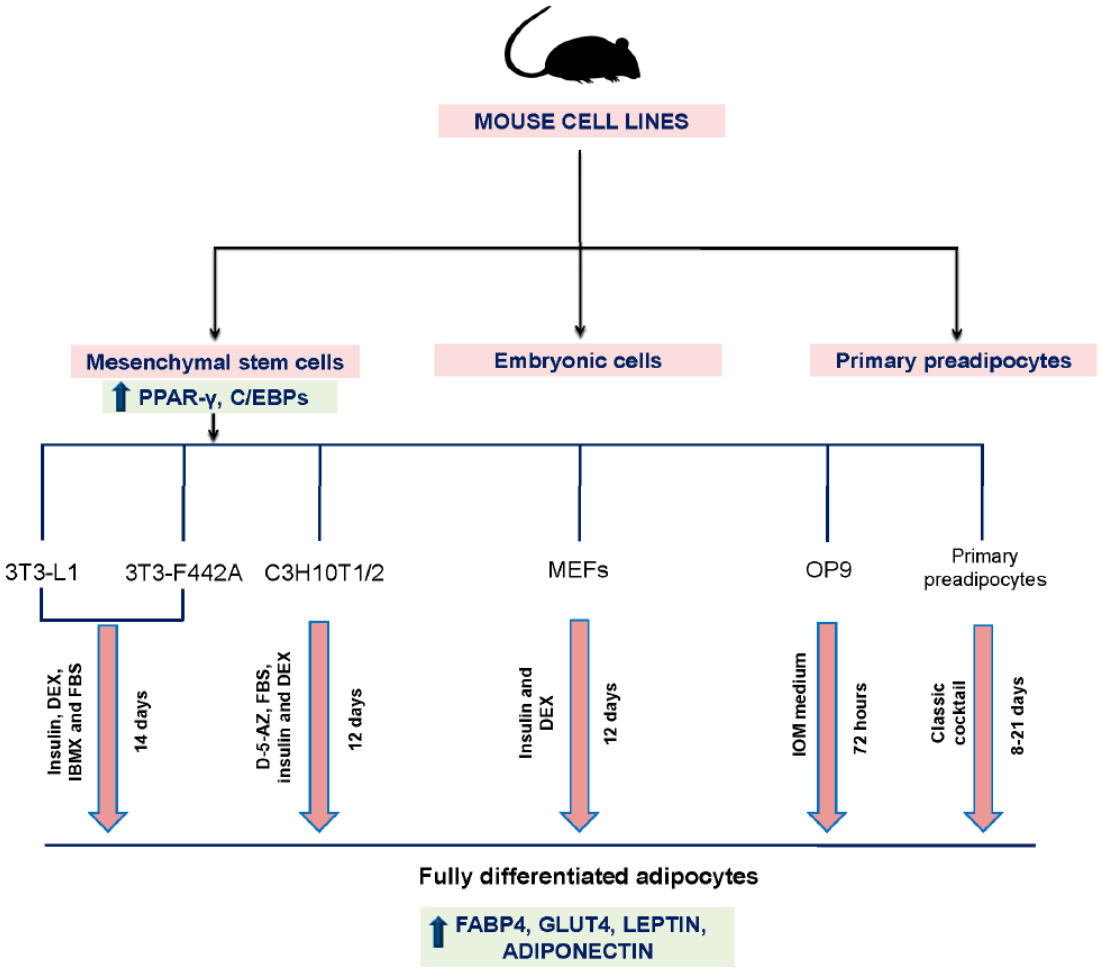

Figure 3. Mouse cell lines used to study adipocyte differentiation *in vitro*. Abbreviations: 3T3-L1, Murine Swiss 3T3 cells from embryos; 3T3-F442A, Murine Swiss 3T3 cells; C3H10T1/2, Mouse embryonic stem cell precursor; MEFs Mouse embryonic fibroblasts; OP9, Mouse stromal cells, DEX, dexamethasone; FBS, fetal bovine serum; IBMX, 3-isobutyl-1-methylxanthine; D-5-AZ, demethylating agent 5-azacytidine; IOM medium, 10% FBS, 175nM Insulin, 0.25mM DEX, 0.5mM IBMX, 2mM L|-glutamine, 100 U/mL penicillin, and 100 mg/mL streptomycin. Adapted from Ruiz-Ojeda et al. (2016)[46].

The 3T3-L1 pre-adipocyte cell line, committed to the adipose lineage, is widely used and very well characterized[47]. The 3T3-L1 cell line was derived from disaggregated 17- to 19-day-old Swiss 3T3 mouse embryo fibroblasts[48,49]. Green and Meuth (1974) showed that (Swiss) 3T3 fibroblasts have the ability to convert to adipocytes in culture; a conversion that begins upon growth arrest of the cells[48]. Green and Kehinde, in 1976, suggested that distinct changes in gene expression are responsible for the conversion of preadipocytes to adipocytes[49]. In the case of 3T3-L1 cells, the process generally involves culturing cells to 100% confluence, allowing them to reach growth arrest for 24-48 hours, and then treating with a differentiation cocktail of dexamethasone (DEX), isobutyl-methyl-xanthine (IBMX), rosiglitazone (Rosi) and insulin[47,50]. Upon stimulation, adipocytes undergo two rounds of cell division (mitotic clonal expansion) that takes place over additional 48 hours[35,51,52]. Following 3 days of differentiation, 3T3-L1 cells begin to accumulate small lipid droplets, which fuse to become large lipid droplets in the developing adipocyte over one to two weeks (Figure 4)[35,51,52].

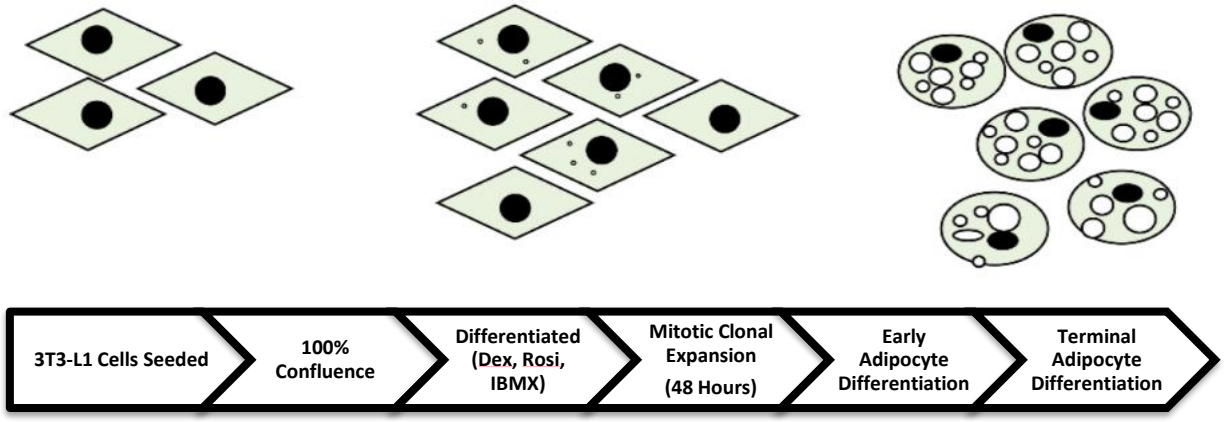

Figure 4. Sequence of 3T3-L1 cell differentiation. 3T3-L1 cells are seeded and allowed to reach confluence. Upon confluence, cells are allowed 24 to 48 hours for growth arrest and then they are differentiated. Within the first 48 hours of differentiation, 3T3-L1 cells are undergoing several rounds of mitosis, followed by growth arrest. Day 3 onwards, 3T3-L1 cells begin to accumulate small lipid droplets, which fuse to become large lipid droplets over one to two weeks. Adapted from Moseti et al. (2016)[51].

Adipocyte differentiation is characterized by appearance of early, intermediate, and late mRNA/protein markers and triglyceride accumulation[35,51,52]. Changes in expression of these markers takes place largely at the transcription level, with posttranscriptional regulation occurring for some adipogenic markers. Thus, gene expression studies conducted *in vitro* using committed preadipocyte cells lines, such as 3T3-L1, have characterized changes in gene expression during the early, intermediate and late phase of adipocyte differentiation[35,34,43].

There are also factors that keep preadipocytes in their undifferentiated form, such as preadipocyte factor-1 (PREF-1)[53]. PREF-1 is known to be a molecular gatekeeper of adipogenesis[53]. PREF-1 is highly expressed in preadipocytes, downregulated during differentiation and is known to be absent in mature adipocytes[53]. It is suggested that PREF-1 activates the MEK/ERK pathway, which is required to inhibit adipocyte differentiation[54]. PREF-1 expression is reduced by DEX during adipocyte differentiation; DEX induces the expression of C/EBPδ, initiating adipogenesis[55]. Overexpression of PREF-1 leads to inhibition of lipid accumulation, downregulation of transcription factors such as PPARγ and C/EBPα, as well as decreased expression of adipocyte markers such as FAS and FABP4[55]. Conversely, decreasing PREF-1 expression enhances adipogenesis[55]. Therefore, PREF-1 plays an important role in maintaining the preadipocyte phenotype and its overexpression results in inhibition of adipogenesis[53,55].

Upon induction of 3T3-L1 cells by DEX, IBMX, Rosi and insulin[50], expression of early differentiation factors CCAAT/enhancer binding protein β (C/EBP-β) and CCAAT/enhancer binding protein δ (C/EBPδ) is increased, which decreases post 48 hours of differentiation[56]. C/EBPβ is primarily induced by IBMX, and C/EBP-δ is primarily induced by DEX[45,57]. Within 48

hours, C/EBPβ and C/EBPδ upregulate the expression of intermediate differentiation factors PPARγ and C/EBPα, which co-regulate their expression and activation throughout adipocyte maturity[52,57]. Both PPARγ[58] and C/EBPα[59] are key transcription factors that modulate expression of genes involved in adipogenesis, lipid metabolism, and endocrine function, including adiponectin (AdipoQ), glucose transporter 4 (GLUT4), and fatty acid binding protein 4 (FABP4)[58].

During the late/terminal phase of differentiation, adipocytes *in vitro* display increased lipid synthesis and sensitivity to insulin[52]. This results in increased gene and protein expression of enzymes involved in triacylglycerol metabolism and carbohydrate intake, as well as levels of adipokines (hormones, proteins and molecules produced by mature adipocytes)[52,60]. Insulin induces glucose uptake through activation of several markers, including SREBP1c, which is a transcription factor that modulates expression of genes involved in glucose utilization and fatty acid synthesis[61]. SREBP1c activates lipogenic genes for carbohydrate intake, including fatty acid synthase (FAS), lipoprotein lipase (LPL) and acetyl-CoA carboxylase (ACC)[61,62]. In addition to fatty acid synthesizing proteins, other markers of terminal differentiation of adipocytes include adipokines, such as leptin and adipsin[63,64].

In summary, the expression of C/EBPβ and C/EBPδ is induced early during adipocyte differentiation[65]. This is followed by upregulation of PPARγ and C/EBPα expression, which are key transcription factors involved in activating genes of adipocyte specific proteins (FABP4, adiponectin) and lipid synthesizing enzymes[65]. Increased expression of enzymes involved in lipid accumulation (LPL) and fatty acid synthesis (FAS and ACC), as well as adipokines (Leptin, Adiponectin and Adipsin) marks the terminal differentiation stage of adipocyte differentiation[65].

White Adipose Tissue Function

The metabolic role of WAT is classified into triglyceride (TG) storage and release for energy homeostasis (also known as lipogenesis and lipolysis)[66]. In times of excess energy, free fatty acids (FFAs), which are present in the circulation bound to albumin, can be taken up[66]. FFAs can also enter adipocytes following the hydrolysis of triglycerides (TGs) from TG-rich lipoproteins[67]. FFAs are re-esterified into TGs through sequential actions of multiple enzymes, including glycerol-3-phosphate acyltransferase (GPAT), 1-acylglycerol-3-phosphate acyltransferase (AGPAT), phosphatidic acid phosphatase (PAP), and diacylglcerol acyltransferase (DGAT)[62,67].

Adipocytes can also synthesize lipid from carbohydrates through *de novo* lipogenesis[66,68]. For this process to occur, glucose enters the adipocyte through a glucose transporter and is metabolized to pyruvate through glycolysis[69]. Then, pyruvate enters the mitochondria and it is converted to citrate. Citrate exists the mitochondria and is converted to acetyl-CoA carboxylase, by an enzyme called ATP citrate-lyase (ACLY). Then acetyl-Co is converted to malonyl CoA by acetyl-CoA carboxylase (ACC). Finally, malonyl-CoA is converted to palmitate in a rate-limiting step by fatty acid synthase (FAS). Palmitate is processed into complex fatty acids and marks the end of the *de novo* lipogenesis process[69]. In presence of high glucose levels, insulin plays a key role in translocating the glucose transporters to the plasma membrane of the adipocyte, which facilitates the uptake of glucose into the cell[62]. Insulin also plays a role in upregulating the lipogenic genes (ACLY, ACC, FAS) through increased expression of the sterol regulatory element binding protein -1 (SREBP-1)[61].

When energy levels are low, enzymes including adipose triglyceride lipase (ATGL), hormone-sensitive lipase (HSL), and monoglyceride lipase (MGL) hydrolyze triglycerides and release free fatty acids (FFAs) back into circulation[70,71]. ATGL selectively performs the first rate-limiting step in the lipolysis process by hydrolyzing triglycerides into diglycerides. Then, HSL performs the rate-limiting step of breaking down diglycerides to monoglycerides. HSL is a multifunctional enzyme that is also able to breakdown TGs, DGs, and MGs[55]. Finally, MGL cleaves monoglycerides into glycerol and non-esterified fatty acids (NEFAs).

Lipid droplets are surrounded by proteins, such as perilipin (PLIN), adipose differentiation-related protein (ADRP), tail-interacting protein of 47 kDa (TIP47), which regulate both storage and release of lipids[72]. PLIN expression is specific to adipocytes, whereas ADRP and TI47 are activated in various other tissues[73]. During lipolysis, activated proteins kinase A (PKA) phosphorylates PLIN and HSL. Phosphorylation of PLIN increases the accessibility of HSL to the lipid droplet, which allows the rate-limiting step of lipolysis to take place[73].

The WAT is also an active endocrine organ that regulates diverse activities, such as insulin sensitivity, lipid metabolism and satiety, along with participation in physiological processes such as reproduction, apoptosis, inflammation, angiogenesis, blood pressure and immunity[9,39]. The WAT accomplishes these functions through secretion of hormones, cytokines and proteins, collectively known as adipokines[39]. The endocrine role of WAT was largely recognized with the discovery of leptin (a critical hormone involved in regulating satiety, primarily produced by the WAT)[74]. Adipokines discovered to date are adiponectin (glucose homeostasis, fatty acid catabolism), apelin (blood pressure), RBP4 (insulin resistance), resistin (insulin resistance), visfatin (insulin secretion), serpin, lipocalin-2, PAI-1, omentin, and chemerin[10,39,60,63,75].

Adipocytes are also known to secrete cytokines such as TNF**α**, IL-6, and MCP-1, which exert inflammatory responses[76]. Altered adipokine secretion results in inflammation, reticulum endoplasmic stress, and hypoxia, which are key characteristics of obesity[77–80]. Therefore, changes in WAT function are largely implicated in the development of obesity and insulin resistance[41].

White Adipose Tissue Extracellular Matrix

During adipocyte differentiation, preadipocytes convert from fibroblast-like cells to round, lipid-filled spherical adipocytes[25]. While the change in shape allows for maximal lipid storage in adipocytes, inhibition of this process results in cell spreading, increased matrix deposition and reduced lipid accumulation[81]. This transition of spindly fibroblasts to round adipocytes involves major remodeling of intracellular and extracellular structures through dramatic changes in expression of integrins, cadherins, cytoskeletal proteins and ECM proteins[82].

Changes in cytoskeletal gene and protein expression represent very early events in adipocyte differentiation[52]. In 3T3-F442A cells undergoing differentiation, actin synthesis is decreased by 90% and tubulin synthesis decreased by 95%[83]. Furthermore, alterations in the cytoskeleton gene expression can influence the expression and function of key adipocyte transcription factors and lipogenic enzymes. 3T3-F442A cells seeded onto fibronectin coated plates (*in vitro),* and stained with Oil Red O, displayed significantly decreased lipid accumulation[25]. Fibronectin blocked the downregulation of actin expression in 3T3-F442A, which resulted in decreased expression of glycerophosphate dehydrogenase (a key enzyme in lipid metabolism)[25]. The α5 integrin binds fibronectin and is expressed highly by preadipocytes[84]. Liu et al., (2005) demonstrated that overexpression of α5 integrin in 3T3-L1 cells blocks adipocyte differentiation by maintaining high levels of active Rac[84]. Rac is a GTPase from the Rho-family of

GTPases, which must be reduced in 3T3-L1 cells for adipogenesis to proceed[84]. Altogether, key changes in the cytoskeleton leading to the transition of spindly fibroblasts to a round shape of adipocytes is facilitated through interaction of cell receptors (i.e., integrins) with the ECM[81,82]. Therefore, changes in the ECM composition play a major upstream role in adipogenesis and lipid accumulation[81,82].

The relative mRNA levels of ECM markers dramatically change throughout adipocyte differentiation[52]. *In vitro* studies have reported that fibronectin (a major component of the preadipocyte ECM) is significantly downregulated during adipocyte differentiation[85]. Type 1 and Type 3 collagen mRNA decrease by 90% in 3T3-L1 cells during adipogenesis[52]. Adipocytes are surrounded by a specialized ECM known as the basement membrane (BM)[86]. Expression levels of adipocyte BM proteins, which include collagen 4, entactin and laminin, increase during adipocyte differentiation. Weiner et al. demonstrated that undifferentiated 3T3-L1 cells express type 1, type 3, and type 4 collagen[87]. Whereas, type 1 and type 3 collagen levels decrease during differentiation, mRNA levels of type 4 collagen are upregulated by 2.6 folds in differentiated 3T3-L1 cells[87]. Similarly, Aratani and Kitagawa found a strong upregulation of collagen 4, nidogen-1 (entactin), and laminin during the 6-day differentiation period of 3T3-L1 cells[88]. Ojima et al. investigated the changes in 3T3-L1 ECM protein secretion at different stages of differentiation and found consistent results as gene expression studies[89]. They reported that adipocytes secrete type 1 and type 3 collagen during the early phase of differentiation, followed by secretion of type 4, type 5 and type 6 collagen at the intermediate stage of differentiation, which is accompanied by lipid accumulation[89]. They also reported that proteins of the adipocyte basement membrane, including heparin sulfate proteoglycan 2 (HSPG2), laminin, nidogen and collagen 4, attained their

peak during the intermediate stage of adipogenesis upon appearance of lipid droplets, suggesting the importance of the development of basement membrane during lipid synthesis[89].

Differentiation of preadipocytes to round lipid-filled adipocytes is accompanied by continuous remodeling of the ECM. ECM remodeling is assisted by special modifiers, including matrix metalloproteinases (MMPs)[16,90]. MMPs are a family of endopeptidases that degrade ECM proteins to facilitate turnover[90]. MMP2 is responsible for the breakdown of collagen IV and its expression is upregulated during differentiation to assist ECM remodeling during lipid accumulation[90]. Complete inhibition of MMP activity blocks the differentiation of committed preadipocytes and impairs adipose tissue development *in vivo*[90]**.** Preadipocytes lacking MMP14 can differentiate under 2D growth conditions, but not when embedded in 3D collagen gels[91].

WAT ECM undergoes constant changes to accommodate triglyceride storage and other WAT functions[20,92]. *In vitro* studies show enhanced synthesis and continuous turnover of ECM proteins during differentiation[22,88,93]. Synthesis and deposition of the basement membrane components is a key event for adipocyte maturation[16]. Overall, evidence suggests that ECM plays an imperative role in adipocyte differentiation and function. Cells perceive and react to their extracellular environment[94]. Moreover, changes in the fibroblastic cell shape of preadipocytes to round spherical adipocytes, arising through interaction between integrins, cytoskeletal proteins and ECM proteins, precedes adipocyte differentiation and lipid accumulation. Therefore, the extracellular environment of adipocytes impacts the adipocyte structure, differentiation and function. Incorporation of an appropriate ECM in cell culture may be an important step in moving towards replicating an *in vivo* cellular environment, investigating molecular pathways in a physiological milieu, and understanding cell-ECM interactions.

CHAPTER 2: PROJECT PROPOSAL

Hydrogels are widely used for cell culture purposes due to their high water content, softness, flexibility and biocompatibility. Matrigel is a commercially available hydrogel with basement membrane components and is widely used for cell culture and high-throughput screening[28]. It is extracted from Engelbreth-Holm-Swarm (EHS) mouse sarcoma, a tumor rich in extracellular matrix proteins, and is composed of laminin, collagen IV, entactin, perlecan and growth factors[28]. The heterogeneous composition of Matrigel and its BM components provides a very close mix of proteins found in the BM surrounding adipocytes[88]. As discussed earlier, the basement membrane of adipocytes is developed during the crucial stage of differentiation when cells begin to accumulate lipid.

The current body of evidence suggests that Matrigel enhances adipocyte differentiation. Viravaidya and Shuler (2002) investigated the effect of collagen, matrigel, and polylysine on adipocyte cell behaviour relative to tissue culture plastic[95]. They found that over 21 days, 3T3-F442A preadipocytes grown on Matrigel and differentiated to adipocytes displayed 30% increase in lipid accumulation, as compared to cells differentiated on polystyrene[95]. O'Connor et al. (2003) explored the effect of Collagen 1, Fibronectin and Matrigel on adipogenic differentiation of primary stromal vascular (SV) cells[24]. They reported that after 24 days of differentiation, less than 5% of SV cells converted to adipocytes on Fibronectin and 59% cells converted to adipocytes on Matrigel, relative to 13% on tissue culture plastic[24]. They also found highest cell spreading of preadipocytes on Fibronectin; and significantly increased adipocyte yield and lipid volume in SV cells on Matrigel[24]. Results from both studies indicate that the ECM composition dictates

preadipocyte differentiation, with the fibroblastic matrix inhibiting adipogenesis and the matrix containing proteins in the adipocyte basement membrane promoting differentiation.

The positive influence on differentiation upon seeding cells on a basement membrane rich ECM has been observed with other cell types, including primary mouse mammary epithelial cells that secreted increased levels of milk proteins when cultured on a reconstituted basement membrane, an ability that is lost when these cells are cultured on plastic[96]. Furthermore, rat hepatocytes cultured on a laminin-rich gel matrix displayed stable secretion of a key protein (i.e., albumin) over 3 weeks[97]; differentiation of endothelial cells is accelerated upon being cultured on a reconstituted gel composed of basement membrane proteins[98]; and alveolar type II epithelial cells cultured on EHS tumor basement membrane displayed higher differentiation and physiological phenotype than cells cultured on plastic[99]. These studies indicate that cells, which secrete a basement membrane *in vivo*, display a higher differentiated phenotype and physiological morphology upon being cultured on a matrix composed of basement membrane proteins than plastic.

It is clear that Matrigel enhances lipid accumulation upon differentiation of preadipocytes, however the molecular mechanism underpinning this increased accumulation is unclear. Changes in mRNA levels of adipogenic and lipogenic markers or adipocyte ECM gene markers during differentiation have not been characterized in cells differentiated on Matrigel. We propose that lipid accumulation will be potentiated in adipocytes differentiated on Matrigel and this will be accompanied by an increase in mRNA levels of adipogenic and lipogenic markers. Furthermore, we propose that the enhanced differentiation of 3T3-L1 cells will be coincident with altered mRNA levels of ECM protein. As discussed above, 3T3-L1 cells secrete proteins of the

basement membrane during the intermediate differentiation stage when cells accumulate lipid. However, if differentiating cells are provided with a matrix composed of basement membrane proteins then it is possible that resources of the cell can be devoted to a greater extent to lipid accumulation. Therefore, the specific research objectives of this study are:

I. **Objective 1:** to assess the impact of Matrigel on 3T3-L1 proliferation, lipid accumulation and expression of adipogenic and lipogenic markers.

   HYPOTHESIS: Matrigel will decrease 3T3-L1 proliferation, increase lipid accumulation and enhance the mRNA levels of adipocyte differentiation and lipid synthesis markers.

   Experimental Rationale: We will investigate the impact of Matrigel on 3T3-L1 cell proliferation and lipid accumulation over 21 days (long-term). Lipid accumulation will be assessed at day 4, day 7, day 14 and day 21 post differentiation. Day 4 is chosen as a representative of the intermediate differentiation stage, day 7 is designated to represent a time point between the intermediate and terminal stage of differentiation, day 14 is selected to determine the impact of Matrigel at the terminal differentiation stage and day 21 is selected to represent a very late stage of adipocyte differentiation. To determine the impact of Matrigel on 3T3-L1 differentiation, mRNA levels of the following markers will be investigated at days 0, 4, 14 and 21: anti-adipogenic marker PREF-1[100]; key transcription factors PPARγ, C/EBPα, and SREBP1c[45,47,44], lipogenic markers FAS and LPL[48]; a key indicator of lipid size PLIN1[57]; an adipocyte marker FABP4; and key adipokines adiponectin and leptin[9,32,59,49]. The day 0 time point is selected to obtain expression of all markers in undifferentiated 3T3-L1 cells.

II. **Objective 2:** to investigate the impact of Matrigel on mRNA levels of ECM genes from all stages of adipocyte differentiation.

HYPOTHESIS: 3T3-L1 cells cultured on Matrigel will express altered levels of ECM genes from all stages of adipocyte differentiation.

Experimental Rationale: The mRNA levels of ECM genes were assessed in 3T3-L1 cells at time points day 0, day 4 and day 14. Day 0 is selected to determine the expression of markers in undifferentiated 3T3-L1 cells. Day 4 is chosen as the representative of the intermediate differentiation stage, and day 14 is selected to determine the impact of Matrigel at the terminal differentiation stage. The selected genes for analysis include the ECM marker expressed by preadipocytes: Fibronectin[81]; ECM genes expressed by preadipocytes and adipocytes at an early stage of differentiation type 1 and type 3 Collagen[73]; markers of the basement membrane type 4 Collagen and Laminin[73,82]; and MM2 as it is involved in breakdown of collagen 4 during adipocyte differentiation[75].

III. **Objective 3:** To assess whether culturing adipocytes on an ECM, as model system, will impact the response of 3T3-L1 cells to pharmaceuticals when compared to culturing cells on tissue culture plastic. Rosiglitazone, an insulin-sensitizing drug that increases lipid accumulation in adipocytes, was used as an example.

HYPOTHESIS: 3T3-L1 cells differentiated on Matrigel will present higher sensitivity to Rosiglitazone relative to control.

Experimental Rationale: We propose to test the effect of various concentrations (0µM, 0.01µM, 0.025µM, 0.1 µM, 0.5µM, 2.0 µM) of the Rosiglitazone on lipid accumulation in 3T3-L1

cells cultured on Matrigel. Rosiglitazone is an antidiabetic drug that belongs to the class of thiazolidinediones. Rosiglitazone acts as an insulin sensitizer by binding to PPARγ and enhancing its response to insulin resulting in increased lipid accumulation[83,84]. Rosiglitazone (2.0 µM) is used to differentiate 3T3-L1 cells and its absence results in lower lipid accumulation[37]. The various concentrations of rosiglitazone were selected from several studies that use this molecule as a control for lipid accumulation[85–87]. Therefore, using Rosiglitazone is a simple and effective method for us to investigate the effect of Matrigel on lipid accumulation in 3T3-L1 cells in response to the various concentrations of Rosiglitazone.

This study will use the 3T3-L1 preadipocyte cell line. We will culture 3T3-L1 cells on Corning® Matrigel matrix and investigate the changes in preadipocyte growth and proliferation, lipid accumulation, and differentiation over long term. The 3T3-L1 preadipocytes will be cultured on the surface of Matrigel at two different thickness; 70µm and 250µm. The 70µm height of Matrigel represent the thinnest possible layer coated on tissue culture plastic plates. The 250µm height of Matrigel is representative of a thickness able to provide three-dimensional support to lipid-filled adipocytes, while being under the limit of diffusion of small molecules, such as oxygen (~150-250µm)[80].

CHAPTER 3. METHODS

3T3-L1 Cell Culture

3T3-L1 cells were obtained from American Type Culture Collection (ATCC)®, were cultured on 100x20 mm cell culture plates (Corning®) in DMEM, 1X (Dulbecco's Modification of Eagle's Medium) with 1g/L glucose, L-glutamine & sodium Pyruvate (Corning 10-014-CV), supplemented with 10% Fetal Bovine Serum (Thermo Fisher Scientific, Gibco®), 1% Penicillin-Streptomycin (Fisher Scientific, Gibco™), and 1% L-glutamine (Thermo Fisher Scientific, Gibco™). 3T3-L1 cells were kept at 37^0C in 95% air and 5% CO_2 incubators (Heracell™ 150i CO_2, ThermoFisher Scientific). For routine maintenance cells were grown to 70-80% confluence and subdivided and re-plated at a ratio of 1:10. Since cells obtained from ATCC are not defined with respect to their passage number at the time of purchase, the initial thaw within the Raha Laboratory was designated Passage 1 (P1). Differentiation of 3T3-L1 cells is decreased with passage number, therefore 3T3-L1 cells were used only up to Passage 8 (P8). Upon expansion of 3T3-L1 (ATCC® CL-173™) cells up to 60-70% confluence, the cells were collected in Recovery™ Cell Culture Freezing Medium (ThermoFisher Scientific), in aliquots of 1mL per 100x21mm plate and stored in liquid nitrogen.

3T3-L1 Cell Differentiation

For differentiation, 3T3-L1 cells were seeded at 30,000 cells/cm^2 in 12-well plates. Upon seeding, 3T3-L1 cells were allowed to reach 100% confluence in 24 hours, and then allowed additional 48 hours to reach growth arrest. The time point at which 3T3-L1 cell differentiation was initiated was referred to as day 0. Differentiation was initiated by feeding growth arrested 3T3-L1 cells with DMEM 1X (Dulbecco's Modification of Eagle's Medium) with 4.5g/L glucose, L-

glutamine & sodium Pyruvate (Corning 10-013-CV), supplemented with 10% Fetal Bovine Serum (Thermo Fisher Scientific, Gibco®), 1% Penicillin-Streptomycin (Fisher Scientific, Gibco™), and 1% L-glutamine (Thermo Fisher Scientific, Gibco™), 1µg/ml insulin (insulin solution from bovine pancreas in 25mM HEPES, pH8.2, bioreagent, Sigma-Aldrich), 0.25mM dexamethasone (DEX) (Sigma-Aldrich), 2µM Rosiglitazone (Rosi) (Sigma-Aldrich), and 0.5µM isobutyl-methyl-xanthine (IBMX) (Sigma-Aldrich). 48 hours post induction of differentiation, the media is replaced with Maintenance media (DMEM with 4.5g/L glucose, L-glutamine & sodium Pyruvate, supplemented with 10% fetal bovine serum, 1% penicillin streptomycin, 1% L-glutamine, and 1ug/ml insulin). The differentiated cells were then resupplemented with maintenance media every 48 hours until the cells were harvested for analysis.

Matrigel Coating

Matrigel® (Corning®, high concentration, growth factor reduced) was thawed overnight in ice at 4^0C. Once thawed, Matrigel® was diluted to 10mg/ml with serum-free and phenol-red free DMEM, 1X (Dulbecco's Modification of Eagle's Medium) with 4.5g/L glucose, L-glutamine & sodium Pyruvate (Corning®). The diluted matrigel was aliquoted in 1.5mL eppendorf tubes and stored at -20^0C for use when required. When needed for experiments, Matrigel® aliquots were thawed on ice at 4^0C overnight, and diluted to 5mg/mL with serum-free and phenol red free DMEM, 1X (Dulbecco's Modification of Eagle's Medium) with 4.5g/L glucose, sodium Pyruvate; without L-glutamine (Corning®). Pipette tips and tissue culture plates of choice were prechilled by placing in the freezer at -20^0C the night before coating. The amount of matrigel per well was calculated by using the 'volume=(area of the base) x (height)' formula. Therefore, the volume of the Matrigel® was determined based on a predetermined thickness of Matrigel® and a defined

surface area. 12-well tissue culture plates (Corning®), with surface area of 3.9cm^{2,}; Matrigel® of heights 70 µm and 250 µm were used for all experiments conducted for this study. Upon coating the plates with the appropriate volume of Matrigel®, the plates were placed in an incubator (Heracell™ 150i CO_2, ThermoFisher Scientific) at 37^{0}C for gelling for 120 minutes. Following this, PBS (Thermo Fisher Scientific), previously warmed to room temperature, was added to the plates and the coated plates were placed back in the incubator at 37^{0}C. The plates were then used the next day for 3T3-L1 seeding. The 3T3-L1 preadipocytes were plated at 30 000 cells/cm^2 on plates coated with Matrigel® and on tissue culture plates without Matrigel® (control) for all experiments.

Oil Red O Assay and Imaging

3T3-L1 preadipocytes and differentiated 3T3-L1 adipocytes were washed with PBS (Thermo Fisher Scientific), and then fixed with a mixture of 1% Gluteraldehyde Solution (Sigma-Aldrich®) and 0.5% Paraformaldehyde (Sigma-Aldrich®) for 45 minutes.

Lipid accumulation of adipocytes was visualized and quantified through conducting an Oil Red O Assay. The Oil Red O Solution, 0.5% in isopropanol (Sigma-Aldrich®), was diluted 1:1 in double distilled water (ddH_2O, Milli Q) and incubated at room temperature for 20 minutes. Following incubation, the Oil Red O solution was filtered through a 0.2 Micron Filter (Thomas Scientific) using a sterile syringe (Thomas Scientific). Once the solution was filtered, fixed cells (according to the protocol above) were incubated in 60% isopropanol (Sigma-Aldrich®) for 5 minutes, followed by 20 minutes of incubation in the filtered Oil Red O solution. The Oil Red O solution was removed after 20 minutes of incubation and the stained 3T3-L1 cells were washed with ddH_2O. Washed 3T3-L1 cells were allowed to dry for 30 minutes and imaged under a phase-contrast microscope at 20x magnification. After 30 minutes of drying, the Oil Red O dye was

extracted with 100% Butanol (Sigma-Aldrich®) for quantification (600 mL in each well of a 12-well plate [Corning®]). The dye was collected in a 96 well plate and visualized for spectrophotometric quantification (Multiskan Spectrum, Thermo Electron Corporation) at 510nm.

Fluorescence Staining with DAPI

3T3-L1 cells were stained with 4',6-diamidino-2-phenylindole (DAPI) (Sigma-Aldrich®) to fluorescently visualize and image cellular nucleus for cell counting purposes. The DAPI (Sigma-Aldrich®) powder was mixed with double distilled water (ddH_2O) to a concentration of 1mg/ml and stored at -20^0C. The working solution was further diluted to 0.1µg/ml in PBS (Thermo Fisher Scientific) and used to stain 3T3-L1 cells. 3T3-L1 cells were incubated in 100µl/cm^2 of the 0.1µg/ml DAPI solution for five minutes. This was followed by removal of stain, washing of cells with PBS and viewed under a fluorescent microscope (Nikon Eclipse, Ti, Japan). Stained cells were imaged at 20x magnification, using the 461nm (blue) emission wavelength.

Cell Count for Quantification of Proliferation

3T3-L1 preadipocytes were seeded at a density of 5000 cells/cm^2 on 12-well tissue culture plates, which were coated with 70 µm of Matrigel, 250 µm of Matrigel, and no Matrigel (control). Three wells were seeded for each condition. At days 1, 2, 3, 4 and 5, 3T3-L1 cells were viewed under a phase-contrast microscope (Motic AE2000), imaged using the MoticamX^2 (0700), fixed (using the protocol above) and stained with DAPI. The DAPI stained cells were then viewed a fluorescent microscope (Nikon Eclipse, Ti, Japan) and imaged at 20x magnification for cell counting. Five different fields of view were imaged per well and processed using the Nikon Imaging Software Elements, Version 4.51.01, Laboratory Imaging). Image J software (NIH ImageJ

bundled with Java 1.8.0_172) was used to count the nuclei for each image. The number of nuclei was used to determine the number of 3T3-L1 cells in each condition.

Cell Count for Quantification of Lipid Accumulation

The differentiated 3T3-L1 cells were harvested at days 4, 7, 14 and 21 for staining with DAPI (Sigma-Aldrich®). At the appropriate time points, the differentiated 3T3-L1 cells were fixed (using the protocol above) and incubated in PBS-Triton (X-100) (Sigma-Aldrich®) to permeabilize the nuclear membrane. Nuclei were then stained incubating the permeabilized cells in the 0.1ug/mL DAPI in PBS solution for 5 minutes. After staining, the DAPI in PBS solution was removed, and the cells were washed three times with PBS-Tween. This experiment was carried out in a dark room and upon completion of the experiment; the plate was covered with aluminum foil to avoid light exposure. The DAPI stained cells visualized using fluorescence microscopy (Nikon Eclipse, Ti, Japan) and imaged at 20x magnification for cell counting. Five fields of view were imaged per well were taken and processed using the Nikon Imaging Software Elements, Version 4.51.01, Laboratory Imaging). Image J software (NIH ImageJ bundled with Java 1.8.0_172) was used to count the nuclei in each image.

Gene Expression

For gene expression analysis, RNA was extracted from 3T3-L1 preadipocytes at Day 0, prior to induction of differentiation, as well as at day 4, 7, 14, and 21 post differentiation. To extract RNA, 3T3-L1 cells were washed with cold PBS, and incubated in cell recovery solution (Corning®) for one hour at 4^0C on a shaker to separate the cells from Matrigel®. After an hour of shaking, the 3T3-L1 cells were centrifuged at 800 xg for 5 minutes to separate the collected cells from Matrigel®. The first spin was followed by 2 additional spins with PBS to wash the cell pellet

of any Matrigel® residue. The experiment up to this point was conducted in a cold room at 4^0C. After the final wash, the supernatant was removed and the cell pellet was resuspended in Trizol™ (ThermoFisher Scientific) reagent. Following the addition of Trizol™ (ThermoFisher Scientific), 3T3-L1 cells were needled (BD PrecisionGlide™ Needle, 20G) to rupture the cell membrane, up to 70 times to allow for successful RNA isolation.

The Direct-zol™ RNA MiniPrep kit w/ Zymo-Spin™ IIC Columns (Zymo Research, Cedarlanelabs) was used for isolation of high quality RNA. RNA was isolated out of each biological replicate and eluted in 25uL of Ultra-Pure H_2O. The concentration and purity of the RNA sample was measured by a NanoDrop™ spectrophotometer, using 1uL of RNA. The purity of the RNA was assessed by the ratio of absorbance at 260nm and 280nm, with a ratio of 1.8-2 generally accepted at pure RNA. The RNA samples were stored at -80^0C until required for use. For qPCR analysis, RNA samples were prepared for cDNA using 1µg of RNA, with the High-Capacity cDNA Reverse Transcription Kit (Applied Biosystems™), as per manufacturer's instructions. 20uL of cDNA was made using the BioRad iCycler (Version 4.006) at conditions: 25^0C for 10 mins, 37^0C for 120 minutes, and 85^0C for 5 minutes. The cDNA samples are stored at -20^0C until further use.

Primer Design

Primers were designed using Pubmed and Primer-BLAST (National Center for Biotechnology Information, USA). Upon selecting the gene of interest on Pubmed, primers are picked on Primer-BLAST. PCR product size is set to 100-200 base pairs. Melting temperature conditions are as follows: Minimum 59^0C; Optimal 60^0C; Maximum 60^0C; Maximum difference 1^0C. Each primer was verified for 'CCGG' runs, CCC and GGG runs at the end of each primer, and the complimentary values were set to a maximum of 6 on the 5' and 3 on the 3'. Each primer

sequence was run through OligoAnalyzer to check for hairpin, self-dimer, and heterodimerization. Sequences with a ΔG (kcal/mol) more than -9 for all parameters were selected, as that value represents thermodynamic stability to form steady state structures in real time. Upon selection, primers were ordered through the MOBIX LAB (Sanger Sequencing and Oligo Synthesis Facility) at McMaster University, Hamilton, ON, Canada. Refer to Table 1 for the list all primers sequences.

Gene	Forward Primer	Reverse Primer
HPRT	AGTCCCAGCGTCGTGATTAG	TTTCCAAATCCTCGGCATAATGA
L32	TGAATGTGGTCACCTGAAGCA	GAGCCCCTATTTGTTGTCTGAT
PREF-1	CCCAGGTGAGCTTCGAGTG	GGAGAGGGGTACTCTTGTTGAG
PPARγ	GCGGAAGAAGAGACCTGGG	GTGACTTCTCCTCAGCCCG
C/EBPα	CCGTGGTGGTTTCTCCTTGA	TTTTTGCTCCCCCTACTCGG
SREBP1c	GTCAAAACCAGCCTCCCAAG	GTCCCCGTCCACAAAGAAAC
FAS	CACGAGTGAGTGTACGGGAG	GATCGGAGCATCTCTGGTGG
PLIN-1	CTGTGTGCAATGCCTATGAGA	CTGGAGGGTATTGAAGAGCCG
FABP4	ATTTCCTTCAAACTGGGCGTG	CTTTCCATCCCACTTCTGCAC
LPL	ATGGCAAGCAACACAACCAG	AGCAGTTCTCCGATGTCCAC
Leptin	TCATACCAAGCGCCCCCAAACT	CATGCCTGCCTGCCCCTCTTA
Adiponectin	AAGGACAAGGCCGTTCTCT	TATGGGTAGTTGCAGTCAGTTGG
Fibronectin	ACCAGAGGGGTCACCTACAA	GGGAAACCGTGTAAGGGTCA
Collagen 1	ATCGACCCTAACCAAGGCTG	GAACGGGAATCCATCGGTCA
Collagen 3	ACCAAGGCTGCAAGATGGAT	TCTGTCCACCAGTGCTTACG
Collagen 4	CCTAACGGTTGGTCCTCACT	CTATGGTGGCGAGCCAAAAG
Laminin	TGAGGAGAACAAAGTAGTTAAGCGA	TCTTCGGGTCTTCCTTTCTGG
Collagen 6	AGGGTTCACACTTGGTGCTT	CTTCCATGACTCCATGCTGTTG
MMP2	ACCTGAACACTTTCTATGGCTG	CTTCCGCATGGTCTCGATG

Table 1. Primer Sequences for RT-qPCR.

Quantitative Reverse Transcription Polymerase Chain Reaction (RT-qPCR) Analysis

RT-qPCR was performed using SSoAdvanced™ Universal SYBR® Green Supermix (BIORAD) to determine the relative fold change of selected gene transcripts. The RT-qPCR uses fluorescent signals by special probes or DNA binding dyes. Each biological replicate was plated in triplicates in Hard-Shell® 384-well PCR Plates, thin wall, skirted, black (BIORAD). The plate was centrifuged

at 100g for 2 minutes at 4^0C in Allegra X-14R Centrifuge. The plates were analyzed in Bio-Rad C1000 Thermal Cycler (CFX384 Touch™ Real-Time PCR Detection System) at conditions: polymerase activation (95^0C for 10 minutes); 39 cycles of denaturing (95^0C for 10 seconds), denaturing (60^0C for 10 seconds), elongation (72^0C for 15 seconds). The threshold cycle (Ct) value was used to calculate the relative gene expression, using HPRT and L32 as housekeeping genes, and quantified by the relative ΔΔCT method. Ribosomal protein L32 (L32) is commonly used as a reference gene, which encodes a ribosomal protein that is a component of the 60S subunit of the ribosome[101–104]. Hypoxanthine phosphoribosyl-transferase I (HPRT) encodes the HPRT protein, which is a transferase enzyme that uses purines from degraded DNA and introduces into purine synthesis pathways[101,105].

Statistics

Statistical analysis was performed using the GraphPad Prism software (Prism 5 for Mac OS X, Version 5.0a, GraphPad Software, Inc.). All data points were expressed as mean ± SEM, and analysed using a two-way analysis of variance (ANOVA) with Bonferroni's Multiple Comparison post-test. Results represent data collected from three biological replicates. Biological replicates were separated by passage and time of culturing. $P \leq .05$ was considered significant, $P \leq .01$ is represented as **, and $P \leq .001$ is represented as ***.

CHAPTER 4. RESULTS

**Notes:*

- *In all figures, 'control' refers to 3T3-L1 cells cultured on tissue culture plastic plates.*
- *In the results below, the Matrigel 70µm condition is referred to as the 'thin layer of Matrigel' or 'thin Matrigel', and the Matrigel 250µm condition is referred to as the 'thick layer of Matrigel' or 'thick Matrigel'*

Matrigel Facilitates Clustering of 3T3-L1 Cells and Significantly Decreases Proliferation

3T3-L1 cells seeded on plastic grow in a monolayer over 5 days, as expected (Figure 5)[106,107]. However, upon seeding 3T3-L1 cells at the same density on Matrigel, they grow in a distinct cluster-like manner (Figure 5). Figure 5 represents 3T3-L1 cells, seeded at a density of 30,000 cells/cm^2 on plastic, as well as on a thin and thick layer of Matrigel. The clustering is apparent as early as 24 hours post cell seeding and is more prominent in 3T3-L1 cells cultured on the thick layer of Matrigel (Figure 5). This pattern of cell clustering/aggregation is not only observed at a high cell density of 3T3-L1 cells on Matrigel, but also on Matrigel at a low cell density of 5000 cells/cm^2 (Supplementary Figure 1a).

Clustering of 3T3-L1 cells on Matrigel is accompanied by lower cell proliferation (Supplementary Figure 1c). 3T3-L1 cells were seeded at 5000 cells/cm^2 on plastic, as well as on a thin and thick layer of Matrigel for five days, stained with DAPI and imaged (Supplementary Figure 1b). DAPI stained nuclei were counted (ImageJ Software), and the growth curve was plotted for analysis (GraphPad Prism Software) (Supplementary Figure 1c). Overall, 3T3-L1 cells in all conditions proliferated over the 5 days (Supplementary Figure 1c). However, Matrigel

decreases 3T3-L1-cell proliferation in a thickness dependent manner. Proliferation is significantly higher at days 3, 4 and 5 in 3T3-L1 cells cultured on plastic (control), followed by 3T3-L1 cells on a thin layer of matrigel and 3T3-L1 cells on a thick layer of Matrigel (Supplementary Figure 1c). Therefore, 3T3-L1 cells proliferate at a lower rate on Matrigel, this rate of cell growth decreases with increasing thickness of Matrigel, and cells grow in aggregates on Matrigel relative to monolayers on plastic.

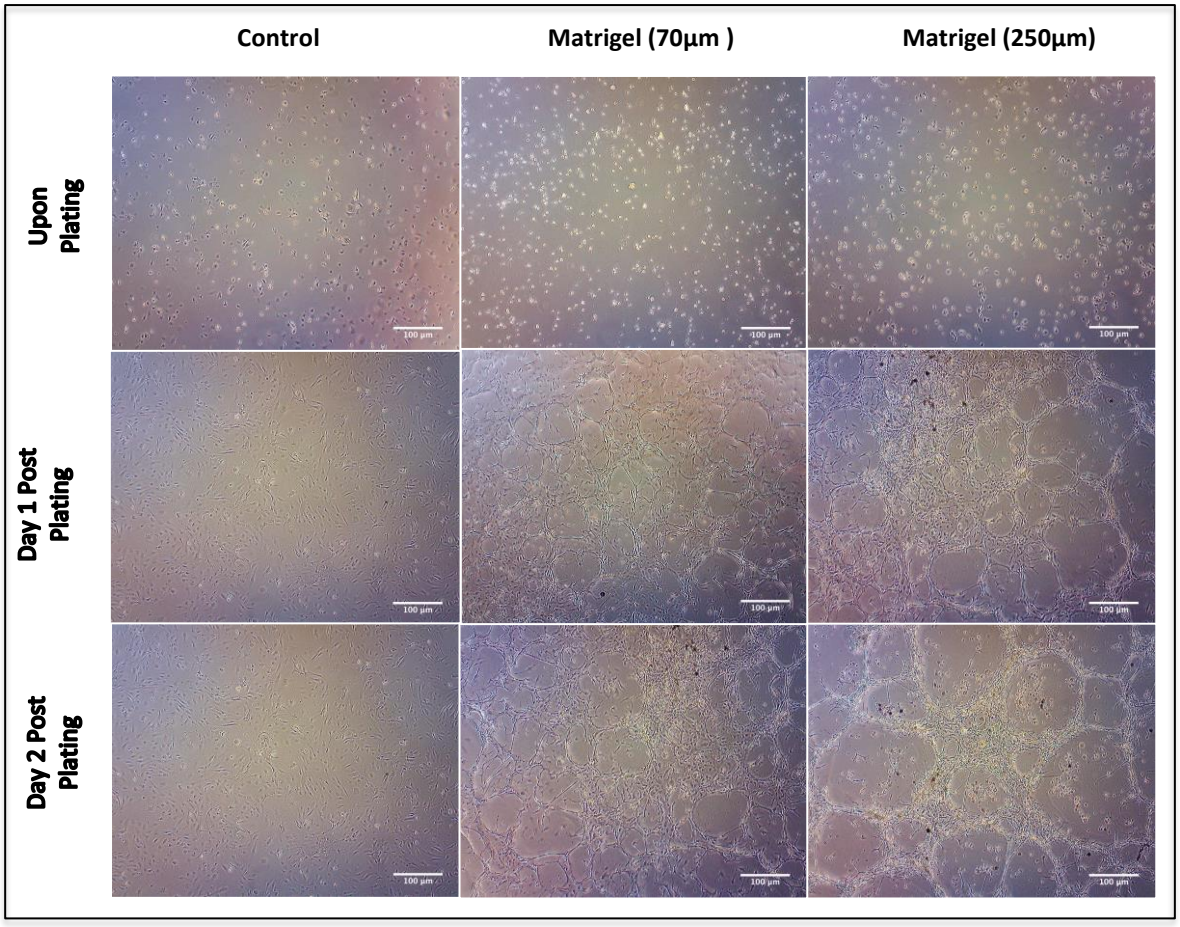

Figure 5. Matrigel induces 3T3-L1 cell aggregation in a thickness dependent manner. Phase-contrast images of 3T3-L1 cells seeded at a density of 30,000 cells/cm^2 on tissue culture plates, a thin (70 µm) and thick (250 µm) layer on Matrigel. Images were taken of the 3T3-L1 cells upon plating, 24 hours post seeding (referred to as Day 1), and 48 hours post seeding (referred to as day 2). Each image was taken at 20x magnification, (n=3).

Matrigel Enhances Lipid Accumulation in 3T3-L1 Cells

Lipid accumulation in 3T3-L1 cells differentiated on Matrigel and plastic was assessed by conducting an Oil Red O Assay (Figure 6a). Differentiated 3T3-L1 cells were fixed, stained with DAPI for cell count (Supplementary Figure 2), and stained with Oil Red O to assess lipid accumulation (Figure 6a). Oil Red O within 3T3-L1 cells was extracted, measured at 510nm for absorbance and divided by cell number to find lipid accumulation per cell. Figure 6b depicts that 3T3-L1 cells under all conditions display increased lipid accumulation over 21 days of differentiation. At day 4, 3T3-L1 cells differentiated on a thick layer of Matrigel exhibited significantly higher lipid accumulation per cell, relative to 3T3-L1 cells on plastic. At day 7, 3T3-L1 cells cultured on both thicknesses demonstrate significantly higher lipid accumulation per cell, relative to control. At day 14, 3T3-L1 cells on the thick layer of Matrigel display significantly increased lipid accumulation, relative to control and 3T3-L1 cells on the thin layer of Matrigel. In addition, the 3T3-L1 cells on the thin layer of Matrigel show increased lipid accumulation, relative to control. Finally at day 21, both thicknesses of Matrigel enhance lipid accumulation in 3T3-L1 cells, relative to control (Figure 6b).

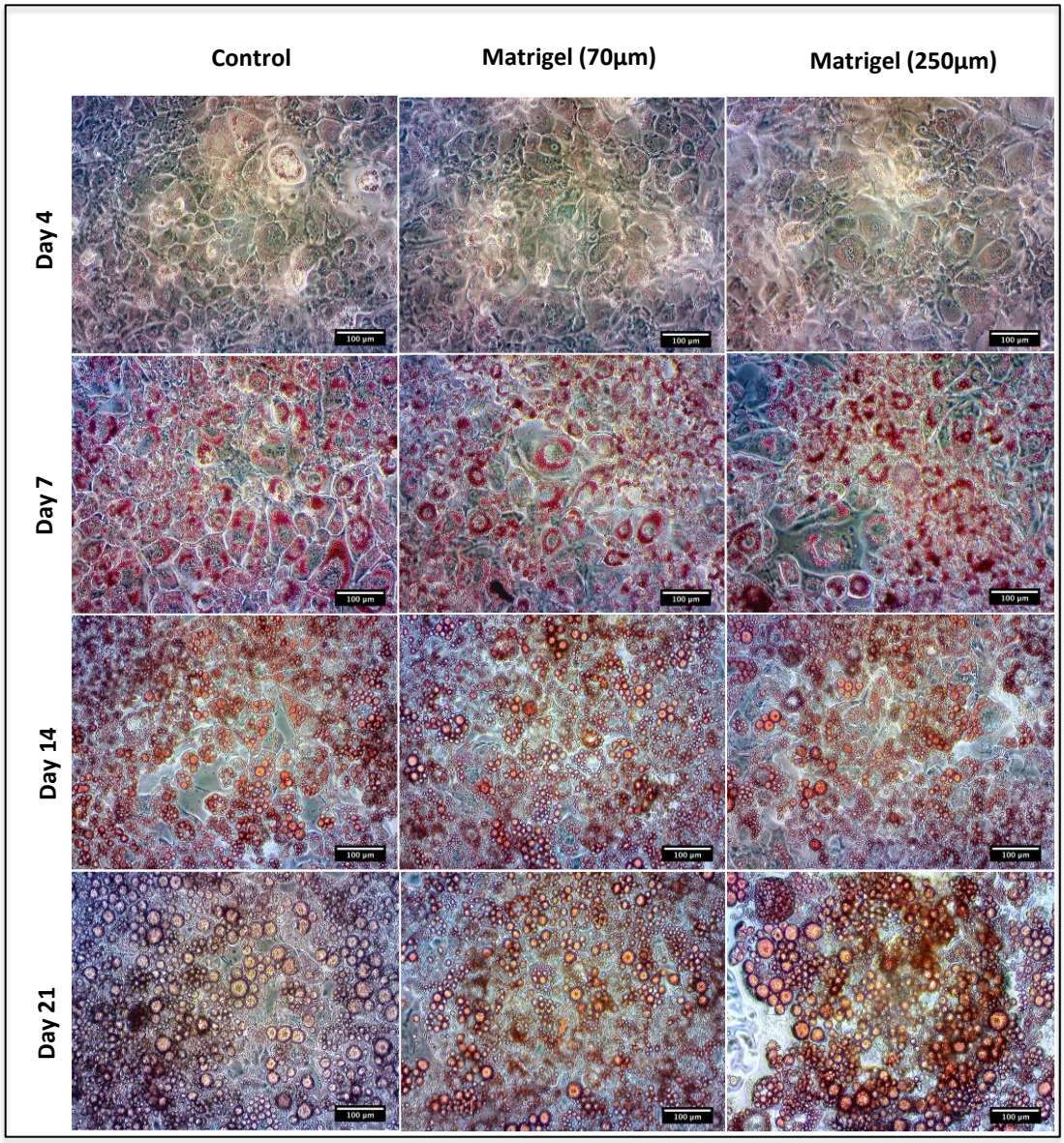

Figure 6a. Lipid accumulation in 3T3-L1 cells differentiated on Matrigel and tissue culture plastic over 21 days, visualized by Oil Red O staining. Phase-contrast images of Oil Red O stained 3T3-L1 cells cultured and differentiated on tissue culture plates, a thin (70 µm) and thick (250 µm) layer on Matrigel. Differentiated 3T3-L1 cells were imaged at day 4, 7, 14 and 21. Images were taken at 20x magnification, (n=3).

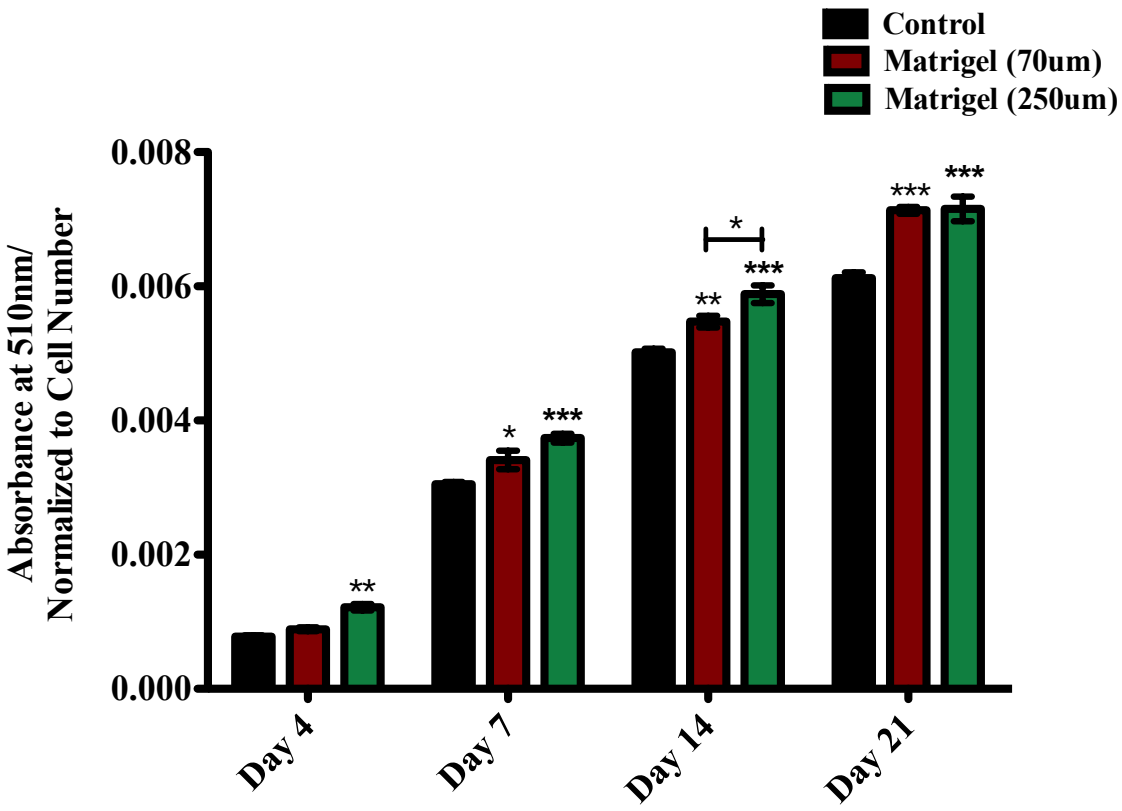

Figure 6b. Matrigel significantly enhances lipid accumulation in 3T3-L1 cells. 3T3-L1 cells were cultured and differentiated on a thick (250 µm) and thin (70 µm) layer of Matrigel, as well as on tissue culture plates. At day 4, 7, 14 and 21, 3T3-L1 cells were harvested, stained with DAPI and imaged for cell counting purposes. Following that, the 3T3-L1 cells were stained with Oil Red O, imaged and extracted for lipid quantification using a spectrophotometer at an absorbance of 510 nm. Results from absorbance were divided by cell counts obtained from DAPI stained images. Data points were plotted in GraphPad Prism Software for analysis. To determine statistical significance, results from Control, Matrigel (70µm) and Matrigel (250µm) were compared at each day, (n=3). $P \leq .05$ was considered significant, $P \leq .01$ is represented as **, and $P \leq .001$ is represented as ***.

Matrigel Down Regulates PREF-1 Expression in 3T3-L1 Cells

Preadipocyte factor 1 (PREF-1) is known as a molecular gatekeeper of adpogenesis, which acts by keeping cells in a preadipocyte state and preventing adipocyte differentiation[53]. It is reported that PREF-1 expression is decreased during differentiation[100]. In this study, PREF-1 expression in 3T3-L1 cells cultured under all conditions, decreased following differentiation (days 4 and 14), as compared to day 0 (Supplementary Figure 3). This is followed by a significant increase in PREF-1 expression at day 21 in 3T3-L1 cells under all conditions (Supplementary Figure 3). At day 0, 3T3-L1 cells grown on both thicknesses of Matrigel resulted in down regulation of PREF-1 expression, relative to control (Figure 7). At day 4, there is no significant difference in PREF-1 mRNA levels between 3T3-L1 cells on plastic, thin and thick layer of Matrigel (Figure 7). At day 14, PREF-1 expression was significantly lower in 3T3-L1 cells on the thin layer of Matrigel relative to control (plastic). Conversely, at day 14, mRNA level of PREF-1 was upregulated in 3T3-L1 cells on the thick layer of Matrigel relative to plastic (Figure 7). Finally at day 21, there was no significant difference in PREF-1 mRNA levels between 3T3-L1 cells on plastic, thin and thick layer of Matrigel (Figure 7).

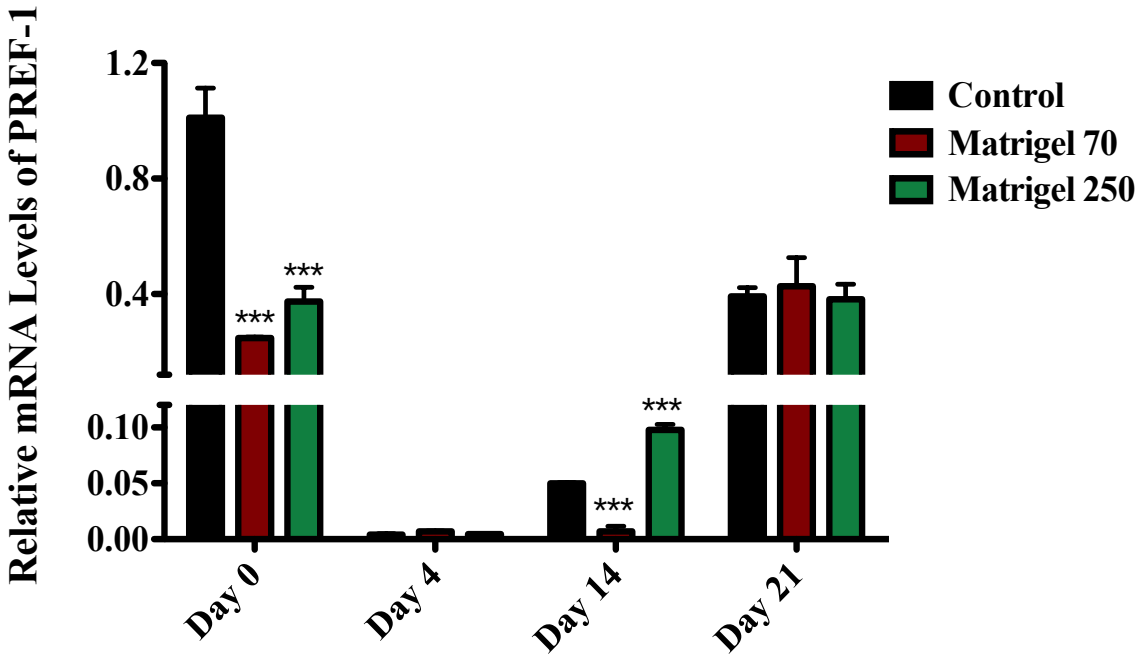

Figure 7. Culturing 3T3-L1 cells on Matrigel results in downregulation of an anti-adipogenic marker PREF-1. 3T3-L1 cells were cultured and differentiated on the thin (70 µm) and thick (250 µm) layer on Matrigel, as well as tissue culture plates (control). Cells were harvested at days 0, 4, 14, and 21 for RT- qPCR. Day 0 represents 3T3-L1 cells that were not differentiated. Results are expressed as the mean relative mRNA levels of PREF-1, normalized to HPRT and L32, ± standard error of mean. GraphPad Prism Software was used for statistical analysis. Results from Control, Matrigel (70µm) and Matrigel (250µm) were compared at each day, (n=3). $P \leq .05$ was considered significant, $P \leq .01$ is represented as **, and $P \leq .001$ is represented as ***.

Matrigel Enhances mRNA Levels Of Differentiation Markers in 3T3-L1 Cells

Adipocyte differentiation is tightly regulated by transcription factors, which include the nuclear receptor peroxisome proliferator-activated receptor γ (PPARγ), CCAAT/enhancer-binding protein alpha (C/EBPα), and sterol regulatory element binding protein-1c (SREBP1c)[35,57,58,61]. These transcription factors promote the differentiation of preadipocytes to mature adipocytes[35,57].

In this study, there was a steady increase in PPARγ expression over 21 days of differentiation in 3T3-L1 cells cultured under all conditions, with a significant up regulation of PPARγ levels at day 14 and day 21, relative to day 0 (Supplementary Figure 4). Between culture conditions, at day 0, PPARγ expression was significantly up regulated in 3T3-L1 cells cultured on the thick and thin layer of Matrigel, relative to control (Figure 8). At day 4, only 3T3-L1 cells differentiated on the thick layer of Matrigel demonstrated increased expression of PPARγ, relative to control. At day 14, a significant increase in PPARγ levels was observed in 3T3-L1 cells cultured on both thicknesses of Matrigel, relative to control (Figure 8). Finally at day 21 mRNA levels of PPARγ were not significantly different in 3T3-L1 cells under all conditions (Figure 8).

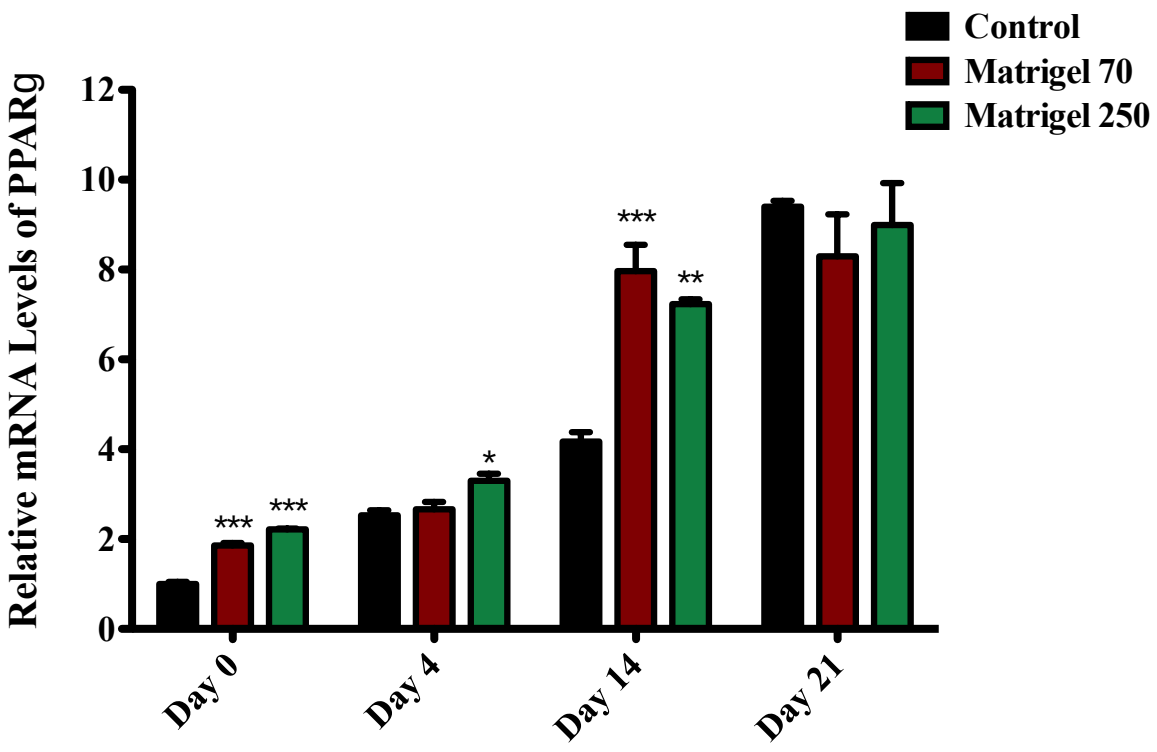

Figure 8. Matrigel enhances expression of the differentiation marker PPARγ in 3T3-L1 cells. 3T3-L1 cells were cultured and differentiated on the thin (70 µm) and thick (250 µm) layer on Matrigel, as well as tissue culture plates (control). Cells were harvested at days 0, 4, 14, and 21 for RT-qPCR. Day 0 represents undifferentiated 3T3-L1 cells. Results are expressed as the mean relative mRNA levels of PPARγ, normalized to HPRT and L32, ± standard error of mean. GraphPad Prism Software was used for statistical analysis. Results from Control, Matrigel (70µm) and Matrigel (250µm) were compared at each day, (n=3). $P \leq .05$ was considered significant, $P \leq .01$ is represented as **, and $P \leq .001$ is represented as ***.

The expression of C/EBPα increased over 21 days of differentiation in 3T3-L1 cells cultured in all conditions (Supplementary Figure 5). This included a significant increase in C/EBPα levels in 3T3-L1 cells cultured under all conditions at day 14 and day 21, relative to day 0 conditions (Supplementary Figure 5). Between conditions, 3T3-L1 cells on both thicknesses of Matrigel up regulated C/EBPα expression at day 0, relative to control (Figure 9). This pattern was consistent at day 4 and day 14. At day 4 and 14, 3T3-L1 cells cultured on both the thin and thick layer of Matrigel displayed increased C/EBPα levels, relative to control. However, at day 21 the 3T3-L1 cells on Matrigel (both thicknesses) demonstrated significantly reduced mRNA levels of C/EBPα, compared to 3T3-L1 cells on plastic (Figure 9).

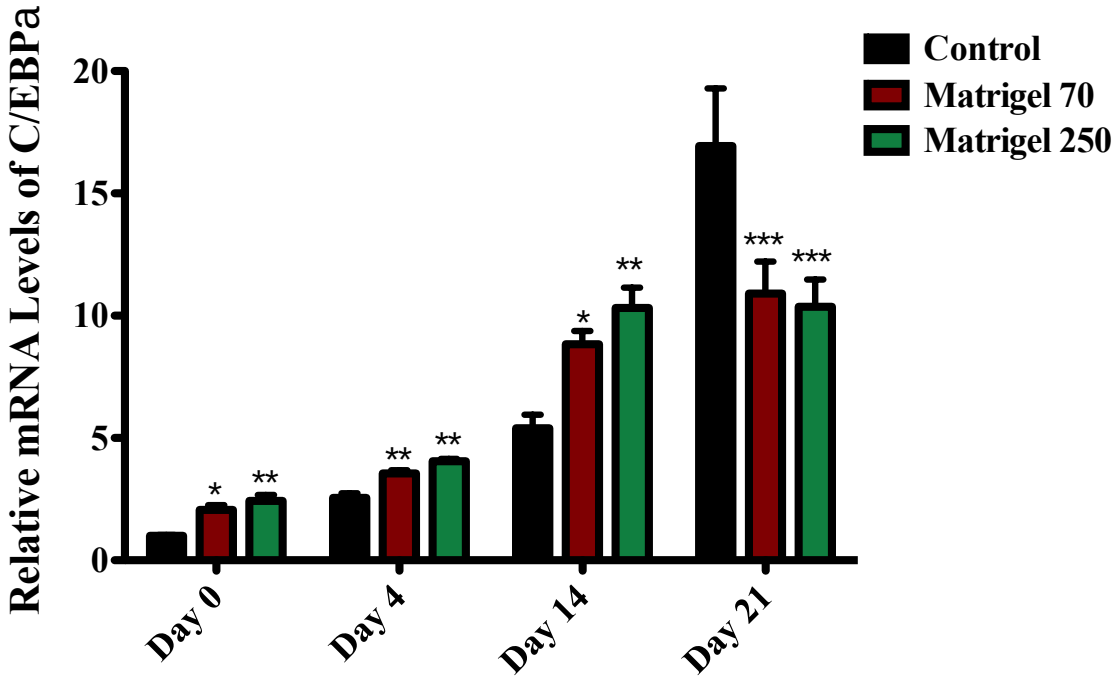

Figure 9. Differentiation of 3T3-L1 cells on Matrigel results in the upregulation of transcription factor C/EBPα. 3T3-L1 cells were cultured and differentiated on the thin (70 µm) and thick (250 µm) layer on Matrigel, as well as tissue culture plates (control). Cells were harvested at days 0, 4, 14, and 21 for RT-qPCR. Day 0 represents 3T3-L1 cells that were not differentiated. Results are expressed as the mean relative mRNA levels of C/EBPα, normalized to HPRT and L32, ± standard error of mean. GraphPad Prism Software was used for statistical analysis. Results from Control, Matrigel (70µm) and Matrigel (250µm) were compared at each day (n=3). $P \leq .05$ was considered significant, $P \leq .01$ is represented as **, and $P \leq .001$ is represented as ***.

SREBP1c mRNA levels significantly increased over 21 days of differentiation in 3T3-L1 cells cultured under all conditions (Supplementary Figure 6). Relative to day 0, there was a significant up regulation of SREBP1c levels at day 21 in 3T3-L1 cells on plastic and the thin layer of Matrigel. The increase in SREBP1c expression in 3T3-L1 cells cultured on the thick layer of Matrigel was observed at day 14, relative to day 0 (Supplementary Figure 6). Between the three conditions, at day 0 the thick layer of Matrigel significantly enhanced SREBP1c expression in 3T3-L1 cells, relative to cells on plastic. At day 4 and day 14, mRNA levels of SREBP1c were significantly up regulated in 3T3-L1 cells cultured on both thicknesses of Matrigel, relative to control. Finally, SREBP1c levels in 3T3-L1 cells under all conditions were not different at day 21 (Figure 10).

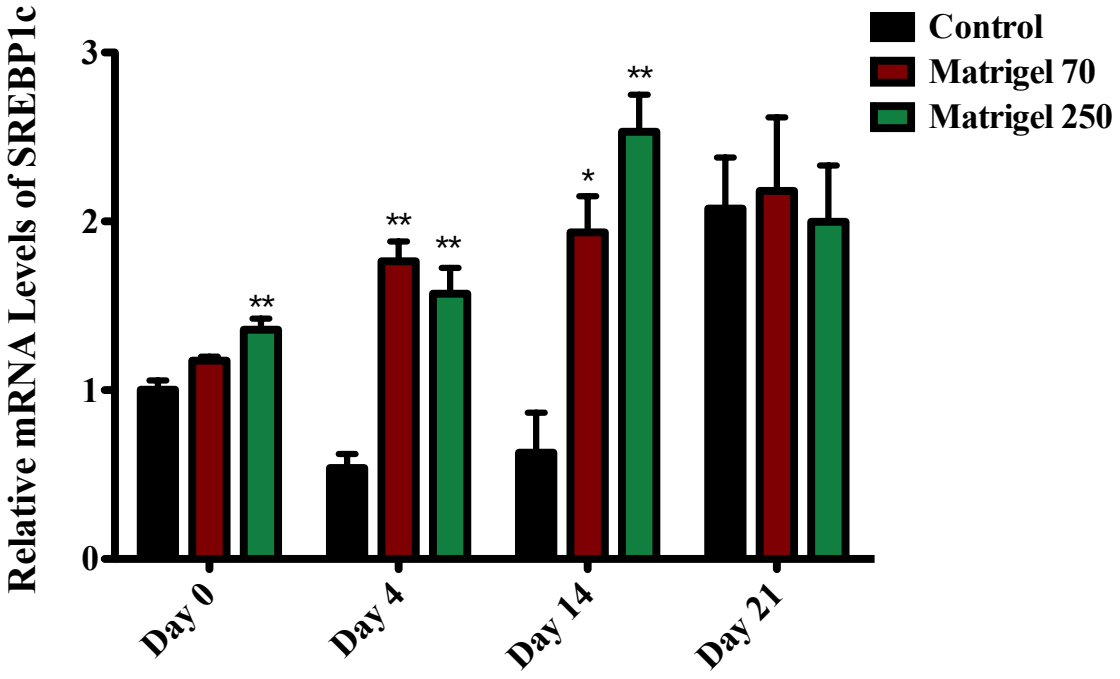

Figure 10. Matrigel significantly increases the expression of a transcription factor SREBP1c in 3T3-L1 cells. 3T3-L1 cells were cultured and differentiated on the thin (70 µm) and thick (250 µm) layer on Matrigel, as well as tissue culture plates (control). Cells were harvested at days 0, 4, 14, and 21 for RT-qPCR. Day 0 represents undifferentiated 3T3-L1 cells. Results are expressed as the mean relative mRNA levels of SREBP1c, normalized to HPRT and L32, ± standard error of mean. GraphPad Prism Software was used for statistical analysis. Results from Control, Matrigel (70µm) and Matrigel (250µm) were compared at each day, (n=3). $P \leq .05$ was considered significant, $P \leq .01$ is represented as **, and $P \leq .001$ is represented as ***.

Matrigel Significantly Increases FABP4 Expression in 3T3-L1 Cells

Fatty acid binding protein 4 (FABP4), commonly known as adipocyte protein 2 (aP2) is referred to an early marker of adipocytes, and is a key target gene of the transcription factors PPARγ and C/EBPα[108–110]. In this study, 3T3-L1 cells under all culture conditions displayed a dramatic and significant increase in FABP4 expression following differentiation (day 4, 14 and 21), relative to day 0 (Supplementary Figure 7). Between conditions, at day 0, 3T3-L1 cells cultured on the thick layer of Matrigel expressed significantly increased FABP4 levels, relative to control (Figure 11). At day 4, FABP4 expression was up regulated in 3T3-L1 cells on the thick layer of Matrigel as compared on 3T3-L1 cells on plastic. Finally at day 14 and day 21, mRNA levels of FABP4 stabilized in 3T3-L1 cells under all growth conditions (Figure 11).

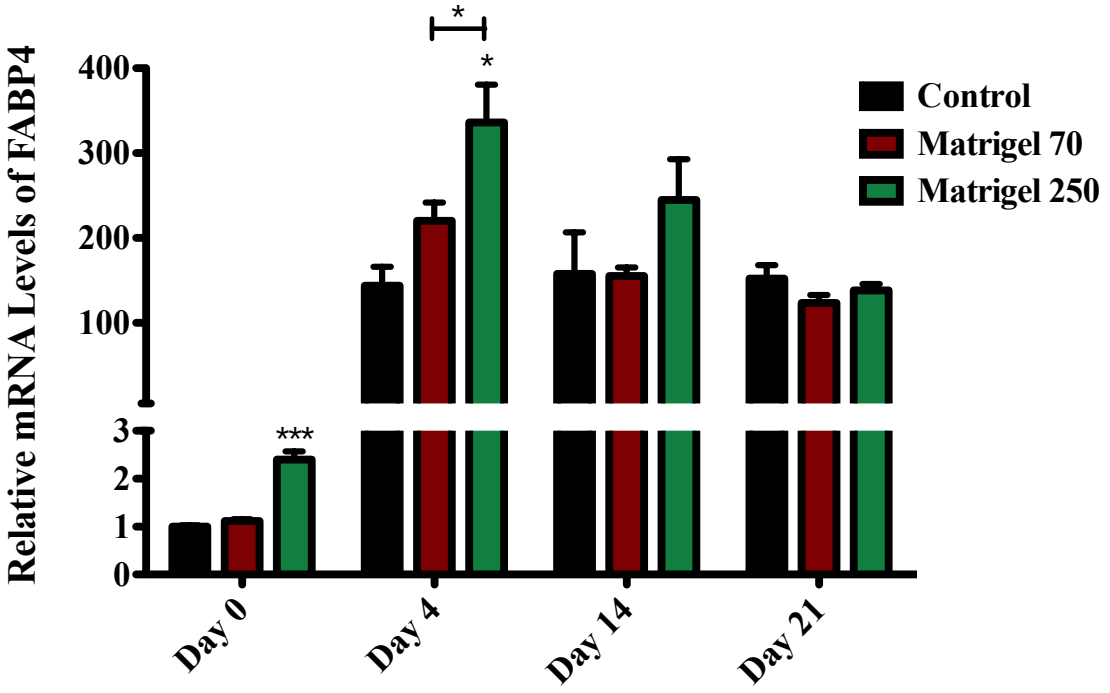

Figure 11. Matrigel enhances the expression of an adipocyte marker FABP4 in 3T3-L1 cells. 3T3-L1 cells were cultured and differentiated on the thin (70 µm) and thick (250 µm) layer on Matrigel, as well as tissue culture plates (control). Cells were harvested at days 0, 4, 14, and 21 for RT-qPCR. Day 0 represents undifferentiated 3T3-L1 cells. Results are expressed as the mean relative mRNA levels of FABP4, normalized to HPRT and L32, ± standard error of mean. GraphPad Prism Software was used for statistical analysis. Results from Control, Matrigel (70µm) and Matrigel (250µm) were compared at each day (n=3). $P \leq .05$ was considered significant, $P \leq .01$ is represented as **, and $P \leq .001$ is represented as ***.

Matrigel Upregulates Gene Expression of a Lipid Size Marker and Lipogenic Enzymes in 3T3-L1 Cells

Perilipin 1 (PLIN1) is known as a lipid-droplet associated protein, which localizes to the surface of lipid droplets[72]. 3T3-L1 cells grown under all conditions demonstrate a dramatic upregulation of PLIN1 expression upon differentiation (Supplementary Figure 8). This includes a significant increase in PLIN1 expression at day 14 and day 21, relative to day 0, in 3T3-L1 cells on plastic and the thick layer of Matrigel; and a significant increase in PLIN1 levels at day 21 in 3T3-L1 cells on the thin layer of Matrigel, relative to day 0 (Supplementary Figure 8). Between all conditions, at day 0, the thick layer of Matrigel significantly enhances the expression of PLIN1 in 3T3-L1 cells, relative to cells on plastic (Figure 12). At day 4, 3T3-L1 cells on the thick layer of Matrigel display a significant increase in PLIN1 expression, relative to control. At day 14 and day 21, 3T3-L1 cells show no significant difference in PLIN1 expression between any of the growth conditions (Figure 12).

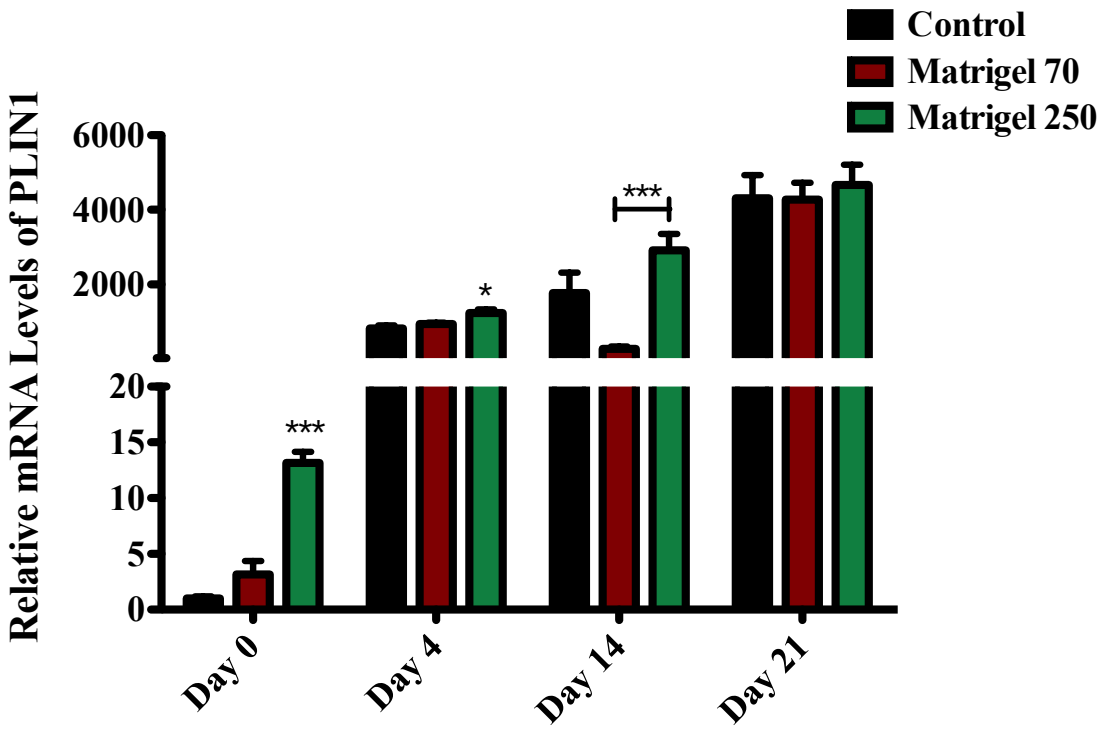

Figure 12. 3T3-L1 cells on Matrigel demonstrate upregulation of a lipid size marker Perilipinin. 3T3-L1 cells were cultured and differentiated on the thin (70 µm) and thick (250 µm) layer on Matrigel, as well as tissue culture plates (control). Cells were harvested at days 0, 4, 14, and 21 for RT-qPCR. Day 0 represents 3T3-L1 cells that were not differentiated. Results are expressed as the mean relative mRNA levels of Perilipin, normalized to HPRT and L32, ± standard error of mean. GraphPad Prism Software was used for statistical analysis. Results from Control, Matrigel (70µm) and Matrigel (250µm) were compared at each day, (n=3). $P \leq .05$ was considered significant, $P \leq .01$ is represented as **, and $P \leq .001$ is represented as ***.

Fatty Acid Synthase (FAS) is an essential enzyme and performs a rate-limiting step in de novo lipogenesis[111]. In all growth conditions, FAS expression in 3T3-L1 cells is stable at day 0 and day 4. At day 14, there is a significant upregulation of FAS expression in 3T3-L1 cells cultured on the thick Matrigel layer, relative to day 0. At day 21, the expression of FAS significantly increases in 3T3-L1 cells cultured under all conditions, relative to day 0 (Supplementary Figure 9). Between conditions, at day 0 and day 4, mRNA levels of FAS are not different in 3T3-L1 cells cultured on plastic, thin and thick layer of Matrigel (Figure 13). At day 14, 3T3-L1 cells cultured on the thick layer of Matrigel display a significant increase in FAS expression, relative to control (Figure 9). Finally at day 21, the FAS expression in 3T3-L1 cells is not significantly different among any of conditions (Thick Matrigel, Thin Matrigel, Control) (Figure 13).

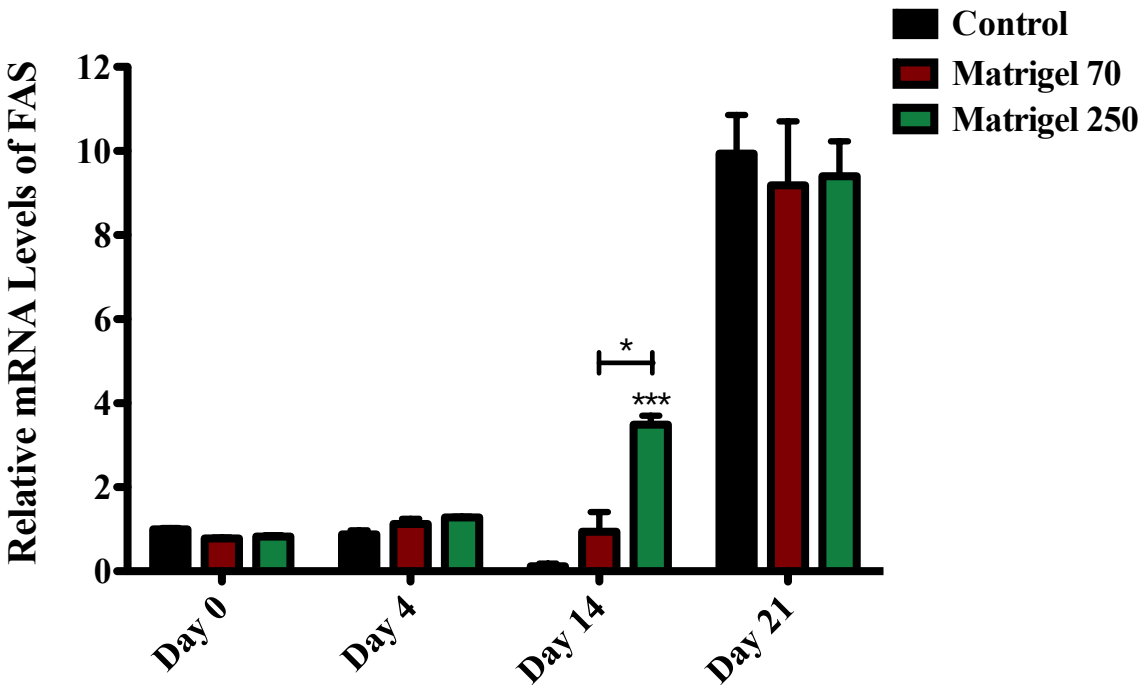

Figure 13. Matrigel significantly enhances the expression of a lipogenic gene marker FAS in 3T3-L1 cells. 3T3-L1 cells were cultured and differentiated on the thin (70 µm) and thick (250 µm) layer on Matrigel, as well as tissue culture plates (control). Cells were harvested at days 0, 4, 14, and 21 for RT-qPCR. Day 0 represents undifferentiated 3T3-L1 cells. Results are expressed as the mean relative mRNA levels of FAS, normalized to HPRT and L32, ± standard error of mean. GraphPad Prism Software was used for statistical analysis. Results from Control, Matrigel (70µm) and Matrigel (250µm) were compared at each day, (n=3). $P \leq .05$ was considered significant, $P \leq .01$ is represented as **, and $P \leq .001$ is represented as ***.

Lipoprotein Lipase (LPL) plays a role in the hydrolysis of triglyceride rich lipoproteins, allowing uptake FFA into the adipocyte[38,62]. 3T3-L1 cells on Matrigel demonstrate a significant increase in LPL expression at day 4 and day 14, relative to day 0 (Supplementary Figure 10). At day 21, 3T3-L1 cells differentiated in all three conditions display a significant up regulation of FAS expression, compared to day 0. Between all conditions, at day 0, mRNA levels of LPL are not different among any of the conditions (Figure 14). LPL expression is stable among conditions at day 4 as well. At day 14, the thick layer of Matrigel significantly enhances LPL levels in 3T3-L1 cells, relative to control and 3T3-L1 cells in the thin layer of Matrigel. Finally, at day 21 mRNA levels of LPL are not different in 3T3-L1 cells in any of the conditions (Figure 14).

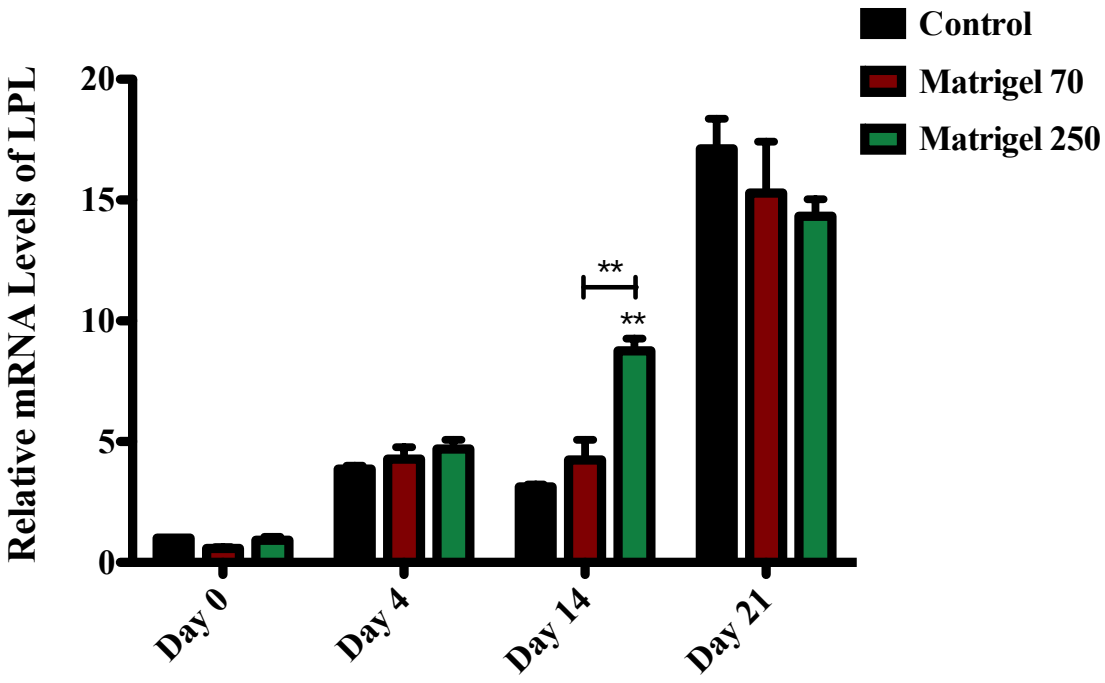

Figure 14. 3T3-L1 cells differentiated on Matrigel demonstrate upregulation of a lipogenic marker LPL. 3T3-L1 cells were cultured and differentiated on the thin (70 µm) and thick (250 µm) layer on Matrigel, as well as tissue culture plates (control). Cells were harvested at days 0, 4, 14, and 21 for RT-qPCR. Day 0 represents undifferentiated 3T3-L1 cells. Results are expressed as the mean relative mRNA levels of LPL, normalized to HPRT and L32, ± standard error of mean. GraphPad Prism Software was used for statistical analysis. Results from Control, Matrigel (70µm) and Matrigel (250µm) were compared at each day, (n=3). $P \leq .05$ was considered significant, $P \leq .01$ is represented as **, and $P \leq .001$ is represented as ***.

Matrigel Alters mRNA Levels of Endocrine Markers of Adipocytes in 3T3-L1 Cells

Leptin is an adipocyte-derived hormone that functions as a signalling molecule functioning in a feedback loop regulating adipose tissue mass[63]. Leptin is a key secretome of adipocytes and its expression is significantly increased in mature adipocytes as compared to preadipocytes[63]. In this study, mRNA levels of Leptin dramatically and significantly increase after 21 days of differentiation in 3T3-L1 cells under all conditions, relative to day 0 (Supplementary Figure 11). At day 0, 3T3-L1 cells on the thin layer of Matrigel demonstrate a significant increase in Leptin expression, relative to control (Figure 15). At day 0, mRNA levels of leptin in 3T3-L1 cells on the thick layer of Matrigel appear to be 5-fold higher, however no statistical significance was found. At day 4, leptin expression was not different in 3T3-L1 cells among any of the conditions. At day 14, 3T3-L1 cells on the thick layer of matrigel displayed a small but significant increase in leptin expression, relative to control. Finally at day 21, there was no significant difference in leptin expression among any of the conditions (Figure 15).

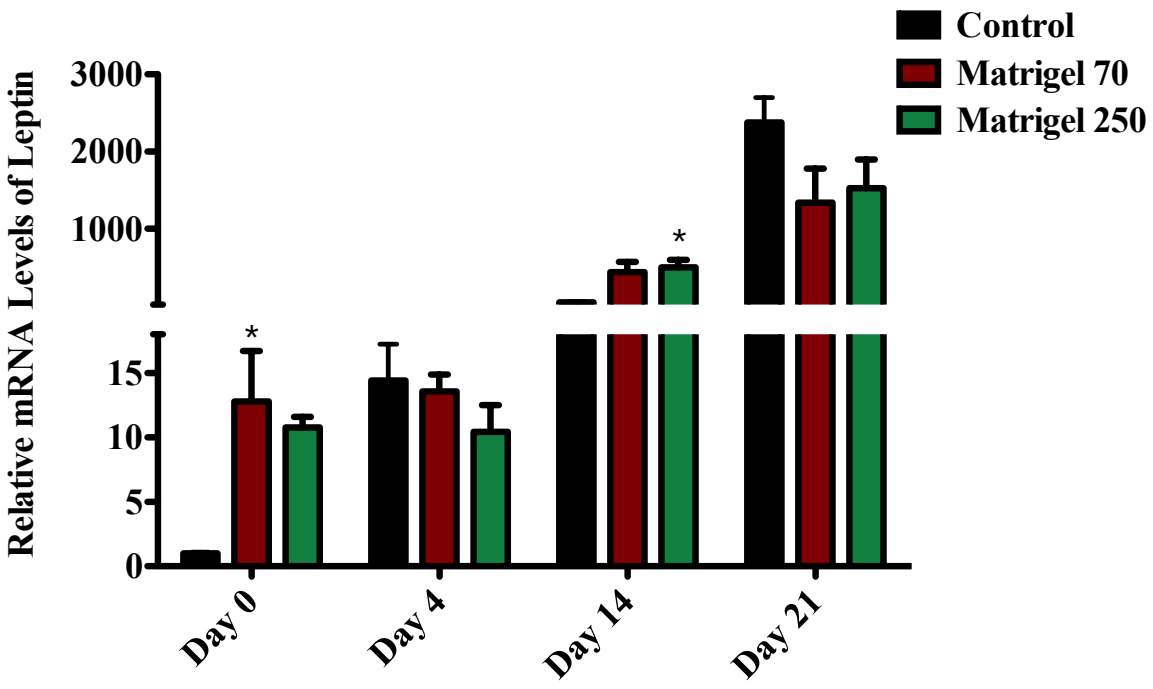

Figure 15. Matrigel enhances the expression of Leptin in 3T3-L1 cells. 3T3-L1 cells were cultured and differentiated on the thin (70 µm) and thick (250 µm) layer on Matrigel, as well as tissue culture plates (control). Cells were harvested at days 0, 4, 14, and 21 for RT-qPCR. Day 0 represents undifferentiated 3T3-L1 cells. Results are expressed as the mean relative mRNA levels of Leptin, normalized to HPRT and L32, ± standard error of mean. GraphPad Prism Software was used for statistical analysis. Results from Control, Matrigel (70µm) and Matrigel (250µm) were compared at each day, (n=3). $P \leq .05$ was considered significant, $P \leq .01$ is represented as **, and $P \leq .001$ is represented as ***.

Adiponectin is a key secretome of adipocytes and it is an important signalling molecule that modulates glucose and lipid metabolism[9,112]. Adiponectin is known to promote fatty acid oxidation and energy expenditure, and its reduced expression is linked to increased adipose tissue mass[64]. Adiponectin gene expression significantly increased following differentiation in 3T3-L1 cells under all condition, relative to day 0 (Supplementary Figure 12). At day 0, the thin layer of Matrigel significantly enhanced Adiponectin levels in 3T3-L1 cells, relative to control (Figure 16). At day 0, the 3T3-L1 cells on the thick layer of Matrigel expressed almost a 10-fold increase in mRNA levels of Adiponectin relative to control, however no statistical significance was found (Figure 16). At day 4, Adiponectin expression is stabilized among 3T3-L1 cells on plastic, thin and thick layer of Matrigel. At day 14, Matrigel (thick and thin layer) significantly decreased Adiponectin expression in 3T3-L1, relative to control. Finally at day 21, there is no difference in expression of Adiponectin among 3T3-L1 cells cultured on all three conditions (Figure 16).

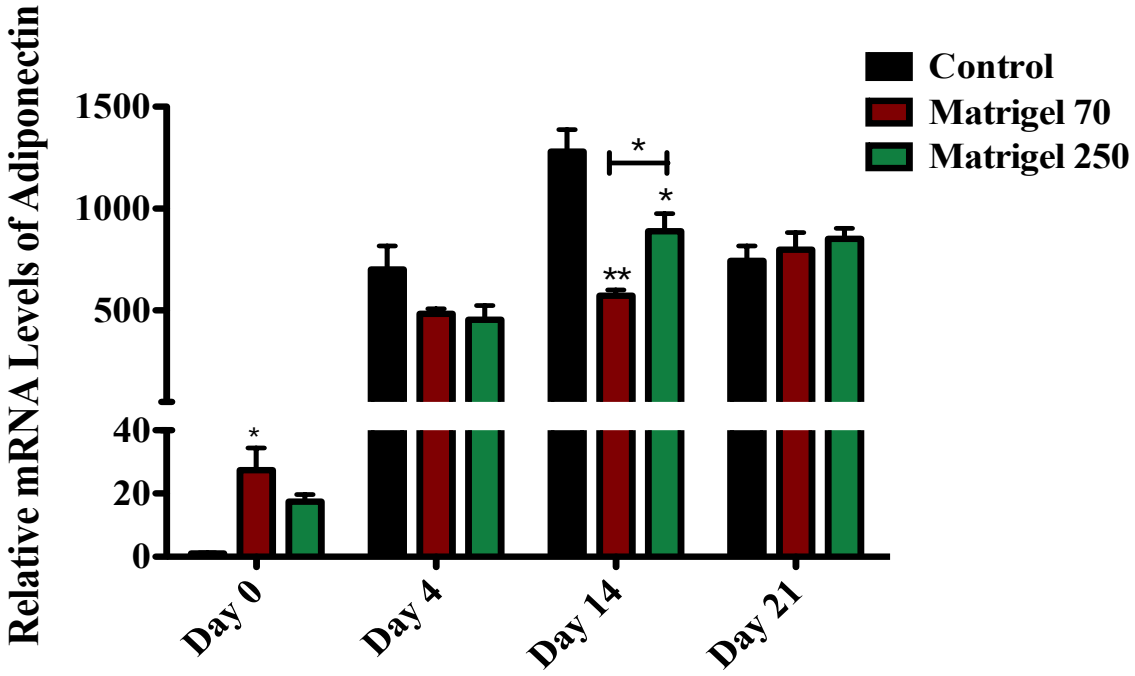

Figure 16. Matrigel results in downregulation of an endocrine marker Adiponectin in 3T3-L1 cells. 3T3-L1 cells were cultured and differentiated on the thin (70 µm) and thick (250 µm) layer on Matrigel, as well as tissue culture plates (control). Cells were harvested at days 0, 4, 14, and 21 for RT-qPCR. Day 0 represents undifferentiated 3T3-L1 cells. Results are expressed as the mean relative mRNA levels of Adiponectin, normalized to HPRT and L32, ± standard error of mean. GraphPad Prism Software was used for statistical analysis. Results from Control, Matrigel (70µm) and Matrigel (250µm) were compared at each day, (n=3). $P \leq .05$ was considered significant, $P \leq .01$ is represented as **, and $P \leq .001$ is represented as ***.

3T3-L1 Cells Cultured on Matrigel Display Significantly Reduced Expression of Genes Encoding ECM Proteins

Fibronectin: A Preadipocyte ECM Protein

Fibronectin is synthesized, secreted and expressed by preadipocytes[113]. Upon induction of differentiation, gene and protein expression of Fibronectin is down regulated in differentiating adipocytes[85]. 3T3-L1 cells cultured on all three conditions demonstrate a dramatic decrease in Fibronectin expression following differentiation (at day 4), relative to day 0; with significant decrease found for 3T3-L1 cells on plastic and the thick layer of Matrigel only (Supplementary Figure 13). However, at day 14 mRNA levels of Fibronectin in 3T3-L1 cells under conditions increased relative to day 4, and were similar to day 0 levels. Between conditions, at day 0, the thick and thin layer of Matrigel significantly down regulated Fibronectin expression in 3T3-L1 cells, relative to control (Figure 17). At day 4, 3T3-L1 cells on the thick layer of Matrigel displayed significant reduction in Fibronectin levels, relative to control. Finally at day 14, both the thin and thick layers of Matrigel significantly decrease Fibronectin expression in 3T3-L1 cells, relative to 3T3-L1 cells on plastic (Figure 17).

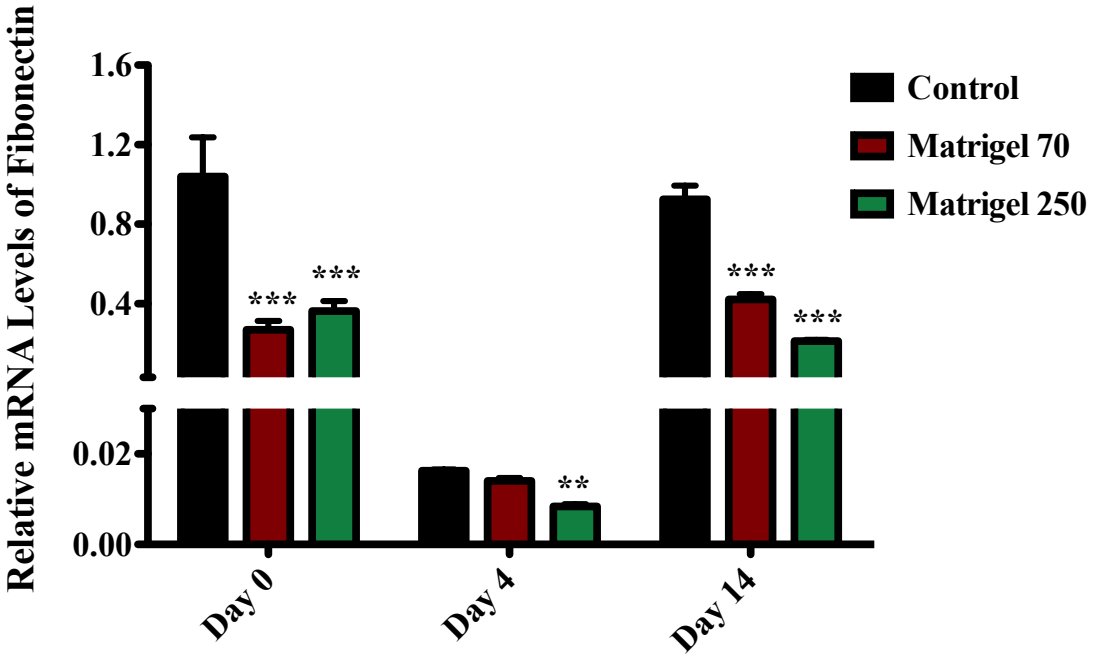

Figure 17. Matrigel decreases the expression of Fibronectin in 3T3-L1 cells. 3T3-L1 cells were cultured and differentiated on the thin (70 µm) and thick (250 µm) layer on Matrigel, as well as tissue culture plates (control). Cells were harvested at days 0, 4 and 14 for RT-qPCR. Day 0 represents undifferentiated 3T3-L1 cells. Results are expressed as the mean relative mRNA levels of Fibronectin, normalized to HPRT and L32, ± standard error of mean. GraphPad Prism Software was used for statistical analysis. Results from Control, Matrigel (70µm) and Matrigel (250µm) were compared at each day, (n=3). $P \leq .05$ was considered significant, $P \leq .01$ is represented as **, and $P \leq .001$ is represented as ***.

Collagen 1 and Collagen 3: Early Phase Adipocyte ECM Proteins

Collagen type 1 and collagen type 3 are the primary proteins that compose the collagen fibrils in the ECM surrounding WAT[87]. Preadipocytes release collagen type 1 and collagen Type 3, and adipocytes secrete these proteins at a very early stage of differentiation[22]. In this study, 3T3-L1 cells under all conditions displayed significant downregulation of collagen 1 after differentiation, at day 4, relative to day 0 (Supplementary Figure 14). However, at day 14, collagen 1 expression increased in 3T3-L1 cells in all conditions, relative to day 4; and was back at similar levels to day 0 (Supplementary Figure 14). Between all conditions, at day 0, Matrigel significantly decreased collagen 1 expression in 3T3-L1 cells, relative to control (Figure 18). At day 4, 3T3-L1 cells cultured on the thick layer of Matrigel displayed significantly reduced levels of collagen 1, compared to control (Figure 18). Finally at day 14, 3T3-L1 cells on both thicknesses of Matrigel demonstrated down regulation of collagen 1 expression, relative to control (Figure 18).

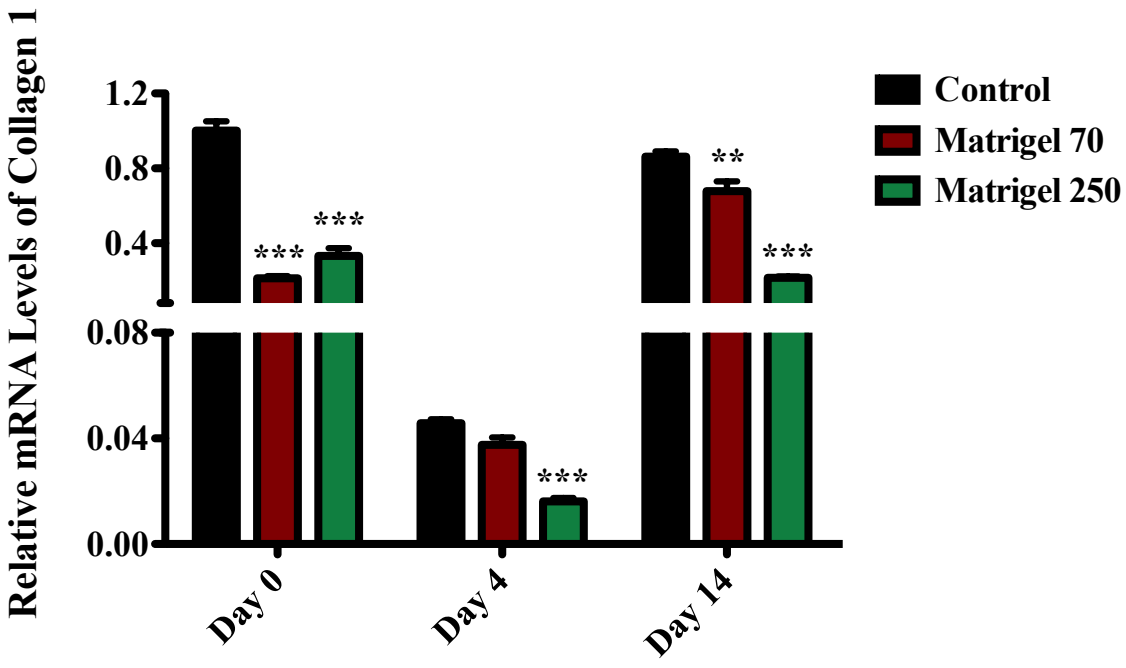

Figure 18. Matrigel results in downregulation of Collagen 1 expression in 3T3-L1 cells. 3T3-L1 cells were cultured and differentiated on the thin (70 µm) and thick (250 µm) layer on Matrigel, as well as tissue culture plates (control). Cells were harvested at days 0, 4 and 14 for RT-qPCR. Day 0 represents undifferentiated 3T3-L1 cells. Results are expressed as the mean relative mRNA levels of Collagen 1, normalized to HPRT and L32, ± standard error of mean. GraphPad Prism Software was used for statistical analysis. Results from Control, Matrigel (70µm) and Matrigel (250µm) were compared at each day, (n=3). $P \leq .05$ was considered significant, $P \leq .01$ is represented as **, and $P \leq .001$ is represented as ***.

The expression of Collagen 3 significantly decreased at day 4, relative to fay 0, in 3T3-L1 cells cultured on plastic, thin and thick layer of Matrigel, following differentiation (Supplementary Figure 15). At day 14, mRNA levels of collagen 1 in 3T3-L1 cells in all conditions increased relative to day 4, and appeared at similar levels to day 0 (Supplementary Figure 15). Between all culture conditions, at day 0, Matrigel (both thicknesses) significantly downregulated the expression of Collagen 3 in 3T3-L1 cells, relative to control (Figure 19). At day 4, 3T3-L1 cells cultures on a thick layer of Matrigel displayed reduced levels of collagen 3, relative to control. Finally at day 14, collagen 3 mRNA levels in 3T3-L1 cells were not different in any of the culture conditions (Figure 19).

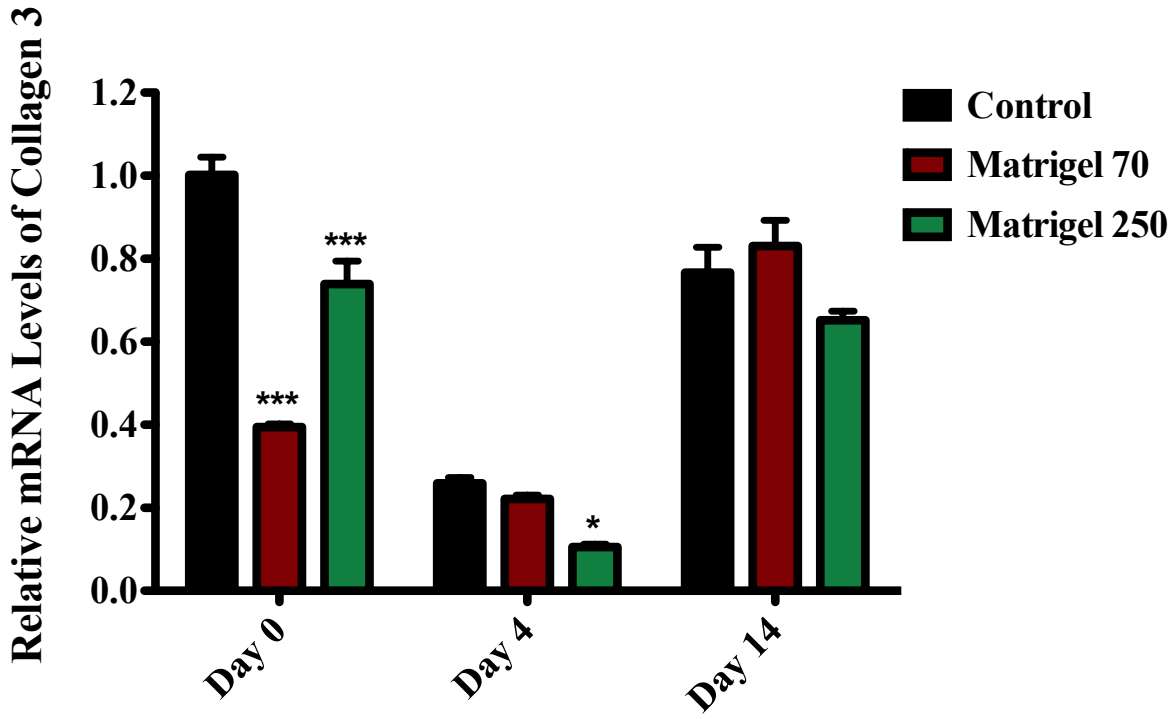

Figure 19. 3T3-L1 cells on Matrigel display decreased Collagen 3 expression. 3T3-L1 cells were cultured and differentiated on the thin (70 µm) and thick (250 µm) layer on Matrigel, as well as tissue culture plates (control). Cells were harvested at days 0, 4 and 14 for RT-qPCR. Day 0 represents undifferentiated 3T3-L1 cells. Results are expressed as the mean relative mRNA levels of Collagen 3, normalized to HPRT and L32, ± standard error of mean. GraphPad Prism Software was used for statistical analysis. Results from Control, Matrigel (70µm) and Matrigel (250µm) were compared at each day, (n=3). $P \leq .05$ was considered significant, $P \leq .01$ is represented as **, and $P \leq .001$ is represented as ***.

Collagen 4 and Laminin: Adipocyte Basement Membrane Proteins

Within the WAT, each adipocyte is surrounded by the basement membrane that is composed of Collagen type 4, Laminin, Entactin and Heparin Sulfate Proteoglycan[88]. In this study, changes expression of Collagen 4 and Laminin were assessed over 14 days of differentiation in 3T3-L1 cells cultured on plastic, thin and thick layer of Matrigel. Following differentiation, expression of Collagen 4 significantly increased in 3T3-L1 cells cultured under all conditions, at day 4 and day 14, relative to day 0 (Supplementary Figure 16). Between conditions, at day 0, Matrigel (both thin and thick layer) significantly reduced Collagen 4 expression in 3T3-L1 cells relative to control (Figure 20). At day 4, the thick layer of Matrigel down regulated the expression of Collagen 4 in 3T3-L1 cells, relative to control. Finally at day 14, 3T3-L1 cells cultured on all thicknesses of Matrigel demonstrated significant downregulation of Collagen 4 levels, compared to 3T3-L1 cells on plastic (Figure 20).

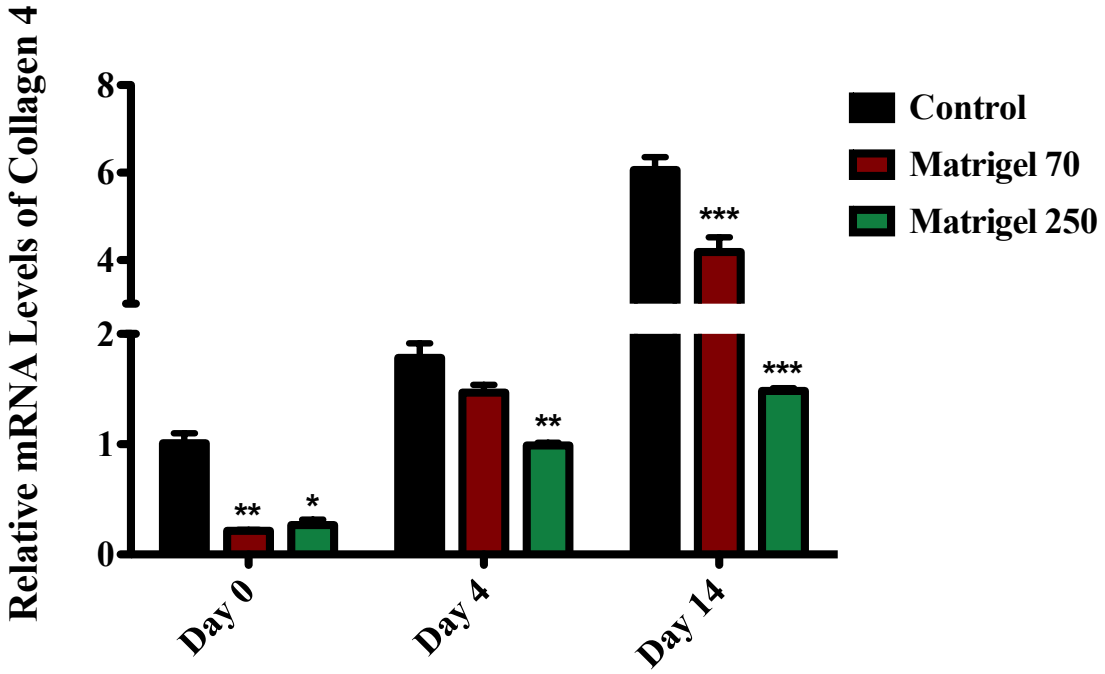

Figure 20. 3T3-L1 cells on Matrigel demonstrate significant downregulation of Collagen 4. 3T3-L1 cells were cultured and differentiated on the thin (70 µm) and thick (250 µm) layer on Matrigel, as well as tissue culture plates (control). Cells were harvested at days 0, 4 and 14 for RT-qPCR. Day 0 represents undifferentiated 3T3-L1 cells. Results are expressed as the mean relative mRNA levels of Collagen 4, normalized to HPRT and L32, ± standard error of mean. GraphPad Prism Software was used for statistical analysis. Results from Control, Matrigel (70µm) and Matrigel (250µm) were compared at each day, (n=3). $P \leq .05$ was considered significant, $P \leq .01$ is represented as **, and $P \leq .001$ is represented as ***.

The expression of Laminin significantly increased at day 14, relative to day 0 and day 4, in 3T3-L1 cells cultured on plastic and the thin layer of Matrigel (Supplementary Figure 17). However, in 3T3-L1 cells cultured on the thick layer of Matrigel, expression of Laminin did not increase following differentiation (Supplementary Figure 17). Between all conditions, at day 0 both thickness of Matrigel down regulated Laminin expression in 3T3-L1 cells compared to control (Figure 21). At day 4 and 14, 3T3-L1 cells cultured on the thick layer of Matrigel only displayed reduced mRNA levels of Laminin, relative to control (Figure 21)

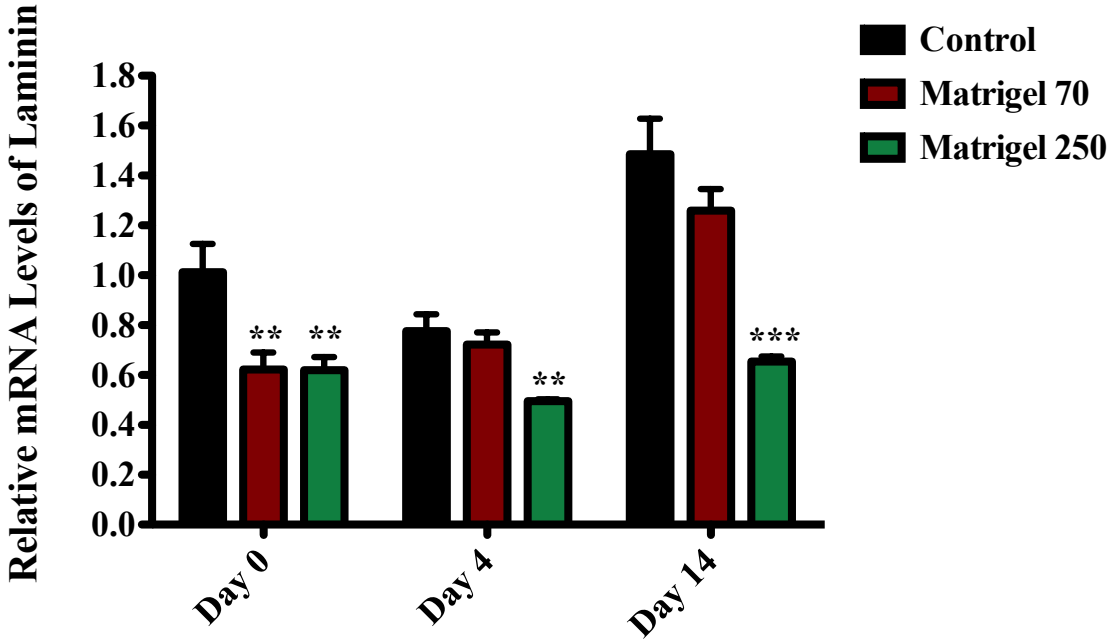

Figure 21. 3T3-L1 cells cultured on Matrigel display decreased levels of Laminin. 3T3-L1 cells were cultured and differentiated on the thin (70 µm) and thick (250 µm) layer on Matrigel, as well as tissue culture plates (control). Cells were harvested at days 0, 4 and 14 for RT-qPCR. Day 0 represents undifferentiated 3T3-L1 cells. Results are expressed as the mean relative mRNA levels of Laminin, normalized to HPRT and L32, ± standard error of mean. GraphPad Prism Software was used for statistical analysis. Results from Control, Matrigel (70µm) and Matrigel (250µm) were compared at each day, (n=3). $P \leq .05$ was considered significant, $P \leq .01$ is represented as **, and $P \leq .001$ is represented as ***.

Collagen 6: A Late Phase Adipocyte ECM Protein

Collagen 6 is secreted by mature adipocytes to facilitate triglyceride accumulation during differentiation[37]. In this study, collagen 6 mRNA levels significantly increased following differentiation (at day 4 and day 14, relative to day 0) in 3T3-L1 cells cultured on plastic, thin and thick layer of Matrigel (Supplementary Figure 18). At day 14, the expression of Collagen 6 significantly decreased in 3T3-L1 cells on plastic and thin layer of Matrigel, relative to day 4. Between all conditions, at day 0 Collagen 6 expression significantly decreased in 3T3-L1 cells on both thicknesses of Matrigel, relative to control (Figure 22). At day 4, mRNA levels of Collagen 6 decreased in 3T3-L1 cells on the thick layer of Matrigel only. Finally at day 14, both thicknesses of Matrigel reduced collagen 6 expression in 3T3-L1 cells, compared to plastic (Figure 22).

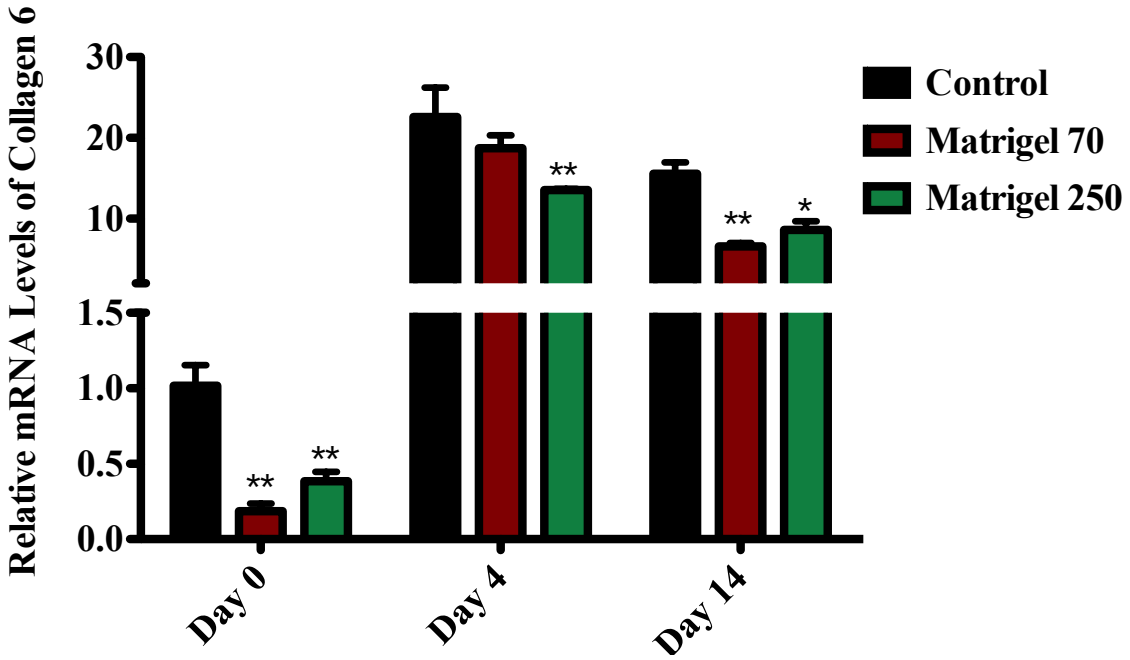

Figure 22. 3T3-L1 cells on Matrigel show decreased expression of a mature adipocyte ECM marker Collagen 6. 3T3-L1 cells were cultured and differentiated on the thin (70 µm) and thick (250 µm) layer on Matrigel, as well as tissue culture plates (control). Cells were harvested at days 0, 4 and 14 for RT-qPCR. Day 0 represents undifferentiated 3T3-L1 cells. Results are expressed as the mean relative mRNA levels of Collagen 6, normalized to HPRT and L32, ± standard error of mean. GraphPad Prism Software was used for statistical analysis. Results from Control, Matrigel (70µm) and Matrigel (250µm) were compared at each day, (n=3). $P \leq .05$ was considered significant, $P \leq .01$ is represented as **, and $P \leq .001$ is represented as ***.

MMP2: A Matrix Metalloprotease that Cleaves Collagen IV

The secretion of matrix metalloprotease (MMP)-2 increases during lipid accumulation and its inhibition hinders adipogenesis[90,91]. MMP2 cleaves Collagen 4 to assist ECM remodelling and is expected to be downregulated during intermediate stage of differentiation[90]. In this study, we observed a significant downregulation of MMP2 expression at day 4 in 3T3-L1 cells cultured under all conditions, relative to day 0 (Supplementary Figure 19). At day 14, MMP2 expression significantly increased in 3T3-L1 cells cultured on plastic and the thin layer of Matrigel, relative to day 4; and was at similar levels to day 0 (Supplementary Figure 19). However, MMP2 levels in 3T3-L1 cells on the thick layer of Matrigel remained significantly reduced at day 14, relative to day 0 (Supplementary Figure 19). When results were compared between all conditions, MMP2 expression at day 0 was significantly up regulated by the thick layer of Matrigel only in 3T3-L1 cells, relative to control (Figure 22). At day 4, MMP2 levels in 3T3-L1 cells cultured on the thick layer Matrigel were increased, compared to control. Finally at day 14, there was a slight but significant decrease in MMP2 expression in 3T3-L1 cells cultured on the thick Matrigel, as compared to 3T3-L1 cells on plastic (Figure 22).

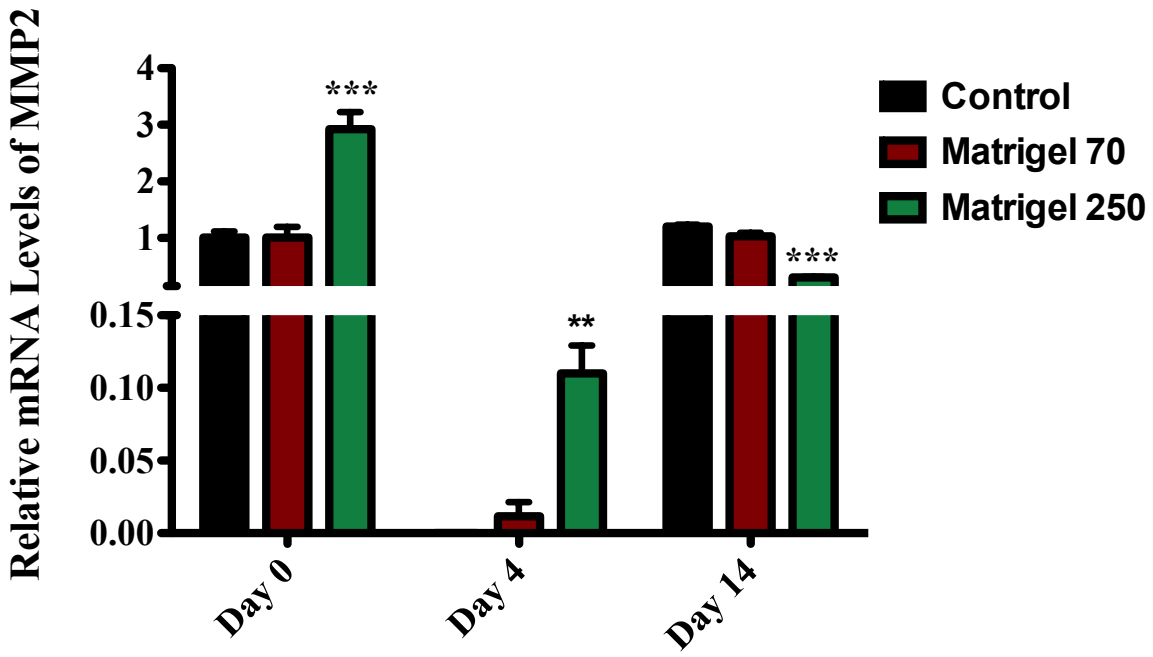

Figure 23. Matrigel alters MMP2 expression in 3T3-L1 cells. 3T3-L1 cells were cultured and differentiated on the thin (70 µm) and thick (250 µm) layer on Matrigel, as well as tissue culture plates (control). Cells were harvested at days 0, 4 and 14 for RT-qPCR. Day 0 represents undifferentiated 3T3-L1 cells. Results are expressed as the mean relative mRNA levels of MMP2, normalized to HPRT and L32, ± standard error of mean. GraphPad Prism Software was used for statistical analysis. Results from Control, Matrigel (70µm) and Matrigel (250µm) were compared at each day, (n=3). $P \leq .05$ was considered significant, $P \leq .01$ is represented as **, and $P \leq .001$ is represented as ***.

Lipid Accumulation in 3T3-L1 Cells Differentiated on Matrigel and Plastic, Treated with 0μm Or 2μm of Rosiglitazone

3T3-L1 cells were cultured on plastic, a thick and thin layer of Matrigel, and treated with 0, 0.01, 0.025, 0.1, 0.5 or 2μM of Rosiglitazone during differentiation. At day 7, 3T3-L1 cells under all growth conditions and treatments were harvested for an Oil Red O assay. The Oil Red O solution from all experimental conditions was extracted and analysed for spectrophotometric observation at absorbance of 510 nm (Supplementary Figure 20). Overall, 3T3-L1 cells in all conditions demonstrated a rise in lipid accumulation with increasing concentration of Rosiglitazone (Supplementary Figure 20). However, no significant changes were observed within the three conditions.

3T3-L1 cells undergo mitotic clonal expansion following differentiation and their proliferation rate is different on Matrigel as compared to plastic. In order to obtain an accurate measure of lipid accumulation in each condition, results must be normalized to cell number. Prior to conducting another full set of experiment with all 6 concentrations to determine lipid accumulation per cell, the two extreme conditions (0 and 2 μM Rosiglitazone) were assessed. In the past, analysis of cell number was not performed in 3T3-L1 cells treated with different concentrations of Rosiglitazone. Therefore, this experiment was conducted first with the two extreme conditions to ensure that the technique was optimized, before conducting it with the full set of concentrations.

Thus, 3T3-L1 cells cultured on all conditions and treated with 0 and 2μM of Rosiglitazone were selected for analysis of lipid accumulation per cell (Figure 24). Figure 25a depicts the results of lipid accumulation per cell for 3T3-L1 cells treated with 0 and 2uM of Rosiglitazone at

differentiation. 3T3-L1 cells cultured under all conditions demonstrate a significant increase in lipid accumulation upon treatment with 2uM of Rosiglitazone as compared to 0uM (Figure 25a). Furthermore, the increase in the lipid accumulation upon treatment with 2uM of Rosiglitazone was obtained and plotted, as seen in Figure 25b. 3T3-L1 cells cultured on the thick Matrigel demonstrate the highest difference in lipid accumulation upon treatment with 2uM of Rosiglitazone, as compared to 3T3-L1 cells on plastic and the thin Matrigel. Furthermore, the 3T3-L1 cells on the thin Matrigel experience higher increase in lipid accumulation upon treatment with 2uM of Rosiglitazone, relative to control (Figure 25b). These results demonstrate that 3T3-L1 cells cultured on plastic and thin and thick layer of Matrigel experience a difference in lipid accumulation per cell in response to various concentration of Rosiglitazone. Therefore, future steps of this study will include a complete analysis of lipid accumulation per cell in 3T3-L1 cells under all conditions subjected to 0, 0.01, 0.025, 0.1, 0.5 or 2uM of Rosiglitazone at differentiation.

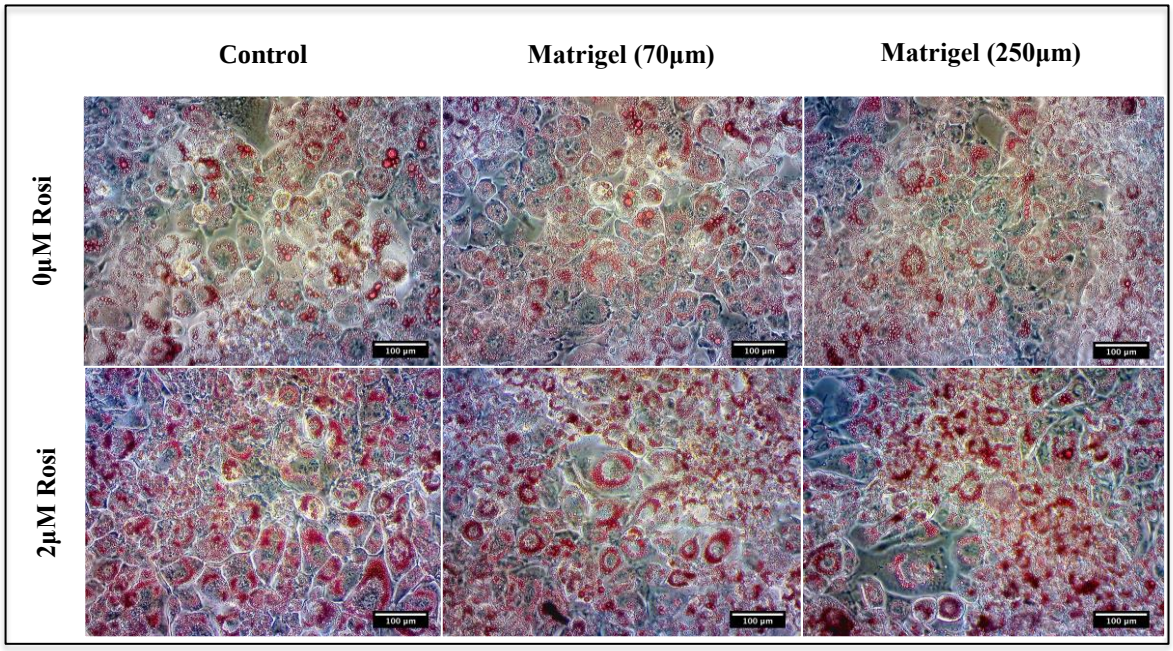

Figure 24. Lipid accumulation in 3T3-L1 cells differentiated on Matrigel and tissue culture plastic at day 7, visualized by Oil Red O staining. 3T3-L1 cells were differentiated on tissue culture plates, a thin (70 µm) and thick (250 µm) layer on Matrigel and treated with 0 or 2.0 µM of Rosiglitazone at differentiation, in addition to DEX, IBMX and Insulin. Differentiated 3T3-L1 cells were stained for Oil Red O and imaged at day 7. Images were taken at 20x magnification, (n=3).

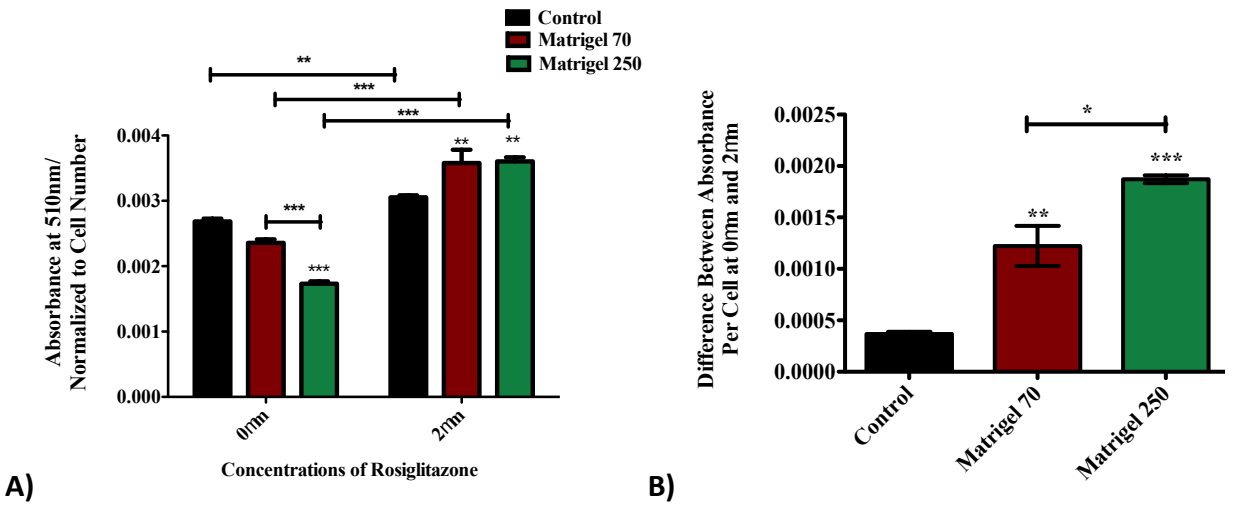

Figure 25. Matrigel enhances the sensitivity of 3T3-L1 cells to Rosiglitazone resulting in higher lipid accumulation. A) 3T3-L1 cells were differentiated on tissue culture plates, a thin (70 µm) and thick (250 µm) layer on Matrigel and treated with 0 or 2.0 µM of Rosiglitazone at differentiation, in addition to DEX, IBMX and Insulin. At day 7, 3T3-L1 cells were stained with DAPI and imaged using a fluorescent microscope to obtain cell count. Following that, 3T3-L1 cells were stained with Oil Red O, imaged, and the dye was extracted and quantified using a spectrophotometer at an absorbance of 510 nm. Absorbance values were divided by an average of the cell number for each condition, and the results were plotted in GraphPad Prism Software. **B)** The difference between the absorbance per cell values of Control 0 and 2uM Rosi, Matrigel 70µm 0 and 2uM Rosi, Matrigel 250µm 0 and 2uM Rosi were plotted in GraphPad Prism Software, (n=3). $P \leq .05$ was considered significant, $P \leq .01$ is represented as **, and $P \leq .001$ is represented as ***.

CHAPTER 5. DISCUSSION

Majority of *in vitro* studies conducted to understand adipocyte differentiation are carried out with committed preadipocyte cell lines, such as the 3T3-L1 cell line[35,48]. These studies primarily assess cellular behavior and function using two-dimensional (2D) monolayer cells cultured directly on tissue culture plastic. Although, these studies have been important in the drug discovery process, there are major limitations to culturing cells on plastic. One of the key drawbacks is that cells lack an appropriate extracellular environment that they are exposed to *in vivo*[114]. This includes an ECM, which is a substrate that cells adhere to *in vivo* is essential for the survival of most cells function[115,116]. The composition of ECM impacts cell shape, cytoskeletal organization and downstream changes such as cell proliferation, differentiation and function[115,116].

There is evidence support the hypothesis that cells grown on an appropriate matrix demonstrate altered response to stimuli and display up regulation of different cellular signaling pathways. Gospodarowicz et al., (1980) demonstrated that adrenal cortex cells and bovine granulosa proliferated actively on tissue culture plates coated with an ECM (comprising of Collagen, glycosaminoglycans and proteoglycans), in contrast to very low proliferation of both cell types on tissue culture plastic[117]. Underwood and Bennett (1993) showed that production of ECM proteins by bovine corneal endothelial (BCE) cells was significantly altered by the nature of the substrate[118]. BCE cells cultured on Collagen 4 resulted in high production of ECM proteins, as compared of cells cultured on Collagen, Fibronectin, Laminin and Vitronectin that produce low or altered levels of the ECM proteins[118]. Gross-Steinmeyer et al. (2005) demonstrated that primary hepatocytes overlaid with Matrigel displayed enhanced expression of genes involved in

hepatocyte differentiation[119]. Therefore, cells demonstrate altered response to substrate and show enhanced differentiation on substrates composed of proteins found in their *in vivo* ECM.

When isolated and cultured on plastic, various cells display high proliferation, low cell viability and low differentiation[21]. The high water content, softness and flexibility of hydrogels make them excellent candidates for cell culture substrates[120]. Matrigel is a biologically derived hydrogel, composed of basement membrane proteins, such as Laminin, Collagen 4, Heparin Sulfate Proteoglycans and Entactin[28], which are also found in the adipocyte basal lamina[28,113]. The purpose of this study was to provide 3T3-L1 cells with a substrate, similar in composition to their *in vivo* ECM, in order to develop an *in vitro* cell culture model that more closely emulates the natural environment of adipocytes. We assessed the impact of Matrigel on 3T3-L1 cell growth, differentiation, function and its ability to impact the cellular signals related to the response of pharmaceuticals, using Rosiglitazone as an example. Developing this model is a first step towards studying molecular pathways, disease mechanism, drug response and cell-to-ECM interactions in a physiological environment.

3T3-L1 Cells Aggregates Formed on Matrigel Represent a Heterogenous Cell Population

In this study, Matrigel facilitates the clustering of 3T3-L1 cells. Formation of aggregates or spheroids on a matrix is commonly found with other cell lines cultured on hydrogels[96,121,122]. Whereas, a monolayer of cells receives a homogenous mixture of nutrients and growth factors from the cell media, cellular aggregates or spheroids respond differently to media availability[120]. Cellular aggregates are composed of cells that are in various stages of growth, including proliferating cells on the outer layers and quiescent cells in the core[121]. The proliferating cells are highly exposed to media, whereas cells in the core experience less oxygen and growth factors[121].

Thus, cells in spheroids or aggregates exhibit properties that are distinct from monolayer cells[123]. Hepatocyte spheroids demonstrate high cell viability and increased detoxification capability than monolayer cultures[124]. Furthermore, endothelial cell spheroids display an inner vascular lumen-like hollow center as compared to cells in monolayer culture[125]. In the body, adipocytes are surrounded by an ECM and co-exist with a population of cells that are exposed to increased nutrients while others are in hypoxic environnment[34,126]. Klingelhutz et al. (2018) developed a scaffold-free method to generate adipocyte spheroids[127]. Adipocytes in the spheroids demonstrated larger lipid droplets, relative to cells in monolayers[127]. Furthermore, upon exposure to toxin-related stress spheroids displayed increased secretion of pro-inflammatory adipokines[127]. Turner et al. (2015) developed a spheroid model of adipocytes using 3T3-L1 cells and demonstrated that cells in spheroids displayed higher lipid accumulation and increased mRNA levels of PPARγ, relative to cells in monolayer culture[128]. Therefore, cellular heterogeneity within cell aggregates or spheroids represent the complex cell organization found *in vivo,* and may result in a more differentiated phenotype relative to cells in monolayers.

The 3T3-L1 cell aggregates on Matrigel appear similar to tube-like formation found in endothelial cells on Matrigel[129]. Corning Matrigel matrix is extracted from the Engelbreth-Holm-Swarm (EHS) mouse sarcoma, a tumor rich in ECM proteins[28]. BALB-3T3 cells belong to a cell line developed from disaggregated mouse embryos, and are highly susceptible to transformation in culture by the murine sarcoma virus[130]. Upon transfection, BALB-3T3 cells display changes in cell morphology and cell growth, relative to non-transfected cells[130]. Based on this data, it can be suggested that 3T3-L1 cells cultured on Matrigel may become susceptible to contamination and as a result display altered growth patterns. However, there is evidence in literature that the

aggregation of 3T3-L1 cells on Matrigel results from interaction between 3T3-L1 cell receptors (i.e., integrins) and ECM proteins in the Matrigel. Liu et al., (2005) differentiated 3T3-L1 cells on Matrigel and reported that the α6 integrin interacts with Laminin in Matrigel and results in the clustering of growth-arrested preadipocytes[84]. Furthermore, inhibition of α6 integrin blocked the formation of 3T3-L1 cell clusters on Matrigel and hindered the ability of 3T3-L1 cells to adopt a round shape[84]. Rather 3T3-L1 displayed fibroblastic morphology and enhanced RhoA activity, which promoted re-entry of 3T3-L1 cells in to the cell cycle. RhoA activity is down regulated during differentiation, allowing fibroblastic cells to become round and differentiate into adipocytes[81]. Therefore, 3T3-L1 cell clustering on Matrigel is facilitated by the interaction of α6 integrin with Laminin in Matrigel, which results in growth arrest and terminal differentiation[84].

In addition, results from our study show that 3T3-L1 cells cultured at a lower cell density represent clustering similar to formation of a spheroid. Since, Figure 5 represents 3T3-L1 cells cultured at a very high density (density at which 3T3-L1 cells are confluent in cell culture), the aggregation may represent contact inhibited growth. Therefore, clustering of 3T3-L1 cells on Matrigel demonstrates interaction of α6 integrin with Laminin in Matrigel, resulting in growth arrest and down regulation of RhoA activity, which is essential for terminal differentiation of adipocytes.

Matrigel Significantly Enhances Lipid Accumulation in 3T3-L1 Cells

Preadipocytes *in vivo* differentiate into large and unilocular lipid-containing adipocytes[35]. Adipocytes require extracellular support in order to expand and differentiate to their full potential *in vitro*[21]. In this study, Matrigel enhanced lipid accumulation in 3T3-L1 cells over 21 days of differentiation. While, 3T3-L1 cells cultured on both thicknesses of Matrigel

demonstrated increased lipid accumulation per cell at days 7, 14, and 21, only the thick layer of Matrigel significantly enhanced lipid accumulation in 3T3-L1 cells relative to control at day 4. The difference in lipid accumulation between 3T3-L1 cells cultured on the thick layer of Matrigel compared to the thin layer of Matrigel may be attributed to the response of cells to the stiffness of the substrate. Cells sense resistance or stiffness in their extracellular environment and respond by making changes in their cytoskeleton[131]. The changes in cytoskeleton are upstream to changes in cell proliferation, differentiation and function[131]. There is evidence that changes in thickness of a gel results in changes in its stiffness[132], which may be the reason underlying changes in lipid accumulation in 3T3-L1 cells cultured on the thick layer of Matrigel relative to thin layer. This topic is discussed in detail below, following the discussion of changes in relative mRNA levels of differentiation markers.

Overall, these results are consistent with other studies that have reported enhanced lipid accumulation in adipocytes differentiated on Matrigel[24,95]. However, these studies do not explore the mechanisms underpinning the observed increase in lipid accumulation in 3T3-L1 cells cultured on Matrigel.

Matrigel Decreases the Expression of an Anti-Adipogenic Marker PREF-1 in 3T3-L1 Cells

In 3T3-L1 cells, a tightly regulated sequential activation of transcription factors initiates and carries out differentiation, resulting in lipid accumulation and formation of the mature adipocyte[35,43,133]. In this study we observed that enhanced lipid accumulation was accompanied by increase in gene expression of adipogenic and lipogenic markers during differentiation. Furthermore, we observed a decrease in an anti-adipogenic marker PREF-1[100] in 3T3-L1 cells cultured on Matrigel, relative to control.

Preadipocyte factor 1 (PREF-1) is a known inhibitor of adipocyte differentiation[100]. PREF-1 is suggested to interact with Fibronectin through the α5β1 integrin; an integrin that binds fibronectin[134]. Furthermore, both PREF-1 and Fibronectin gene expression is high in preadipocytes and is down regulated during differentiation[25,53,100]. In this study, 3T3-L1 cells under all conditions experienced down regulation of PREF-1 and Fibronectin expression post differentiation. At day 0, Matrigel significantly reduced the expression of PREF-1 and Fibronectin in 3T3-L1 cells, relative to control. PREF-1-fibronectin-integrin interaction activates the ERK/MAPK pathway to inhibit adipocyte differentiation[53]. It is possible that down regulation of Fibronectin expression in 3T3-L1 cells on Matrigel leading to a lower secretion of Fibronectin, and resulting in reduced interactions of Fibronectin to α5β1 integrin on 3T3-L1 cells, and manifesting in lower PREF-1 expression.

Overexpression of PREF-1 in adipose tissue results in decreased adipose tissue mass, and reduced expression of adipocyte markers, including C/EBPα and FAS[100]. Decreased expression of PREF-1 in 3T3-L1 cells on Matrigel, relative to cells on plastic may explain the slight but significant increase found in lipid accumulation in 3T3-L1 cells on Matrigel. A dramatic increase in PREF-1 expression was found in 3T3-L1 cells cultured in all conditions at day 21. Pref-1 expression is reduced following differentiation[54], however no study has observed its expression following long term of adipocyte differentiation. PREF-1 is inhibited by DEX[54], so it is possible that following 21 days induction the inhibitory effect on PREF-1 is decreased. While, the adipocyte differentiation is complete at day 21, resulting in mature adipocytes (Figure 6a), and increased PREF-1 expression does not impact adipocyte maturity. Furthermore, PREF-1 inhibits adipogenesis through activation of the MAPK pathway[134], however upon induction of differentiation with DEX,

IBMX and Insulin, MAPK pathway is down regulated and activation of MEK1 induces the expression of within 48 hours of differentiation[135]. Once the activation of such transcription factors PPARγ and C/EBPa occurs, the preadipocytes undergo successful differentiation[135]. Therefore, increased expression of PREF-1 at a late stage of adipogenesis does not impact adipocyte maturity.

Matrigel Enhances Gene Expression of Differentiation Markers in 3T3-L1 Cells

Differentiation markers, such as peroxisome proliferator-activated receptor γ (PPARγ), CCAAT/enhancer-binding protein alpha (C/EBPα), and sterol regulatory element binding protein-1c (SREBP1c), are significantly upregulated post differentiation and ensure the development of the adipocyte phenotype[35,57,58,61]. As expected, 3T3-L1 cells cultured under all conditions showed an increase in expression of these transcription factors following differentiation. However, there are differences found within treatment conditions at different time points. Matrigel enhanced PPARγ expression at days 0, day 4 and day 14 in 3T3-L1 cells, relative to control. As PPARγ is considered the master regulator of adipogenesis[136], its increased levels in 3T3-L1 cells on Matrigel over short term and long term indicate that Matrigel provides a favourable environment for adipocyte differentiation. Furthermore, increased PPARγ expression is also associated with increased lipid accumulation[137,138]. At day 4, only the thick layer of layer enhances PPARγ expression in 3T3-L1 cells, which mimics the increase in lipid accumulation in 3T3-L1 cells on the thick Matrigel, relative to control.

Similarly, C/EBPα expression was enhanced in 3T3-L1 cells cultured on Matrigel at day 0. However, contrary to PPARγ expression at day 4, expression of C/EBPα was significantly higher in 3T3-L1 cells cultured on both thicknesses of Matrigel, which suggests that expression of

differentiation factors is not consistently up regulated for all growth conditions. 3T3-L1 cells cultured on the thick layer of Matrigel demonstrate a significant increase in SREBP1c expression at day 0, consistent with PPARγ and C/EBPα. This, in combination with reduced expression of PREF-1 in 3T3-L1 cells on Matrigel at day 0, indicates that 3T3-L1 cells on Matrigel are more adipogenic relative to cells on plastic, even prior to induction. At day 4 and day 14, Matrigel enhanced SREBP1c expression in 3T3-L1 cells, which further supports that Matrigel enhances differentiation of 3T3-L1 cells leading to the development of a more differentiated phenotype.

Expression of differentiation markers is up regulated at the intermediate stage of adipogenesis (48 hours post induction), and they ensure the activation and expression of genes involved in adipocyte development[38]. Furthermore, regulation of genes, including early and intermediate differentiation markers, takes place at the transcription level[38]. Terminal differentiation is characterized by expression of late and very late markers, which Include enzymes involved in lipogenesis[38]. Terminal differentiation of adipocytes is accompanied by mature lipid-filled adipocytes. In our study, adipocytes demonstrated a lipid-filled phenotype at day 14, which is why it was selected to represent the terminally differentiated state. Furthermore, day 21 was chosen to represent the very late stage of differentiation, primarily to monitor the mRNA levels of adipocyte hormones, such as leptin and adiponectin. Expression of early and intermediate markers of adipocyte differentiation decreases soon after terminal differentiation, and increased expression of lipid synthesizing enzymes and triglyceride accumulation proteins ensures the development of the mature adipocyte phenotype[38].

The mRNA levels of PPARγ and SREBP1c are not significantly different between the three growth conditions at day 21. In contrast, the levels of C/EBPα expression are reduced at day 21.

Since day 21 represents a later stage of terminal differentiation, down regulation of transcription factors is expected. Overall, one key finding is that the thick layer of Matrigel enhanced the expression of all three markers in 3T3-L1 cells at day 4 and day 14, relative to their respective controls. This indicates that the thick Matrigel increases differentiation in 3T3-L1 cells during short-term, whereas both thicknesses of Matrigel enhance differentiation and lipid accumulation in 3T3-L1 cells over long-term.

Matrigel Enhances Gene Expression of an Early Adipocyte Marker FABP4

Fatty acid binding protein 4 (FABP4), commonly known as adipocyte protein 2 (aP2), is extensively used as a marker for differentiated adipocytes[38,45,51]. The mRNA levels of FABP4 dramatically increase in 3T3-L1 cells under all conditions post differentiation (day 4, 14 and 21), relative to the undifferentiated 3T3-L1 cells. FABP4 is known as a key target gene of PPARγ and C/EBPα[108,109]. Significant increase in FABP4 expression, at days 0 and 4, in 3T3-L1 on a thick layer of Matrigel is consistent with increases in the levels of PPARγ and C/EBPα in the same conditions. Limitation of using the FABP4 marker to assess adipocytes differentiation includes reports of FABP4 expression found in adipocyte precursors *in vivo*[139]. Furthermore, it is suggested that the early appearance of FABP4 reflects increased transcription of FABP4 at an earlier point by adipocytes, and not necessarily reflect adipocyte maturity[140].

3T3-L1 Cells on Matrigel Express High mRNA Levels of Perilipin

Perilipin (PLIN) expression is a lipid droplet coating protein, which regulates lipid metabolism in adipocytes by blocking the lipolysis recruitment site to the lipid droplet for lipases[141]. Therefore investigation of PLIN1 expression in differentiating adipocytes provides insight to lipid accumulation, adipocyte maturity and lipid droplet size. In this study, day 4 was

one of the earliest time points when lipid droplets were visible in adipocytes, relative to undifferentiated cells. As expected, 3T3-L1 cells cultured under all conditions demonstrate a dramatic increase in PLIN1 expression, following differentiation. Perilipin, or PLIN1, belongs to a family of lipid-droplet associated proteins that are expressed during adipocyte differentiation and localize on lipid droplets[142]. Inhibition of PLIN1 expression is associated with reduction of fat mass in mice by ~70%[143]. Increase of PLIN1 expression at day 0 and day 4 in 3T3-L1 cells cultured on the thick Matrigel, is consistent with increased expression of adipogenic markers at day 0 and increased lipid accumulation at day 4 in 3T3-L1 cells on the thick Matrigel. However, the lack of difference in PLIN1 expression at day 14 and day 21 suggests that expression of other lipid droplet associated proteins, such as adipose differentiation-related protein (ADRP), may be more representative of lipid droplet size over long term rather than PLIN1 alone. ADRP is also localized to lipid droplets and its mRNA is expressed during adipocyte differentiation, indicating the potential for its use in gene expression studies to investigate lipid droplet size[144].

Matrigel Upregulates Gene Expression of Lipogenic Enzymes in 3T3-L1 Cells

Increased expression of SREBP1c is associated with upregulation of lipogenic enzyme gene expression, including FAS and LPL[145]. Gene expression of lipogenic enzymes marks the terminal phase of differentiation[45,57]. In this study, day 14 was selected to represent the terminal differentiation state of 3T3-L1 cells due to the appearance of lipid-filled adipocytes. Fatty acid synthase (FAS) is a key enzyme involved in de novo lipogenesis[111]. 3T3-L1 cells under all conditions demonstrated upregulation of FAS over the 21 days of differentiation. However, only cells cultured on thick Matrigel displayed increased expression of FAS at day 14, relative to those on the thin Matrigel and control (Figure 13). Upregulation of FAS expression is associated with

increased rate of triglyceride accumulation[146]. Therefore, increased FAS expression at day 14 supports the evidence indicating that the thick layer of Matrigel induces increases lipogenesis.

Lipoprotein Lipase (LPL) mediates hydrolysis of circulating lipoprotein particles and allows their uptake into adipocytes[62]. As expected, expression of LPL increases about 4 to 6 fold in 3T3-L1 cells under all conditions at day 4 and day 14, and dramatically increase at day 21, relative to day 0[147]. At day 14, the thick layer of Matrigel induces increased LPL expression in 3T3-L1 cells, relative to 3T3-L1 cells on the thin Matrigel and control (Figure 14). Gonzales and Orlando (2007) demonstrated that expression of LPL in 3T3-L1 adipocytes directly correlated with lipid storage. Furthermore, they found reduced expression of LPL in adipocytes resulted in decreased LPL mRNA levels, decrease in LPL enzymatic activity by ~50%, and reduction in lipid storage by ~80%[147]. Therefore, increased LPL and FAS expression in 3T3-L1 cells on the thick layer of Matrigel at day 14 (terminally differentiated adipocytes), relative to control and 3T3-L1 cells on thin Matrigel, indicates that the thick Matrigel increases the rate of triglyceride synthesis and enhances lipid accumulation through upregulation of FAS and LPL.

Matrigel Alters mRNA Levels of Endocrine Markers Leptin & Adiponectin

The WAT is considered to be a key endocrine organ in the human body[39]. Its dynamic ability of secretion of biologically active compounds, hormones and signaling molecules plays huge role in maintaining metabolic homeostasis[39]. Leptin is a key endocrine molecule that is secreted by adipocytes to maintain satiety and regulate body weight[63]. Leptin expression is observed to be upregulated in 3T3-L1 cells under all conditions at day 14 and day 21, relative to day 0 and day 4 (Figure 15). At day 14, leptin expression is significantly enhanced in 3T3-L1 cells on the thick layer of Matrigel, relative to control. A study by Skurk et al. (2007) reported that

mRNA expression and secretion of adipokines, including leptin, adiponectin IL-6, IL-8 and MCP-1, positively correlated with adipocyte cell size[75]. Therefore, increased lipid mRNA levels, consistent with high FAS and LPL expression, in 3T3-L1 cells on the thick layer of Matrigel indicate increased adipocyte size, rate of triglyceride synthesis and lipid accumulation.

The mRNA levels of Adiponectin sharply increased following induction of adipogenesis (Figure 16), which is expected as the expression of Adiponectin is dependent on adipocyte differentiation[148]. Adiponectin is a key adipokine secreted by adipocytes and has anti-diabetic and anti-atherogenic effects[75,148]. At day 14, Matrigel significantly down regulated Adiponectin expression in 3T3-L1 cells (Figure 16). Excess accumulation of triglycerides results in increased adipocyte size, which is positively correlated with increased cytokine secretion as well as risk of T2D[75,149]. Adiponectin is an insulin sensitizing, anti-inflammatory adipokine that is secreted in low levels during Obesity[150]. Meyer et al (2013) reported that increase in adipocyte size is associated with decreased expression and secretion of Adiponectin[151]. A limitation to studying Adiponectin is that, while mRNA levels of Adiponectin dramatically increase post differentiation, protein and secretion of Adiponectin is only observed in mature adipocytes[148].

Changes Within the Thick and Thin Matrigel: Cells Sense ECM Stiffness

Cells attach to their neighboring cells and surrounding ECM, and most cells require adhesion for survival[152]. Cells react to their extracellular environment through integrins, which are cell surface receptors that bind ECM ligands and activate intracellular signaling mediators, such as focal adhesion kinases (FAKs), mitogen-activated protein kinases (MAPKs), and Rho-family GTPases[94]. This leads to changes in cell shape, gene expression and function[94]. As cells adhere to their surrounding ECM through integrins, they sense resistance and respond through

changes in their cytoskeleton[131]. A stiff matrix provides more resistance than a soft matrix; and resistance, also known as stiffness, is defined as Young's elastic modulus, E (Pa; newtons/m^2) [131]. Whereas stiffness of living tissue varies from 300Pa to 20kPa, with stiffness of adipose tissue reported as 5kPa, stiffness of tissue culture plastic is in the gigapascal range[153].

In this study, changes in proliferation, differentiation and lipid accumulation seen in 3T3-L1 cells cultured on plastic, thin and thick layer of Matrigel may be attributed to changes in stiffness of the substrate. Leong et al., (2010) reported that a thin Collagen gel (130µm) had a higher elastic modulus (E) than a thick gel (1440µm), indicating that increasing substrate thickness is negatively correlated with stiffness[132]. Based on these findings, in this study, 3T3-L1 cells cultured on the thick Matrigel may have experienced decreased stiffness, relative to the thin Matrigel. This is a possible mechanism underlying the increased lipid accumulation and expression of differentiation markers observed in 3T3-L1 cells on the thick Matrigel, relative to the thin Matrigel and plastic. Cells cultured in an ECM that is closer to stiffness of their natural environment display a higher differentiated phenotype[154]. Future steps involve measuring the stiffness of all gels used in the study and studying stiffness dependent changes in integrin localization, expression and interaction with ECM proteins in 3T3-L1 cells.

Matrigel Significantly Downregulates mRNA Levels of ECM Proteins in 3T3-L1 Cells

Cells cultured *in vitro* are removed from highly complex tissues, surrounded by various molecules and ECM proteins, and are placed into tissue culture plastic[155]. It is natural that these cells begin to rebuild their *in vivo* environment by secreting their own ECM. 3T3-L1 cells are known to secrete various ECM proteins at different stages of differentiation[89]. It is suggested that expression levels of ECM proteins may be higher in cells cultured on plastic, as these cells may

be putting in greater efforts to create their ECM. Streuli and Bissel (1990), demonstrated that mammary epithelial cells expressed lower mRNA and protein levels of ECM markers (laminin, type 4 collagen and fibronectin) when cultured on type 1 collagen gels, compared to cells cultured on plastic[156]. Thus, we hypothesized that 3T3-L1 cells cultured on Matrigel will display decreased mRNA levels of ECM markers.

Fibronectin is expressed and secreted by preadipocytes and a strong decrease in Fibronectin synthesis and secretion is found during adipocyte differentiation[113]. As expected, the mRNA levels of Fibronectin significantly decreased in 3T3-L1 cells under all conditions following differentiation (day 4). Within the three conditions, Matrigel significantly down regulated Fibronectin expression in undifferentiated as well as in differentiated 3T3-L1 cells. Fibronectin promotes cell to-cell adhesion, cell-to-basement membrane attachment, and fibroblast migration[157]. Fibronectin interacts with the cell surface receptor (i.e., integrin α5), which maintains inside-out and outside-in signaling[84]. Whereas, maintaining preadipocytes on Fibronectin-coated dishes inhibits adipocyte differentiation, preventing Fibronectin matrix assembly enhances adipogenesis[158]. In this study, decreased expression of Fibronectin in 3T3-L1 cells on Matrigel is consistent with increased differentiation and lipid accumulation. Furthermore, 3T3-L1 cells cultured on Matrigel displayed decreased proliferation, relative to 3T3-L1 cells on plastic. Increased Fibronectin expression is associated with higher cell spreading, higher proliferation, and reduced adipocyte differentiation through interaction with the α5β1 integrin, which activates Rho GTPases and the MAPK pathway to inhibit differentiation[81,113,84,134]. Thus, 3T3-L1 cells cultured on Matrigel coated plates expressed lower mRNA levels of

Fibronectin, which resulted in lower proliferation and higher differentiation than 3T3-L1 cells cultured on plastic.

Collagen 1 and Collagen 3 are key ECM proteins secreted by preadipocytes as well as adipocytes during early differentiation[155]. As expected mRNA levels of collagen 1 and collagen 3 reduced in 3T3-L1 cells under all conditions after 4 days of differentiation. Furthermore, Matrigel reduced mRNA levels of collagen 1 and collagen 3, similar to fibronectin. Collagen 4 and Laminin are key proteins of the adipocyte basement membrane, and are secreted by adipocytes during differentiation[88]. The mRNA levels of collagen 4 increased in 3T3-L1 cells under all conditions following differentiation, as expected. Moreover, at day 4, only the thick layer of Matrigel decreased mRNA levels of Collagen 4 in 3T3-L1 cells. This is consistent with the enhanced lipid accumulation and increased mRNA levels of differentiation markers on the thick Matrigel in 3T3-L1 cells at day 4. Matrigel significantly decreased the expression of collagen 4 in 3T3-L1 cells, relative to control at days 0 and 14. Collagen 4 is a key component of the adipocyte basement membrane; reduction of collagen 4, fibronectin, collagen 1 and collagen 3 in 3T3-L1 cells on Matrigel indicates that culturing cells on a ECM composed of basement membrane proteins decreases the mRNA levels of ECM proteins predominantly present in preadipocytes as well as mature adipocytes.

During adipogenesis, along with the change from fibroblastic morphology to round cell, there is also a switch in the expression of integrins, from fibronectin binding α5β1 integrin to laminin binding α6β1 integrin[84]. The α6β1 integrin is involved in facilitating 3T3-L1 cell clustering through interaction with Laminin in Matrigel[84]. Overall, the mRNA levels of laminin increased following differentiation in 3T3-L1 cells under all conditions. Within conditions, 3T3-L1 cells on

thick Matrigel demonstrated decreased Laminin levels at day 0, 4, and 14, consistent with Collagen 4. The thick Matrigel decreased the expression of both markers of basement membrane proteins (Collagen 4 and Laminin) in 3T3-L1 cells during differentiation and lipid accumulation.

Collagen 6 expression is upregulated in adipocytes and this ECM protein plays a role in surrounding the adipocyte during lipid accumulation[159]. As expected, 3T3-L1 cells in all conditions display increased expression of Collagen 6 following differentiation. At day 0 and day 14, Matrigel decreased Collagen 6 mRNA levels in 3T3-L1 cells. However, at day 4, 3T3-L1 cells cultured on the thick Matrigel only expressed lower levels of Collagen 6 mRNA; a result that is consistent with Collagen 4 and Laminin expression. These results are supportive of the hypothesis that the thick Matrigel accelerates differentiation in 3T3-L1 cells, but overall differentiation is enhanced in 3T3-L1 cells cultured on both thicknesses in long term.

In this study, Matrigel downregulates mRNA levels of ECM proteins present in preadipocytes and early differentiation (fibronectin, collagen 1, collagen 3), along with basement membrane proteins (collagen 4, laminin and collagen 6) in 3T3-L1 cells. Streuli and Bissel (1990), found that mammary epithelial cells cultured on type 1 collagen secreted increased amount of basement membrane proteins, relative to cells on plastic[156]. They suggested that the secreted basement membrane provided a negative feedback to cells, which resulted in decreased mRNA and protein expression of ECM components[156]. Based on these findings, we suggest that decreased mRNA levels of ECM markers may have resulted from increased secretion of basement membrane on Matrigel and subsequent negative feedback; although this was not explored in the current study, it must be confirmed in future experiments. Furthermore, since basement membrane surrounds mature adipocytes and is essential for adipogenesis, it can be speculated

that increased secretion of basement membrane components by 3T3-L1 cells on Matrigel facilitates enhanced differentiation and lipid accumulation.

Finally, Matrix Metalloprotease 2 (MMP2) cleaves collagen 4 during lipid accumulation to assist ECM remodeling[90]. As expected the expression of MMP2 is down regulated at day 4 in 3T3-L1 cells in all conditions, and increased at day 14. The thick layer of Matrigel expresses significantly higher levels of MMP2 at day 0, relative to control. Similarly, at day 4, levels of MMP2 are significantly higher than control. High expression of MMP2 in 3T3-L1 cells on Matrigel at day 0 and day 4 indicates that cells on Matrigel are able to sense their extracellular environment (i.e., collagen 4) and digest their ECM (using MMP2) in order to regulate the structure and composition of their environment.

Matrigel Enhances the Response of 3T3-L1 Cells to Rosiglitazone

Cells cultured in optimized *in vitro* conditions, including three-dimensional (3D) environment and on an ECM or substrate demonstrate successful cell viability, cell migration and enhanced differentiation[160]. Results in our study are consistent with such findings. In addition, limitations of cell culture conditions translate to lower percentage of drugs showing therapeutic efficacy in clinical trials. For example, only 5% of agents having anticancer activity in preclinical development are licensed for human use[161]. In order to explore whether our optimized cell culture model could be used for drug screening purposes, we decided to subject 3T3-L1 cells to various concentration of Rosiglitazone and observe the changes in lipid accumulation at day 7.

Rosiglitazone is an antidiabetic drug that acts as an insulin sensitizer by binding to PPARγ in adipocytes[29]. By doing this it enhances the response of PPARγ to insulin leading to increased lipid accumulation[29]. Rosiglitazone (2.0 µM) is used to differentiate 3T3-L1 cells and its absence

results in lower lipid accumulation[7]. Therefore, Using Rosiglitazone is a simple and effective method for us to investigate the effect of Matrigel on change in lipid accumulation in response to the various concentrations of Rosiglitazone. The various concentrations of rosiglitazone were selected from various studies that use this molecular as a control for lipid accumulation[5–87]. Figure 22 depicts that the 3T3-L1 cells on Matrigel accumulate greater amounts of lipid upon being exposed to 2µM of Rosiglitazone, as compared to cells grown on plastic. This demonstrates that our model exhibits a difference in sensitivity to a drug molecule, relative to control, and underscores the need to more clearly understand the mechanism for how ECM may impact the response of adipocytes.

CHAPTER 6. FUTURE DIRECTIONS

Future steps of this study include complete assessment of the effect of various concentrations of Rosiglitazone on 3T3-L1 cell differentiation, cultured on plastic and Matrigel. This assessment will include investigation of cell response at an intermediate stage of differentiation (day 4), and at the terminal phase of adipogenesis (day 14). Finally, the study will include investigation of changes in mRNA levels of key adipogenic markers, such as PPARγ and C/EBPα, as well as key lipogenic enzymes, including FAS and LPL. Secretion of key endocrine markers, such as Leptin and Adiponectin may provide a higher insight into the change in function upon drug treatment. This study will provide a validation for this model to be used in the future for larger drug studies.

The cell-to-ECM interactions will be explored in 3T3-L1 cells cultured on Matrigel. This will involve investigation of key integrins with their known ligands in the ECM, including α5 integrin and fibronectin interaction; α6 integrin and laminin interaction; and α1 integrin and collagen 4 interaction[23,84]. Since this study provides evidence that Matrigel enhances adipogenesis, we hypothesize that expression of α5 integrin will be downregulated and mRNA levels of α6 integrin and α1 integrin will be upregulated.

Finally, adipocytes in the WAT are surrounded by a rich vasculature. Therefore, to develop this *in vitro* model further, co-culturing with endothelial cells may be the next step in providing an insight into cell-cell interactions within a physiological environment.

CHAPTER 7. CONCLUSION

3T3-L1 cells grown on Matrigel demonstrated significant changes in cell growth, proliferation, differentiation and response to Rosiglitazone. Matrigel facilitated the formation of cellular aggregates of 3T3-L1 cells, which are representative of morphology of tissues *in vivo*[124]. Lower proliferation of 3T3-L1 cells was associated with decreased expression of Fibronectin, and may be a key factor resulting in increased differentiation[25]. During differentiation, while expression of an anti-adipogenic marker PREF-1 was significantly downregulated in 3T3-L1 cells on Matrigel, mRNA levels of key transcription factors and adipogenic markers, PPARγ, C/EBPα and SREBP1c were significantly increased. The thick layer of Matrigel consistently showed increased levels of differentiation, adipogenic and lipogenic markers. Expression of key lipogenic enzymes (FAS, LPL) and endocrine markers (Leptin) associated with the intermediate stage of differentiation were increased in 3T3-L1 cells on thick Matrigel. Increased expression of FAS, LPL and Leptin is associated with increased lipid accumulation and adipocyte size[75,111,147]. Furthermore, down regulation of Adiponectin is associated with increasing adipocyte size[151]; Adiponectin expression was down regulated in 3T3-L1 cells on Matrigel. Finally, expression of key ECM proteins, including Collagen 1, Collagen 3, Collagen 4, Collagen 6 and Laminin was decreased in 3T3-L1 cells on Matrigel.

Altogether, higher Leptin and decreased Adiponectin expression suggest that Matrigel increased 3T3-L1 adipocyte size, which is consistent with enhanced lipid accumulation per cell on Matrigel. Decreased Fibronectin expression is associated with lower cell spreading and increased cell rounding, which could have been a key mediator resulting in increased 3T3-L1 cell size on Matrigel. Altogether the results suggest that, 3T3-

L1 cells cultured on Matrigel coated plates expressed lower levels of Fibronectin, which resulted in increased cell rounding. This is accompanied by higher α6 integrin interaction with Laminin on Matrigel[84], resulting in cell aggregates that are known to enhance differentiation, as cellular organization within clusters is more physiological. Furthermore, Matrigel enhanced the expression of intermediate differentiation markers and increased mRNA levels of lipogenic enzymes through downregulation of ECM gene expression. This is proposed as a result of cells devoting more resources towards differentiation, rather than ECM development. Finally, this study provided us with a model to study the response of Rosiglitazone in 3T3-L1 cells in a physiological environment. Our model exhibited a difference in sensitivity to lipid accumulation when cells were cultured on Matrigel. Understanding the mechanisms underpinning such phenomenon more thoroughly will facilitate the adoption of 3D-culture models into the drug discovery process.

CHAPTER 8. REFERENCES

1. World Health Organization. WHO | Obesity and overweight. *Fact sheet N°311* (2015). Available at: http://www.who.int/mediacentre/factsheets/fs311/en/#.
2. Khaodhiar, L., McCowen, K. C. & Blackburn, G. L. Obesity and its comorbid conditions. *Clin. Cornerstone* **2,** 17–28 (1999).
3. Navaneelan, T. & Janz, T. Adjusting the scales: Obesity in the Canadian population after correcting for respondent bias. *Stat. Canada Cat. no. 82-624-X* **53,** 1929–1930 (2014).
4. Tran, B. X., Nair, A. V., Kuhle, S., Ohinmaa, A. & Veugelers, P. J. Cost analyses of obesity in Canada: Scope, quality, and implications. *Cost Effectiveness and Resource Allocation* **11,** (2013).
5. WHO. WHO | Obesity and overweight. *Who* (2017).
6. Dobbs, R. *et al. Overcoming obesity : An initial economic analysis*. *McKinsey Global Institute* (2014).
7. Kelly, T., Yang, W., Chen, C. S., Reynolds, K. & He, J. Global burden of obesity in 2005 and projections to 2030. *Int. J. Obes.* **32,** 1431–1437 (2008).
8. Pellegrinelli, V., Carobbio, S. & Vidal-Puig, A. Adipose tissue plasticity: how fat depots respond differently to pathophysiological cues. *Diabetologia* **59,** 1075–1088 (2016).
9. Kershaw, E. E. & Flier, J. S. Adipose tissue as an endocrine organ. *J. Clin. Endocrinol. Metab.* **89,** 2548–56 (2004).
10. Vázquez-Vela, M. E. F., Torres, N. & Tovar, A. R. White Adipose Tissue as Endocrine Organ and Its Role in Obesity. *Archives of Medical Research* **39,** 715–728 (2008).
11. Must, A. *et al.* The Disease Burden Associated With Overweight and Obesity. *JAMA* **282,**

1523–1529 (1999).

12. Divoux, A. & Clément, K. Architecture and the extracellular matrix: The still unappreciated components of the adipose tissue. *Obes. Rev.* **12,** (2011).
13. Frantz, C., Stewart, K. M. & Weaver, V. M. The extracellular matrix at a glance. *J. Cell Sci.* **123,** 4195–4200 (2010).
14. Järveläinen, H. Extracellular matrix molecules: potential targets in pharmacotherapy. *Pharmacol Rev.* **61,** 198–223 (2009).
15. Ben Amor, I. M., Glorieux, F. H. & Rauch, F. Genotype-Phenotype Correlations in Autosomal Dominant Osteogenesis Imperfecta. *J. Osteoporos.* **2011,** 1–9 (2011).
16. Lin, D., Chun, T. H. & Kang, L. Adipose extracellular matrix remodelling in obesity and insulin resistance. *Biochemical Pharmacology* **119,** 8–16 (2016).
17. Boden, G. Obesity, insulin resistance and free fatty acids. *Curr Opin Endocrinol Diabetes Obes.* **18,** 139–143 (2011).
18. Buechler, C., Krautbauer, S. & Eisinger, K. Adipose tissue fibrosis. *World J. Diabetes* **6,** 548–53 (2015).
19. Christiaens, V. & Lijnen, H. R. Angiogenesis and development of adipose tissue. *Molecular and Cellular Endocrinology* **318,** 2–9 (2010).
20. Mariman, E. C. M. & Wang, P. Adipocyte extracellular matrix composition, dynamics and role in obesity. *Cell. Mol. Life Sci.* **67,** 1277–1292 (2010).
21. Kokai, L. E., Marra, K. G. & Kershaw, E. E. Three-dimensional adipocyte culture: The next frontier for adipocyte biology discovery. *Endocrinology* **156,** 4375–4376 (2015).
22. Nakajima, I., Yamaguchi, T., Ozutsumi, K. & Aso, H. Adipose tissue extracellular matrix:

Newly organized by adipocytes during differentiation. *Differentiation* **63,** 193–200 (1998).

23. Rosso, F., Giordano, A., Barbarisi, M. & Barbarisi, A. From Cell-ECM Interactions to Tissue Engineering. *Journal of Cellular Physiology* **199,** 174–180 (2004).
24. O'Connor, K. C., Song, H., Rosenzweig, N. & Jansen, D. A. Extracellular matrix substrata alter adipocyte yield and lipogenesis in primary cultures of stromal-vascular cells from human adipose. *Biotechnol. Lett.* **25,** 1967–1972 (2003).
25. Spiegelman, B. M. & Ginty, C. A. Fibronectin modulation of cell shape and lipogenic gene expression in 3t3-adipocytes. *Cell* **35,** 657–666 (1983).
26. Shoemaker, R. H. The NCI60 human tumour cell line anticancer drug screen. *Nat. Rev.* **6,** 813–823 (2006).
27. Dhiman, H. K., Ray, A. R. & Panda, A. K. Three-dimensional chitosan scaffold-based MCF-7 cell culture for the determination of the cytotoxicity of tamoxifen. *Biomaterials* **26,** 979–986 (2005).
28. Hughes, C. S., Postovit, L. M. & Lajoie, G. A. Matrigel: a complex protein mixture required for optimal growth of cell culture. *Proteomics* **10,** 1886–1890 (2010).
29. Wolffenbuttel, B. H., Sels, J. P. & Huijberts, M. S. Rosiglitazone. *Expert Opin Pharmacother* **2,** 467–478 (2001).
30. Chusyd, D. E., Wang, D., Huffman, D. M. & Nagy, T. R. Relationships between Rodent White Adipose Fat Pads and Human White Adipose Fat Depots. *Front. Nutr.* **3,** (2016).
31. Kwok, K. H. M., Lam, K. S. L. & Xu, A. Heterogeneity of white adipose tissue: molecular basis and clinical implications. *Exp. Mol. Med.* **48,** e215 (2016).
32. Sbarbati, A. *et al.* Subcutaneous adipose tissue classification. *Eur. J. Histochem.* **54,** e48

(2010).

33. Mann, A., Thompson, A., Robbins, N. & Blomkalns, A. L. Localization, Identification, and Excision of Murine Adipose Depots. *J. Vis. Exp.* (2014). doi:10.3791/52174

34. Wronska, A. & Kmiec, Z. Structural and biochemical characteristics of various white adipose tissue depots. *Acta Physiologica* **205,** 194–208 (2012).

35. Ali, A. T., Hochfeld, W. E., Myburgh, R. & Pepper, M. S. Adipocyte and adipogenesis. *European Journal of Cell Biology* **92,** 229–236 (2013).

36. Guo, Y., Cordes, K. R., Farese, R. V. & Walther, T. C. Lipid droplets at a glance. *J. Cell Sci.* **122,** 749–752 (2009).

37. Khan, T. *et al.* Metabolic dysregulation and adipose tissue fibrosis: role of collagen VI. *Mol. Cell. Biol.* **29,** 1575–1591 (2009).

38. Ailhaud, G., Grimaldi, P. & Négrel, R. Cellular and molecular aspects of adipose tissue development. *Annu. Rev. Nutr.* **12,** 207–33 (1992).

39. Musi, N. & Guardado-Mendoza, R. in *Cellular Endocrinology in Health and Disease* 229–237 (2014). doi:10.1016/B978-0-12-408134-5.00014-7

40. Miettinen, S., Sarkanen, J. R. & Ashammakhi, N. Adipose Tissue and Adipocyte Differentiation: Molecular and Cellular Aspects and Tissue Engineering Applications. *Top. Tissue Eng.* **4,** 1–26 (2008).

41. Gu, P. & Xu, A. Interplay between adipose tissue and blood vessels in obesity and vascular dysfunction. *Rev. Endocr. Metab. Disord.* **14,** 49–58 (2013).

42. Poissonnet, C. M., Burdi, A. R. & Bookstein, F. L. Growth and development of human adipose tissue during early gestation. *Early Hum. Dev.* **8,** 1–11 (1983).

43. Ntambi, J. M. & Kim, Y.-C. Adipocyte differentiation and gene expression. *J. Nutr.* **130,** 3122–3126 (Supp) (2000).

44. Young, D. A., Choi, Y. S., Engler, A. J. & Christman, K. L. Stimulation of adipogenesis of adult adipose-derived stem cells using substrates that mimic the stiffness of adipose tissue. *Biomaterials* **34,** 8581–8588 (2013).

45. Gregoire, F. M. *et al.* Understanding adipocyte differentiation. *Physiol. Rev.* **78,** 783–809 (1998).

46. Ruiz-Ojeda, F. J. *et al.* Cell models and their application for studying adipogenic differentiation in relation to obesity: A review. *Int. J. Mol. Sci.* **17,** 1040 (2016).

47. Poulos, S. P., Dodson, M. V & Hausman, G. J. Cell line models for differentiation: preadipocytes and adipocytes. *Exp. Biol. Med. (Maywood, NJ)* **235,** 1185–1193 (2010).

48. Green, H. & Meuth, M. An established pre-adipose cell line and it's differentation in culture. *Cell* **3,** 127–133 (1974).

49. Green, H. & Kehinde, O. Spontaneous heritable changes leading to increased adipose conversion in 3T3 cells. *Cell* **7,** 105–113 (1976).

50. Zebisch, K., Voigt, V., Wabitsch, M. & Brandsch, M. Protocol for effective differentiation of 3T3-L1 cells to adipocytes. *Anal. Biochem.* **425,** 88–90 (2012).

51. Moseti, D., Regassa, A. & Kim, W. K. Molecular regulation of adipogenesis and potential anti-adipogenic bioactive molecules. *International Journal of Molecular Sciences* **17,** (2016).

52. Gregoire, F. M., Smas, C. M. & Sul, H. S. Understanding adipocyte differentiation. *Physiol. Rev.* **78,** 783–809 (1998).

53. Hudak, C. S. & Sul, H. S. Pref-1, a gatekeeper of adipogenesis. *Frontiers in Endocrinology* **4,** (2013).

54. Kim, K.-A., Kim, J.-H., Wang, Y. & Sul, H. S. Pref-1 (Preadipocyte Factor 1) Activates the MEK/Extracellular Signal-Regulated Kinase Pathway To Inhibit Adipocyte Differentiation. *Mol. Cell. Biol.* **27,** 2294–2308 (2007).

55. Sul, H. S. Minireview: Pref-1: Role in Adipogenesis and Mesenchymal Cell Fate. *Mol. Endocrinol.* **23,** 1717–1725 (2009).

56. Cornelius, P., MacDougald, O. a & Lane, M. D. Regulation of adipocyte development. *Annu. Rev. Nutr.* **14,** 99–129 (1994).

57. Guo, L., Li, X. & Tang, Q. Q. Transcriptional regulation of adipocyte differentiation: A central role for CCAAT/ enhancer-binding protein (C/EBP) β. *Journal of Biological Chemistry* **290,** 755–761 (2015).

58. Ahmadian, M. *et al.* PPARgamma signaling and metabolism: the good, the bad and the future. *Nat Med* **19,** 557–566 (2013).

59. Otto, T. C. & Lane, M. D. Adipose development: from stem cell to adipocyte. *Crit. Rev. Biochem. Mol. Biol.* **40,** 229–242 (2005).

60. Proença, A. R. G. *et al.* New concepts in white adipose tissue physiology. *Brazilian Journal of Medical and Biological Research* **47,** 192–205 (2014).

61. Stoeckman, A. K. & Towle, H. C. The role of SREBP-1c in nutritional regulation of lipogenic enzyme gene expression. *J. Biol. Chem.* **277,** 27029–27035 (2002).

62. Ranganathan, G. *et al.* The lipogenic enzymes DGAT1, FAS, and LPL in adipose tissue: effects of obesity, insulin resistance, and TZD treatment. *J. Lipid Res.* **47,** 2444–50 (2006).

63. Hynes, G. R. & Jones, P. J. Leptin and its role in lipid metabolism. *Curr. Opin. Lipidol.* **12,** 321–7 (2001).

64. Trayhurn, P. & Beattie, J. H. Physiological role of adipose tissue: white adipose tissue as an endocrine and secretory organ. *Proc. Nutr. Soc.* **60,** 329–339 (2001).

65. Mori, T. *et al.* Role of kr??ppel-like factor 15 (KLF15) in transcriptional regulation of adipogenesis. *J. Biol. Chem.* **280,** 12867–12875 (2005).

66. Solinas, G., Borén, J. & Dulloo, A. G. De novo lipogenesis in metabolic homeostasis: More friend than foe? *Mol Metab* **4,** 367–377 (2015).

67. Gupta, R. K. Adipocytes. *Curr. Biol.* **24,** R988-93 (2014).

68. Robenek, H. *et al.* Compartmentalization of proteins in lipid droplet biogenesis. *Biochimica et Biophysica Acta - Molecular and Cell Biology of Lipids* **1791,** 408–418 (2009).

69. Hellerstein, M. K. De novo lipogenesis in humans: Metabolic and regulatory aspects. *Eur. J. Clin. Nutr.* **53,** s53–s65 (1999).

70. Lass, A., Zimmermann, R., Oberer, M. & Zechner, R. Lipolysis - A highly regulated multi-enzyme complex mediates the catabolism of cellular fat stores. *Prog. Lipid Res.* **50,** 14–27 (2011).

71. Grahn, T. H. M. *et al.* Fat-specific protein 27 (FSP27) interacts with adipose triglyceride lipase (ATGL) to regulate lipolysis and insulin sensitivity in human adipocytes. *J. Biol. Chem.* **289,** 12029–12039 (2014).

72. Takahashi, Y. *et al.* Perilipin-Mediated Lipid Droplet Formation in Adipocytes Promotes Sterol Regulatory Element-Binding Protein-1 Processing and Triacylglyceride Accumulation. *PLoS One* (2013). doi:10.1371/journal.pone.0064605

73. Hickenbottom, S. J., Kimmel, A. R., Londos, C. & Hurley, J. H. Structure of a lipid droplet protein: The PAT family member TIP47. *Structure* **12,** 1199–1207 (2004).

74. Zhang, Y. *et al.* Positional cloning of the mouse obese gene and its human homologue. *Nature* **372,** 425–432 (1994).

75. Skurk, T., Alberti-Huber, C., Herder, C. & Hauner, H. Relationship between Adipocyte Size and Adipokine Expression and Secretion. *J. Clin. Endocrinol. Metab.* **92,** 1023–1033 (2007).

76. Manteiga, S., Choi, K., Jayaraman, A. & Lee, K. Systems biology of adipose tissue metabolism: Regulation of growth, signaling and inflammation. *Wiley Interdisciplinary Reviews: Systems Biology and Medicine* **5,** (2013).

77. Cinti, S. *et al.* Adipocyte death defines macrophage localization and function in adipose tissue of obese mice and humans. *J. Lipid Res.* **46,** 2347–2355 (2005).

78. Hotamisligil, G. S. Inflammation and metabolic disorders. *Nature* **444,** 860–7 (2006).

79. Xie, Q. *et al.* Hypoxia enhances angiogenesis in an adipose-derived stromal cell/endothelial cell co-culture 3D gel model. *Cell Prolif.* **49,** 236–245 (2016).

80. Weisberg, S. P. *et al.* Obesity is associated with macrophage accumulation in adipose tissue. *J. Clin. Invest.* **112,** 1796–1808 (2003).

81. McBeath, R., Pirone, D. M., Nelson, C. M., Bhadriraju, K. & Chen, C. S. Cell shape, cytoskeletal tension, and RhoA regulate stem cell lineage commitment. *Dev. Cell* **6,** 483–495 (2004).

82. Gumbiner, B. M. Cell adhesion: The molecular basis of tissue architecture and morphogenesis. *Cell* **84,** 345–357 (1996).

83. Spiegelman, B. M. & Farmer, S. R. Decreases in tubulin and actin gene expression prior to

morphological differentiation of 3T3 Adipocytes. *Cell* **29,** 53–60 (1982).

84. Liu, J. *et al.* Changes in integrin expression during adipocyte differentiation. *Cell Metab.* **2,** 165–177 (2005).

85. Pierleoni, C., Verdenelli, F., Castellucci, M. & Cinti, S. Fibronectins and basal lamina molecules expression in human subcutaneous white adipose tissue. *Eur. J. Histochem.* **42,** 183–8 (1998).

86. LeBleu, V. S., Macdonald, B. & Kalluri, R. Structure and function of basement membranes. *Exp. Biol. Med. (Maywood).* **232,** 1121–9 (2007).

87. Weiner, F. R., Shah, a, Smith, P. J., Rubin, C. S. & Zern, M. a. Regulation of collagen gene expression in 3T3-L1 cells. Effects of adipocyte differentiation and tumor necrosis factor alpha. *Biochemistry* **28,** 4094–4099 (1989).

88. Aratani, Y. & Kitagawa, Y. Enhanced synthesis and secretion of type IV collagen and entactin during adipose conversion of 3T3-L1 cells and production of unorthodox laminin complex. *J. Biol. Chem.* **263,** 16163–16169 (1988).

89. Ojima, K., Oe, M., Nakajima, I., Muroya, S. & Nishimura, T. Dynamics of protein secretion during adipocyte differentiation. *FEBS Open Bio* (2016). doi:10.1002/2211-5463.12091

90. Chavey, C. *et al.* Matrix metalloproteinases are differentially expressed in adipose tissue during obesity and modulate adipocyte differentiation. *J. Biol. Chem.* **278,** 11888–11896 (2003).

91. Chun, T. H. & Inoue, M. 3-D adipocyte differentiation and peri-adipocyte collagen turnover. *Methods Enzymol.* **538,** 15–34 (2014).

92. Cummins, T. D. *et al.* Metabolic remodeling of white adipose tissue in obesity. *Am J Physiol*

Endocrinol Metab **307,** E262–E277 (2014).

93. Chen, S. S., Fitzgerald, W., Zimmerberg, J., Kleinman, H. K. & Margolis, L. Cell-cell and cell-extracellular matrix interactions regulate embryonic stem cell differentiation. *Stem Cells* **25,** 553–61 (2007).

94. Boudreau, N. J. & Jones, P. L. Extracellular matrix and integrin signalling: the shape of things to come. *Biochem. J.* **339 (Pt 3,** 481–488 (1999).

95. Viravaidya, K. & Shuler, M. L. The effect of various substrates on cell attachment and differentiation of 3T3-F442A preadipocytes. *Biotechnol. Bioeng.* **78,** 454–458 (2002).

96. Li, M. L. *et al.* Influence of a reconstituted basement membrane and its components on casein gene expression and secretion in mouse mammary epithelial cells. *Proc Natl Acad Sci U S A* **84,** 136–140 (1987).

97. Bissell, D. M., Arenson, D. M., Maher, J. J. & Roll, F. J. Support of cultured hepatocytes by a laminin-rich gel. Evidence for a functionally significant subendothelial matrix in normal rat liver. *J. Clin. Invest.* **79,** 801–812 (1987).

98. Kubota, Y., Kleinman, H. K., Marin, G. R., and Lawley, T. J., Kubota, Y., Kleinman, H. K., Martin, G. R. & Lawley, T. J. Role of laminin and basement membrane in the morphological differentiation of human endothelial cells into capillary like structures. *J. Cell Biol.* **107,** 1589–1598 (1988).

99. Shannon, J. M., Mason, R. J. & Jennings, S. D. Functional differentiation of alveolar type II epithelial cells in vitro: effects of cell shape, cell-matrix interactions and cell-cell interactions. *Biochim. Biophys. Acta* **931,** 143–56 (1987).

100. Wang, Y., Kim, K.-A., Kim, J.-H. & Sul, H. S. Pref-1, a Preadipocyte Secreted Factor That

Inhibits Adipogenesis. *Jounal Nutr.* **136,** 2953–2956 (2006).

101. Kozera, B. & Rapacz, M. Reference genes in real-time PCR. *Journal of Applied Genetics* **54,** 391–406 (2013).

102. Kriegova, E. *et al.* PSMB2 and RPL32 are suitable denominators to normalize gene expression profiles in bronchoalveolar cells. *BMC Mol. Biol.* **9,** (2008).

103. Ahn, K. *et al.* Selection of internal reference genes for SYBR green qRT-PCR studies of rhesus monkey (Macaca mulatta) tissues. *BMC Mol. Biol.* **9,** (2008).

104. Bruynsteen, L. *et al.* Expression of inflammation-related genes is associated with adipose tissue location in horses. *BMC Vet. Res.* **9,** (2013).

105. Arsenijevic, T., Grégoire, F., Delforge, V., Delporte, C. & Perret, J. Murine 3T3-L1 Adipocyte cell differentiation model: Validated reference genes for qPCR gene expression analysis. *PLoS One* **7,** (2012).

106. Kawada, T., Aoki, N., Kawai, R. & Sugimoto, E. Proliferation of 3T3-L1 preadipocytes in a completely defined serum-free medium. *Cell Biol. Int. Rep.* **14,** 567–574 (1990).

107. Russell, T. R. Growth and Cytodifferentiation of 3T3-L1 Preadipocytes into Adipocytes. *Methods Enzymol.* **72,** 720–723 (1981).

108. Atlas, E. *et al.* Bisphenol A increases aP2 expression in 3T3L1 by enhancing the transcriptional activity of nuclear receptors at the promoter. *Adipocyte* **3,** 170–179 (2014).

109. Thompson, G. M. *et al.* A high-capacity assay for PPARγ ligand regulation of endogenous aP2 expression in 3T3-L1 cells. *Anal. Biochem.* **330,** 21–28 (2004).

110. Pomatto, V. *et al.* Plasticizers used in food-contact materials affect adipogenesis in 3T3-L1 cells. *J. Steroid Biochem. Mol. Biol.* **178,** 322–332 (2018).

111. Berndt, J. *et al.* Fatty acid synthase gene expression in human adipose tissue: Association with obesity and type 2 diabetes. *Diabetologia* **50,** 1472–1480 (2007).

112. Ouchi, N., Parker, J. L., Lugus, J. J. & Walsh, K. Adipokines in inflammation and metabolic disease. *Nat Rev Immunol* **11,** 85–97 (2011).

113. Pierleoni, C., Verdenelli, F., Castellucci, M. & Cinti, S. Fibronectins and basal lamina molecules expression in human subcutaneous white adipose tissue. *Eur. J. Histochem.* **42,** 183–8 (1998).

114. Edmondson, R., Broglie, J. J., Adcock, A. F. & Yang, L. Three-Dimensional Cell Culture Systems and Their Applications in Drug Discovery and Cell-Based Biosensors. *Assay Drug Dev. Technol.* **12,** 207–218 (2014).

115. Watt, F. M. The extracellular matrix and cell shape. *Trends Biochem. Sci.* **11,** 482–485 (1986).

116. Ingber, D. Extracellular matrix and cell shape: potential control points for inhibition of angiogenesis. *J Cell Biochem* **47,** 236–241 (1991).

117. Gospodarowicz, D., Delgado, D., Vlodavsky, I. & Biology, C. Permissive effect of the extracellular matrix on cell proliferation in vitro. *Proc. Natl. Acad. Sci. U. S. A.* **77,** 4094–8 (1980).

118. Underwood, P. A. & Bennett, F. A. The effect of extracellular matrix molecules on the in vitro behavior of bovine endothelial cells. *Exp. Cell Res.* **205,** 311–319 (1993).

119. Gross-Steinmeyer, K. *et al.* Influence of Matrigel-overlay on constitutive and inducible expression of nine genes encoding drug-metabolizing enzymes in primary human hepatocytes. *Xenobiotica* (2008).

120. Fang, Y. & Eglen, R. M. Three-Dimensional Cell Cultures in Drug Discovery and Development. *SLAS Discov.* 2472555217696795 (2017). doi:10.1177/2472555217696795

121. Edmondson, R., Broglie, J. J., Adcock, A. F. & Yang, L. Three-dimensional cell culture systems and their applications in drug discovery and cell-based biosensors. *Assay Drug Dev. Technol.* **12,** 207–218 (2014).

122. Barcellos-Hoff, M. H., Aggeler, J., Ram, T. G. & Bissell, M. J. Functional differentiation and alveolar morphogenesis of primary mammary cultures on reconstituted basement membrane. *Development* **105,** 223–235 (1989).

123. Lin, R. Z. & Chang, H. Y. Recent advances in three-dimensional multicellular spheroid culture for biomedical research. *Biotechnology Journal* **3,** 1172–1184 (2008).

124. Abu-Absi, S. F., Friend, J. R., Hansen, L. K. & Hu, W. S. Structural polarity and functional bile canaliculi in rat hepatocyte spheroids. *Exp. Cell Res.* **274,** 56–67 (2002).

125. Korff, T. & Augustin, H. G. Integration of endothelial cells in multicellular spheroids prevents apoptosis and induces differentiation. - PubMed - NCBI. *J. Cell Biol.* **143,** 1341–1352 (1998).

126. Cinti, S. *et al.* The adipose organ at a glance. *Dis. Model. Mech.* **5,** 588–94 (2012).

127. Klingelhutz, A. J. *et al.* Scaffold-free generation of uniform adipose spheroids for metabolism research and drug discovery. *Sci. Rep.* **8,** (2018).

128. Turner, P. A., Tang, Y., Weiss, S. J. & Janorkar, A. V. Three-dimensional spheroid cell model of in vitro adipocyte inflammation. *Tissue Eng Part A* **21,** 1837–1847 (2015).

129. Ponce, M. L. Tube formation: an in vitro matrigel angiogenesis assay. *Methods Mol. Biol.* **467,** 183–188 (2009).

130. Aaronson, S. A. & Todaro, G. J. Development of 3T3-like lines from Balb/c mouse embryo cultures: Transformation susceptibility to SV40. *J. Cell. Physiol.* **72,** 141–148 (1968).

131. Wells, R. G. The role of matrix stiffness in regulating cell behavior. *Hepatology* **47,** 1394–1400 (2008).

132. Leong, W. S. *et al.* Thickness sensing of hMSCs on collagen gel directs stem cell fate. *Biochem. Biophys. Res. Commun.* **401,** 287–292 (2010).

133. Lefterova, M. I. & Lazar, M. A. New developments in adipogenesis. *Trends in Endocrinology and Metabolism* **20,** 107–114 (2009).

134. Wang, Y., Zhao, L., Smas, C. & Sul, H. S. Pref-1 Interacts with Fibronectin To Inhibit Adipocyte Differentiation. *Mol. Cell. Biol.* **30,** 3480–3492 (2010).

135. Prusty, D., Park, B. H., Davis, K. E. & Farmer, S. R. Activation of MEK/ERK signaling promotes adipogenesis by enhancing peroxisome proliferator-activated receptor γ (PPARγ) and C/EBPα gene expression during the differentiation of 3T3-L1 preadipocytes. *J. Biol. Chem.* **277,** 46226–46232 (2002).

136. Shao, X. *et al.* Peroxisome Proliferator-Activated Receptor-γ: Master Regulator of Adipogenesis and Obesity. *Curr. Stem Cell Res. Ther.* **11,** 282–9 (2016).

137. Schadinger, S. E. PPAR 2 regulates lipogenesis and lipid accumulation in steatotic hepatocytes. *AJP Endocrinol. Metab.* **288,** E1195–E1205 (2005).

138. Matsusue, K. PPAR / potentiates PPAR -stimulated adipocyte differentiation. *FASEB J.* **18,** 1477–1479 (2004).

139. Soukas, A., Socci, N. D., Saatkamp, B. D., Novelli, S. & Friedman, J. M. Distinct Transcriptional Profiles of Adipogenesis in Vivo and in Vitro. *J. Biol. Chem.* **276,** 34167–

34174 (2001).

140. Djian, P., Phillips, M. & Green, H. The activation of specific gene transcription in the adipose conversion of 3T3 cells. *J. Cell. Physiol.* **124,** 554–556 (1985).

141. Hansen, J. S., De Maré, S., Jones, H. A., Göransson, O. & Lindkvist-Petersson, K. Visualization of lipid directed dynamics of perilipin 1 in human primary adipocytes. *Sci. Rep.* **7,** (2017).

142. Brasaemle, D. L. *et al.* Adipose differentiation-related protein is an ubiquitously expressed lipid storage droplet-associated protein. *J. Lipid Res.* **38,** 2249–2263 (1997).

143. Tansey, J. T. *et al.* Perilipin ablation results in a lean mouse with aberrant adipocyte lipolysis, enhanced leptin production, and resistance to diet-induced obesity. *Proc. Natl. Acad. Sci.* **98,** 6494–6499 (2001).

144. Jiang, H. P. & Serrero, G. Isolation and characterization of a full-length cDNA coding for an adipose differentiation-related protein. *Proc. Natl. Acad. Sci. U. S. A.* **89,** 7856–60 (1992).

145. Korczynska, J. *et al.* Upregulation of lipogenic enzymes genes expression in white adipose tissue of rats with chronic renal failure is associated with higher level of sterol regulatory element binding protein-1. *Metabolism.* **53,** 1060–1065 (2004).

146. Szolkiewicz, M. *et al.* Upregulation of fatty acid synthase gene expression in experimental chronic renal failure. *Metabolism.* **51,** 1605–1610 (2002).

147. Gonzales, A. M. & Orlando, R. A. Role of adipocyte-derived lipoprotein lipase in adipocyte hypertrophy. *Nutr. Metab.* **4,** (2007).

148. Körner, A. *et al.* Adiponectin expression in humans is dependent on differentiation of adipocytes and down-regulated by humoral serum components of high molecular weight.

Biochem. Biophys. Res. Commun. **337,** 540–550 (2005).

149. Weyer, C., Foley, J. E., Bogardus, C., Tataranni, P. A. & Pratley, R. E. Enlarged subcutaneous abdominal adipocyte size, but not obesity itself, predicts type II diabetes independent of insulin resistance. *Diabetologia* **43,** 1498–1506 (2000).

150. Li, S., Shin, H. J., Ding, E. L. & van Dam, R. M. Adiponectin levels and risk of type 2 diabetes: a systematic review and meta-analysis. *JAMA* **302,** 179–188 (2009).

151. Meyer, L. K., Ciaraldi, T. P., Henry, R. R., Wittgrove, A. C. & Phillips, S. A. Adipose tissue depot and cell size dependency of adiponectin synthesis and secretion in human obesity. *Adipocyte* **2,** 217–226 (2013).

152. Trappmann, B. & Chen, C. S. How cells sense extracellular matrix stiffness: A material's perspective. *Current Opinion in Biotechnology* **24,** 948–953 (2013).

153. Buxboim, A., Rajagopal, K., Brown, A. E. X. & Discher, D. E. How deeply cells feel: Methods for thin gels. *J. Phys. Condens. Matter* **22,** (2010).

154. Mullen, C. A., Vaughan, T. J., Billiar, K. L. & McNamara, L. M. The effect of substrate stiffness, thickness, and cross-linking density on osteogenic cell behavior. *Biophys. J.* **108,** 1604–1612 (2015).

155. Lareu, R. R. *et al.* Collagen matrix deposition is dramatically enhanced in vitro when crowded with charged macromolecules: The biological relevance of the excluded volume effect. *FEBS Lett.* **581,** 2709–2714 (2007).

156. Streuli, C. H. & Bissell, M. J. Expression of extracellular matrix components is regulated by substratum. *J. Cell Biol.* **110,** 1405–15 (1990).

157. Proctor, R. a. Fibronectin: a brief overview of its structure, function, and physiology. *Rev.*

Infect. Dis. **9 Suppl 4,** S317-21 (1987).

158. Kamiya, S. *et al.* Fibronectin peptides derived from two distinct regions stimulate adipocyte differentiation by preventing fibronectin matrix assembly. *Biochemistry* **41,** 3270–3277 (2002).

159. Nakajima, I., Muroya, S., Tanabe, R. I. & Chikuni, K. Positive effect of collagen V and VI on triglyceride accumulation during differentiation in cultures of bovine intramuscular adipocytes. *Differentiation* **70,** 84–91 (2002).

160. Anton, D., Burckel, H., Josset, E. & Noel, G. Three-dimensional cell culture: A breakthrough in vivo. *International Journal of Molecular Sciences* **16,** 5517–5527 (2015).

161. Hutchinson, L. & Kirk, R. High drug attrition rates - Where are we going wrong? *Nature Reviews Clinical Oncology* **8,** 189–190 (2011).

CHAPTER 9: APPENDIX - SUPPLEMENTARY FIGURES

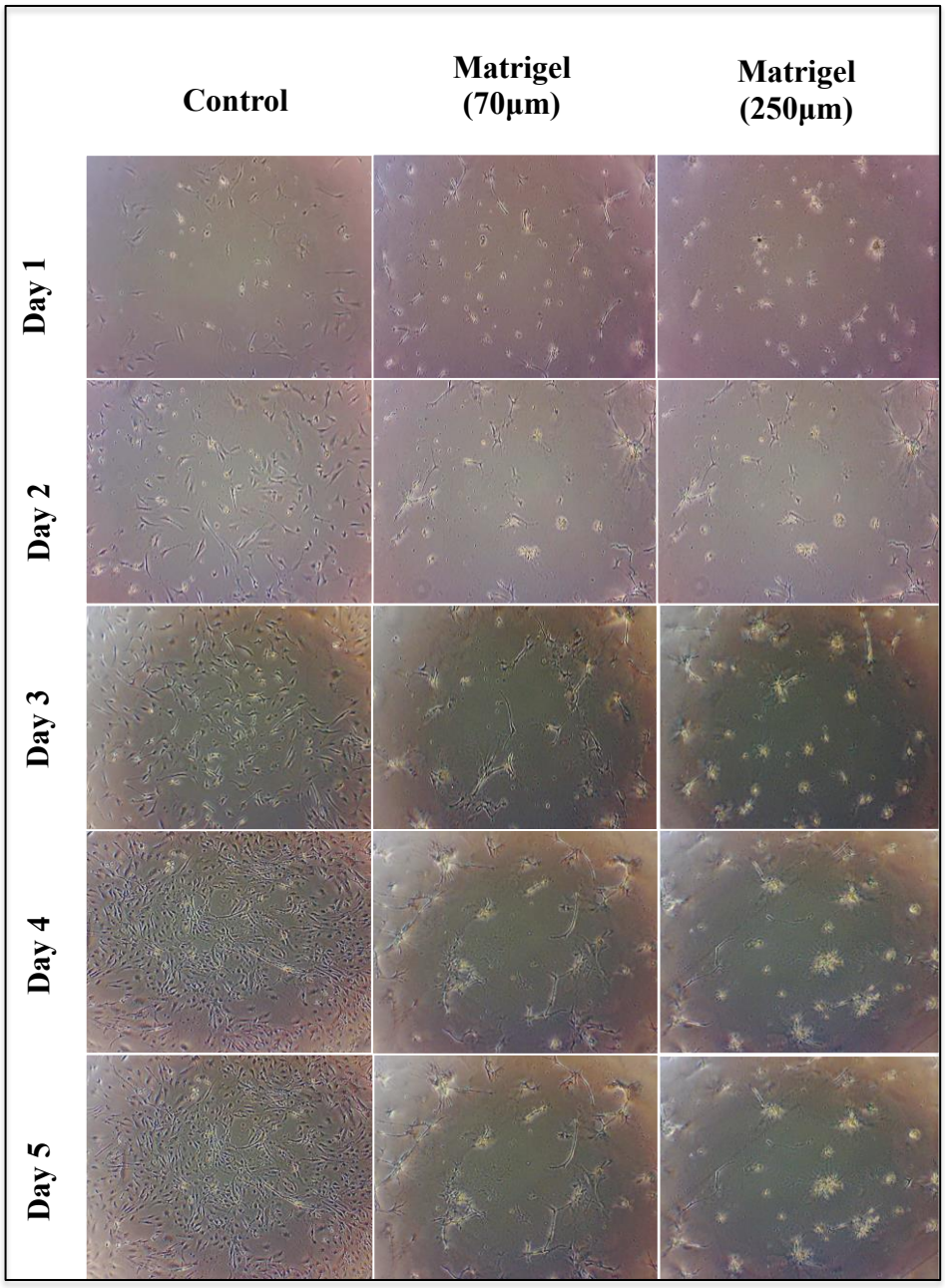

Supplementary Figure 1a. 3T3-L1 cells proliferation in a cluster-like fashion on Matrigel as compared to monolayers on tissue culture plates. Phase-contrast images of 3T3-L1 cells seeded at a density of 5000 cells/cm^2 on tissue culture plates, a thin (70 µm) and thick (250 µm) layer on Matrigel. Images were taken 24 hours post seeding; the time point referred to as day 0, and following that every 24 hours until day 5. Images were taken at 20x magnification, (n=3).

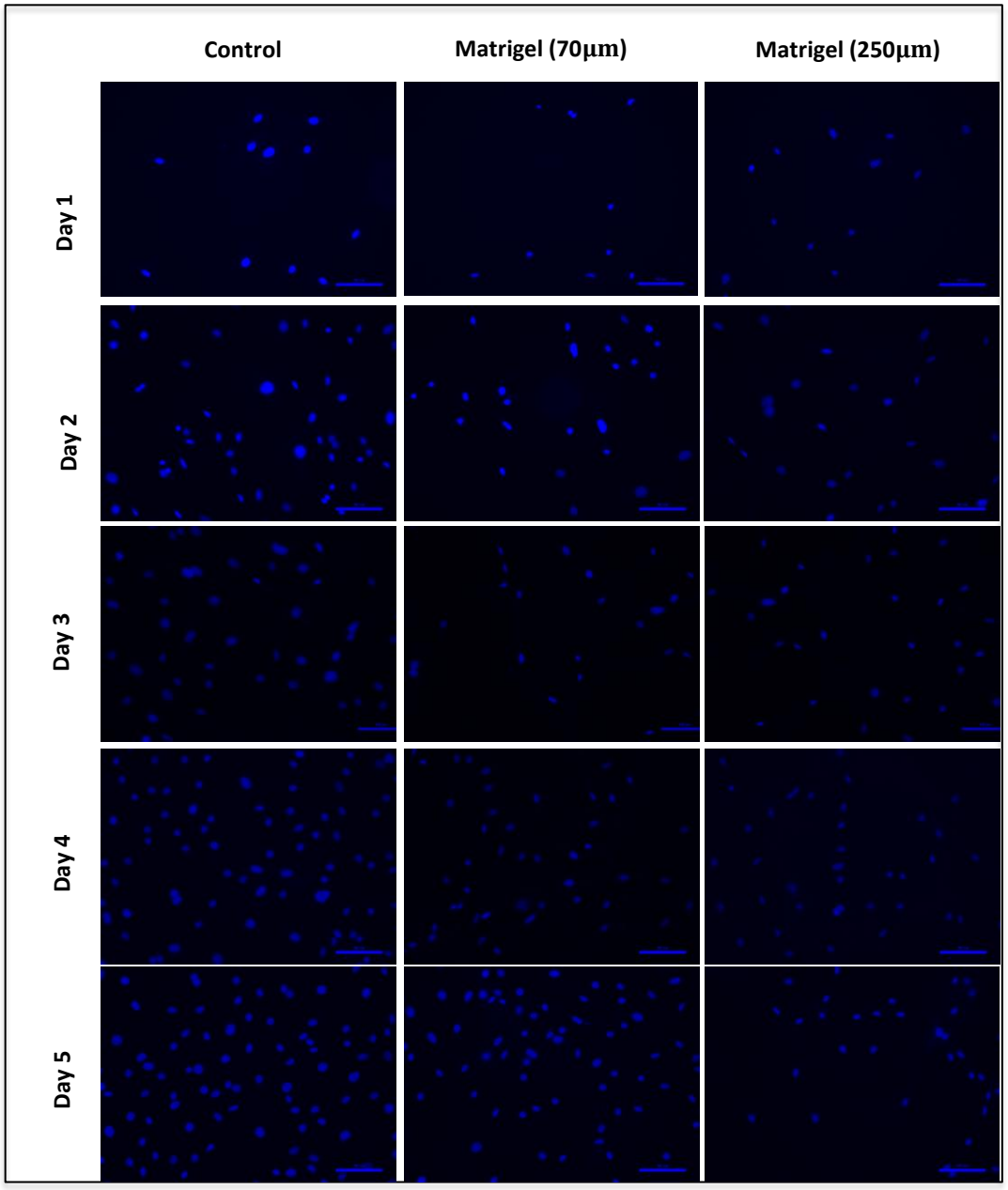

Supplementary Figure 1b. Higher DAPI staining visible in 3T3-L1 growing on tissue culture plates over 5 days as compared to cells cultured on the thin (70 μm) and thick (250 μm) layer on Matrigel. DAPI stained 3T3-L1 cells were imaged using a fluorescent microscope 24 hours post seeding; the time point referred to as day 0, and every 24 hours following that until day 5. Images were taken at 20x magnification, (n=3).

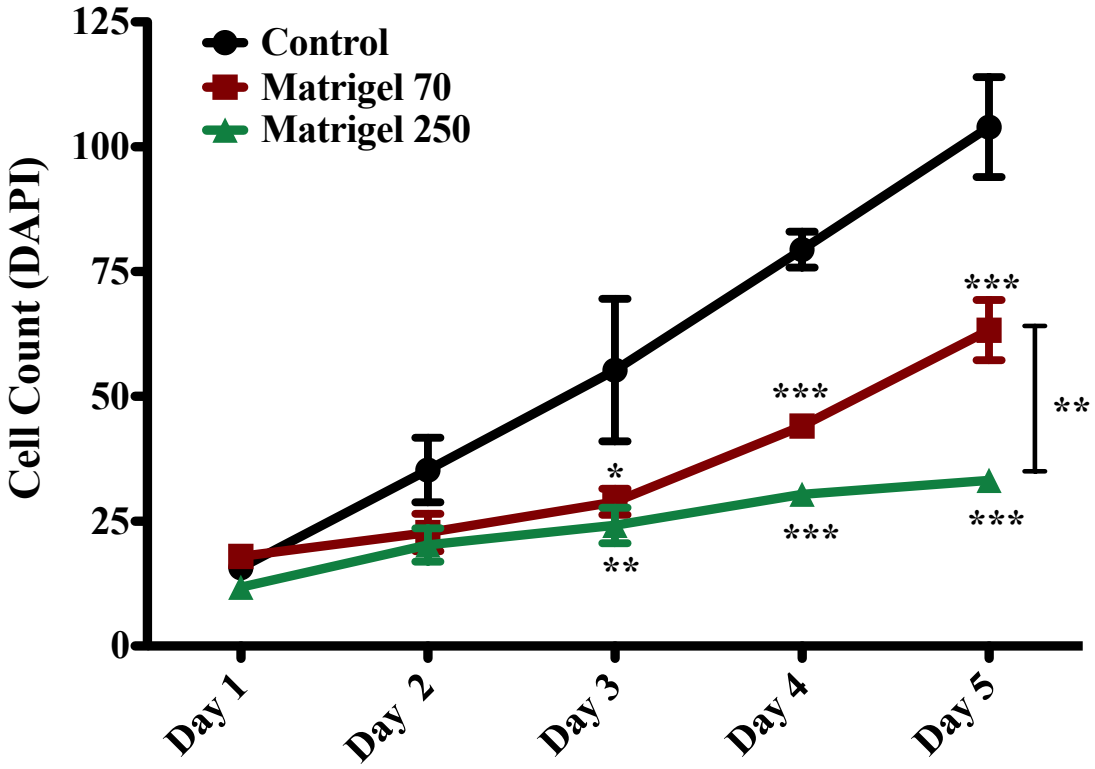

Supplementary Figure 1c. Proliferation of 3T3-L1 cells is highest in cells cultured on tissue culture plates, followed by cells on the thin (70 µm) and thick (250 µm) layer on Matrigel over 5 days. 3T3-L1 cells were stained with DAPI and imaged using a fluorescent microscope 24 hours post seeding; the time point referred to as day 0, and every 24 hours following that until day 5. Images were taken at 20x magnification, (n=3). Image J software was used to count the cells for each image and the results were plotted to make the growth curve and analyzed in GraphPad Prism Software. $P \leq .05$ was considered significant, $P \leq .01$ is represented as **, and $P \leq .001$ is represented as ***.

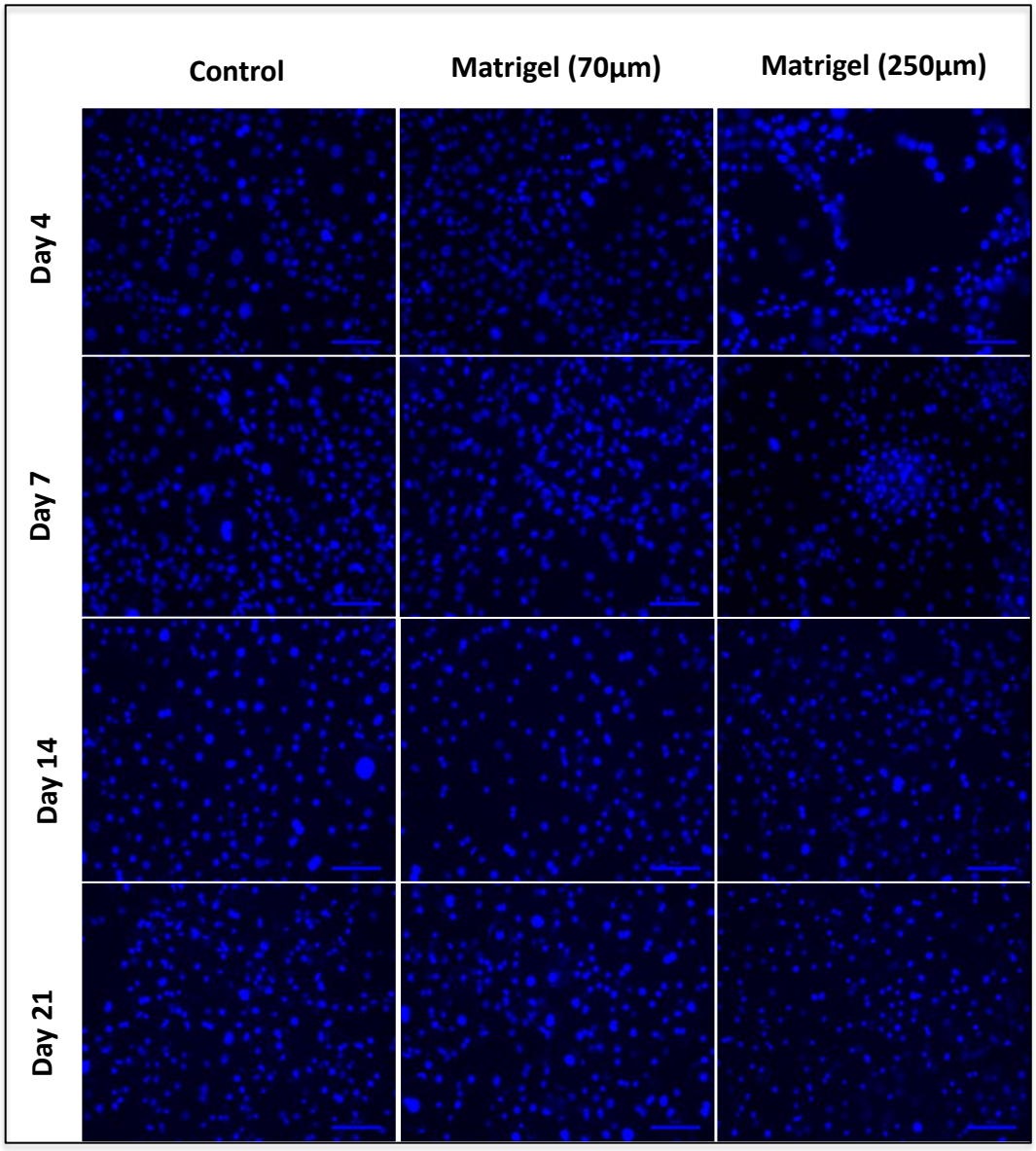

Supplementary Figure 2. Increased DAPI staining visible in 3T3-L1 cells cultured and differentiated on tissue culture plates, followed a thin (70 µm) and thick (250 µm) layer on Matrigel. DAPI stained 3T3-L1 cells were imaged using a fluorescent microscope at day 4, 7, 14 and 21 post differentiation. Images were taken at 20x magnification, (n=3).

**Note: Supplementary Figures 3 to 19 represents the same gene expression data that is represented in the Results section but reorganized to show statistical difference between all days for one condition. For example, the changes in expression of PREF-1 for 3T3-L1 cells cultured on plastic only at days 0, 4, 14 and 21 are analyzed for statistical significance. The same is done for 3T3-L1 cells on the thin layer of Matrigel and the thick layer of Matrigel. This is done to observe changes in expression over the 21 days for each condition.*

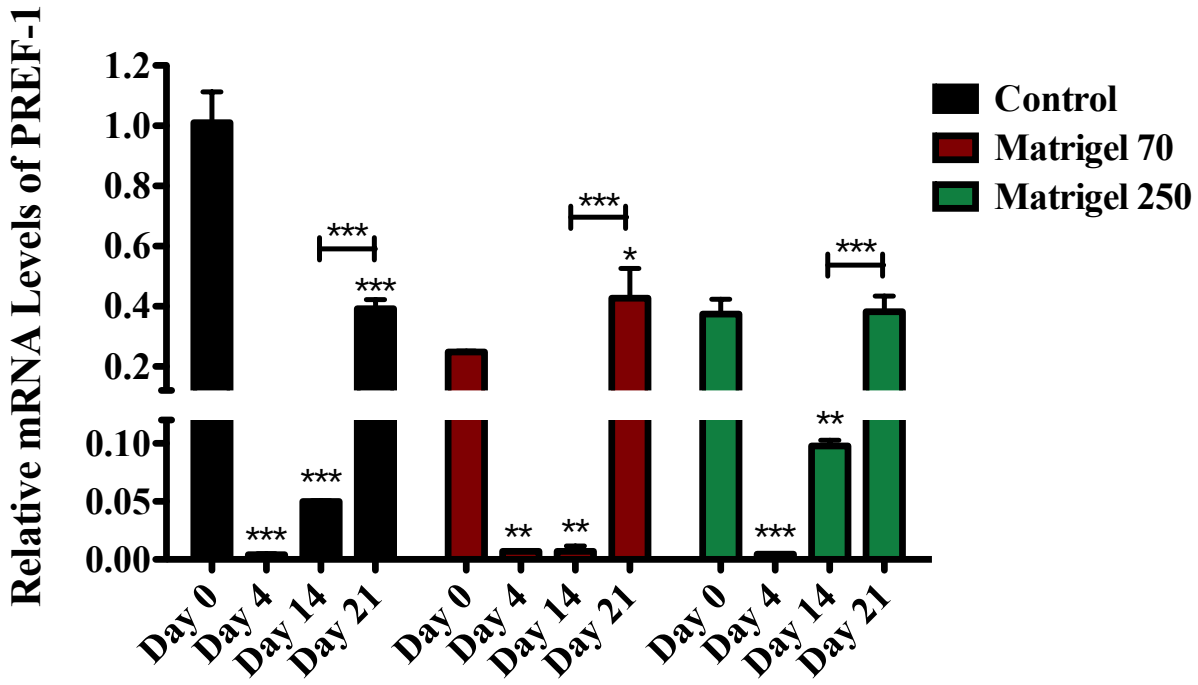

Supplementary Figure 3. PREF-1 expression of 3T3-L1 cells is downregulated post differentiation at day 4 and 14, and increases again at day 21. 3T3-L1 cells were cultured and differentiated on the thin (70 µm) and thick (250 µm) layer on Matrigel, as well as tissue culture plates (control). Cells were harvested at days 0, 4, 14, and 21 for RT- qPCR. Day 0 represents undifferentiated 3T3-L1 cells. Results are expressed as the mean relative mRNA levels of PREF-1, normalized to HPRT and L32, ± standard error of mean. GraphPad Prism Software was used for statistical analysis. Results from day 0, 4, 14 and 21 were compared for each condition, (n=3). $P \leq .05$ was considered significant, $P \leq .01$ is represented as **, and $P \leq .001$ is represented as ***.

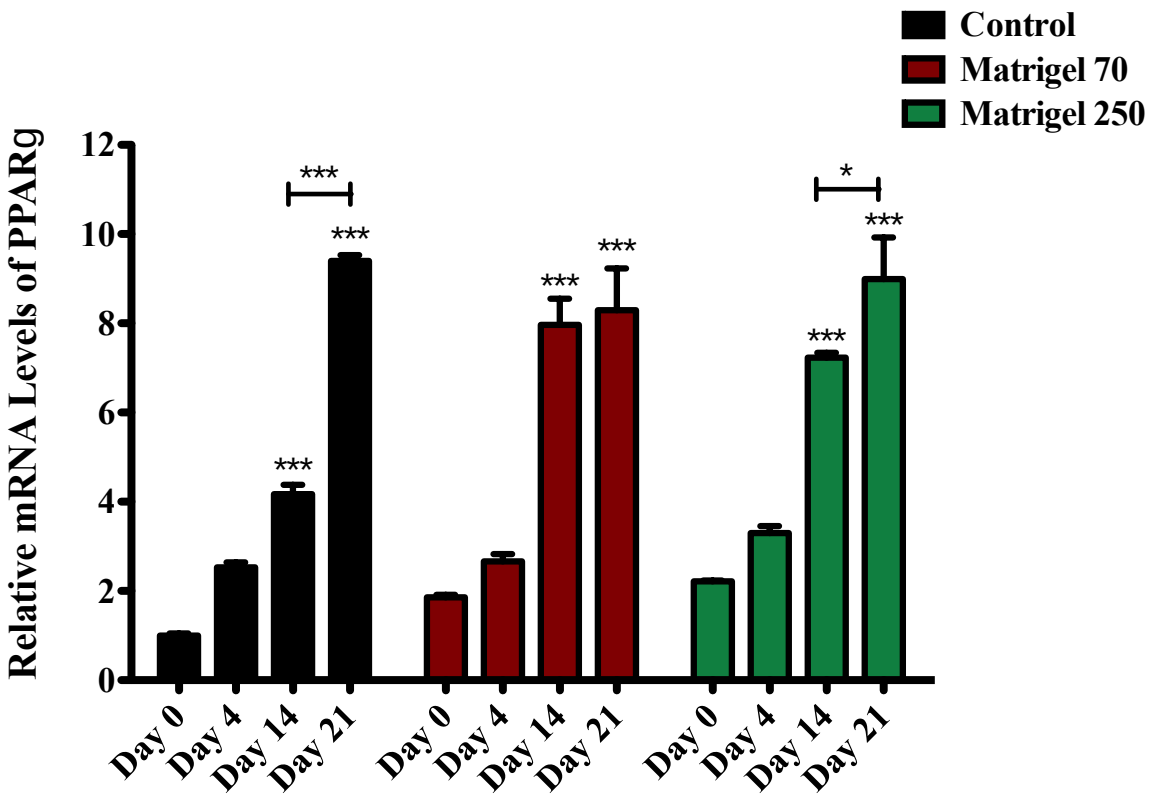

Supplementary Figure 4. PPARγ expression is increased following differentiation in 3T3-L1 cells cultured under all conditions. 3T3-L1 cells were cultured and differentiated on the thin (70 µm) and thick (250 µm) layer on Matrigel, as well as tissue culture plates (control). Cells were harvested at days 0, 4, 14, and 21 for RT-qPCR. Day 0 represents undifferentiated 3T3-L1 cells. Results are expressed as the mean relative mRNA levels of PPARγ, normalized to HPRT and L32, ± standard error of mean. GraphPad Prism Software was used for statistical analysis. Results from day 0, 4, 14 and 21 were compared for each condition, (n=3). $P \leq .05$ was considered significant, $P \leq .01$ is represented as **, and $P \leq .001$ is represented as ***.

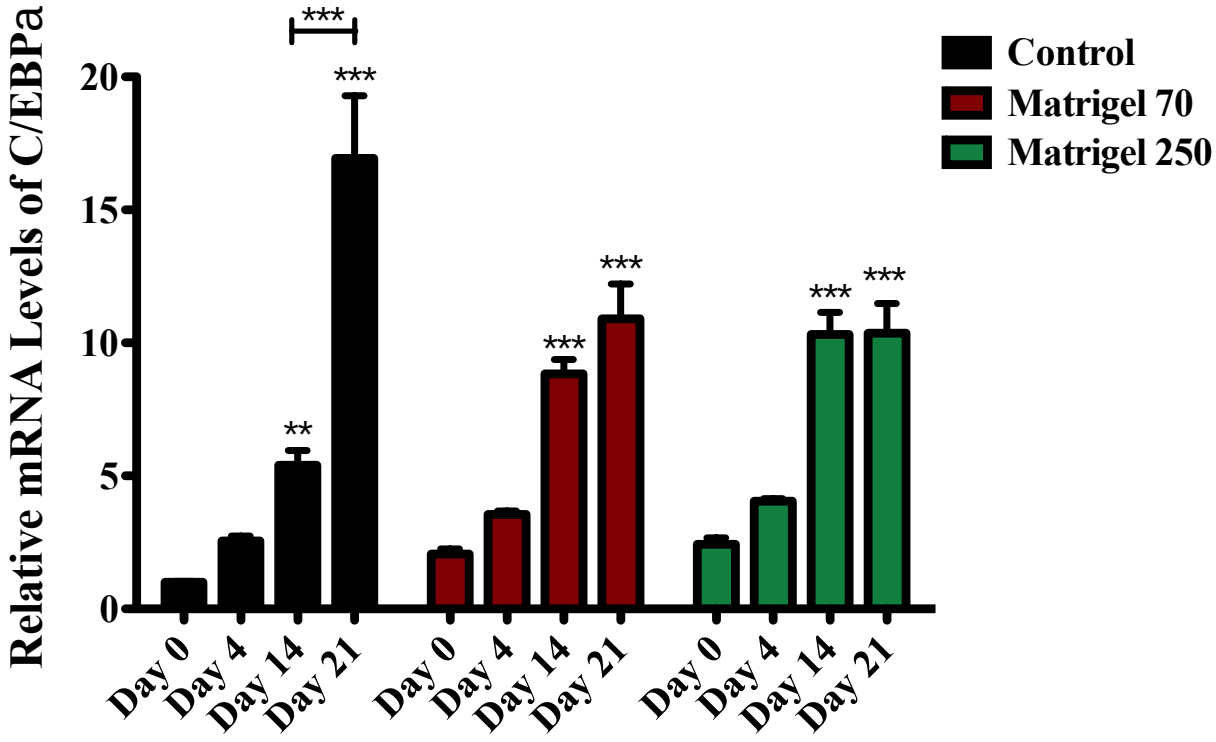

Supplementary Figure 5. Expression of C/EBPα is significantly enhanced following differentiation of 3T3-L1 cells in all culture conditions. 3T3-L1 cells were cultured and differentiated on the thin (70 µm) and thick (250 µm) layer on Matrigel, as well as tissue culture plates (control). Cells were harvested at days 0, 4, 14, and 21 for RT-qPCR. Day 0 represents 3T3-L1 cells that were not differentiated. Results are expressed as the mean relative mRNA levels of C/EBPα, normalized to HPRT and L32, ± standard error of mean. GraphPad Prism Software was used for statistical analysis. Results from day 0, 4, 14 and 21 were compared for each condition, (n=3). $P \leq .05$ was considered significant, $P \leq .01$ is represented as **, and $P \leq .001$ is represented as ***.

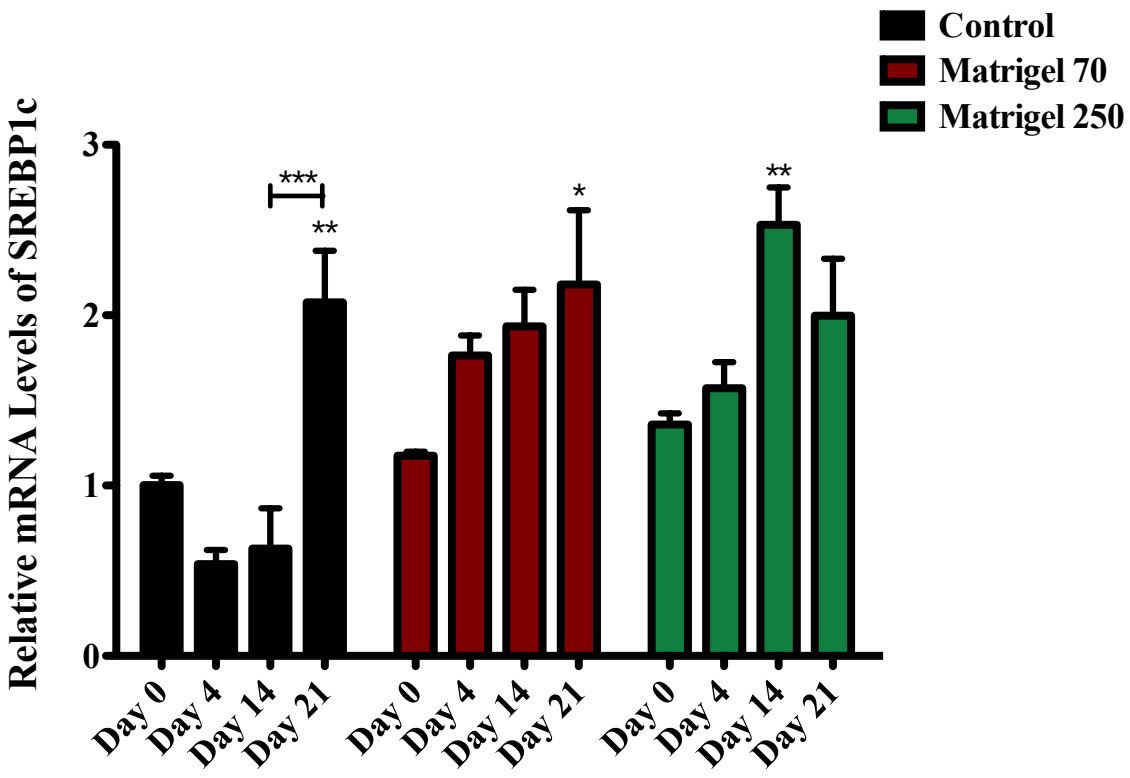

Supplementary Figure 6. SREBP1c gene expression is significantly increased over 21 days in 3T3-L1 cells differentiated under all conditions. 3T3-L1 cells were cultured and differentiated on the thin (70 µm) and thick (250 µm) layer on Matrigel, as well as tissue culture plates (control). Cells were harvested at days 0, 4, 14, and 21 for RT-qPCR. Day 0 represents undifferentiated 3T3-L1 cells. Results are expressed as the mean relative mRNA levels of SREBP1c, normalized to HPRT and L32, ± standard error of mean. GraphPad Prism Software was used for statistical analysis. Results from day 0, 4, 14 and 21 were compared for each condition, (n=3). $P \leq .05$ was considered significant, $P \leq .01$ is represented as **, and $P \leq .001$ is represented as ***.

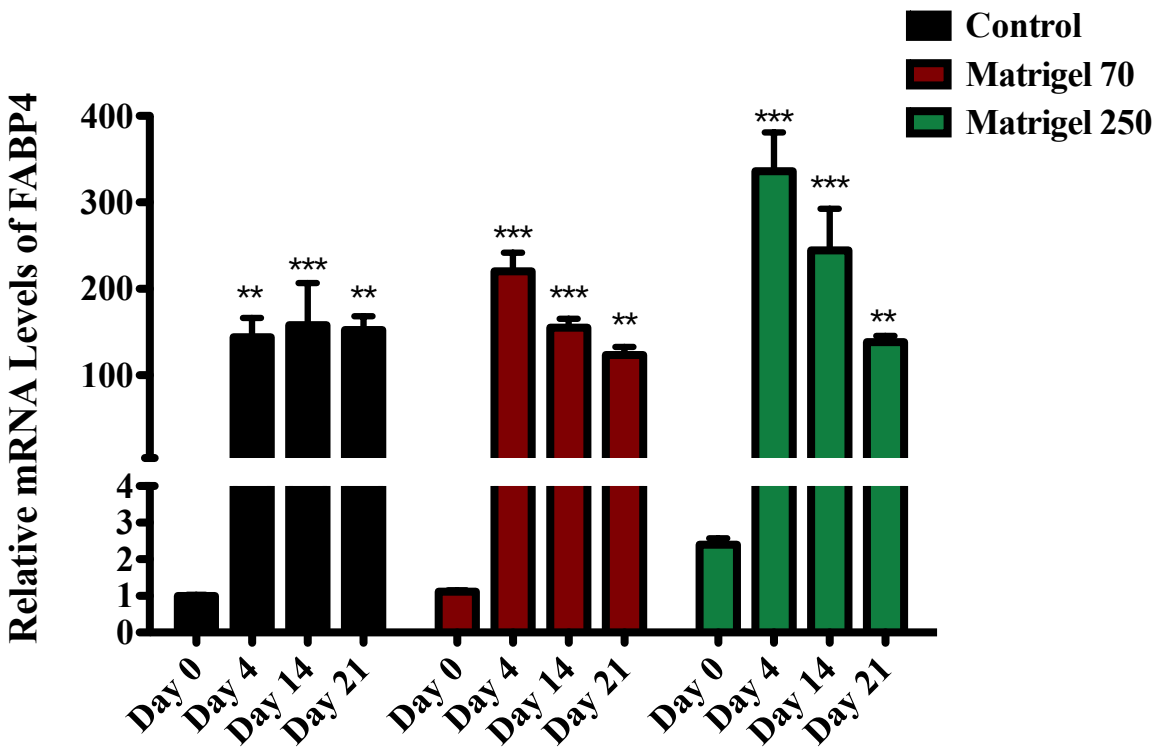

Supplementary Figure 7. FABP4 expression significantly increases after differentiation of 3T3-L1 cells in all conditions. 3T3-L1 cells were cultured and differentiated on the thin (70 µm) and thick (250 µm) layer on Matrigel, as well as tissue culture plates (control). Cells were harvested at days 0, 4, 14, and 21 for RT-qPCR. Day 0 represents undifferentiated 3T3-L1 cells. Results are expressed as the mean relative mRNA levels of FABP4, normalized to HPRT and L32, ± standard error of mean. GraphPad Prism Software was used for statistical analysis. Results from day 0, 4, 14 and 21 were compared for each condition, (n=3). $P \leq .05$ was considered significant, $P \leq .01$ is represented as **, and $P \leq .001$ is represented as ***.

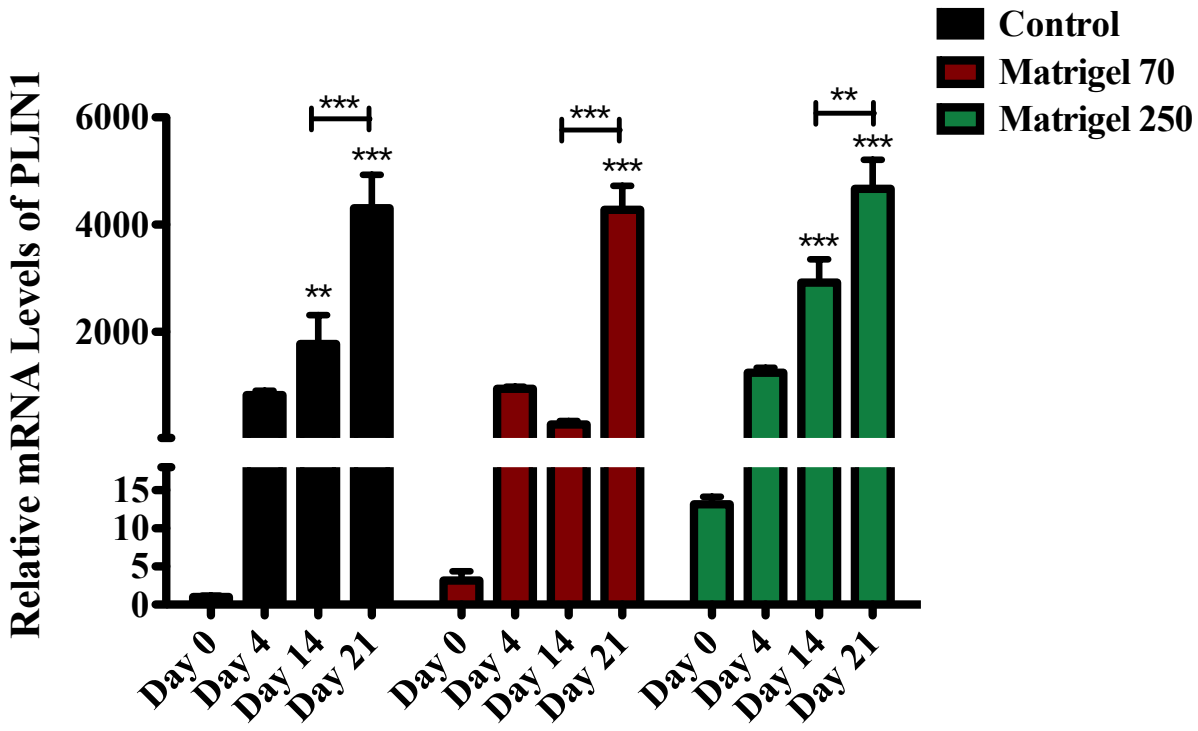

Supplementary Figure 8. Levels of PLIN1 marker are significantly enhanced following differentiation of 3T3-L1 cells in all three conditions. 3T3-L1 cells were cultured and differentiated on the thin (70 µm) and thick (250 µm) layer on Matrigel, as well as tissue culture plates (control). Cells were harvested at days 0, 4, 14, and 21 for RT-qPCR. Day 0 represents 3T3-L1 cells that were not differentiated. Results are expressed as the mean relative mRNA levels of Perilipin, normalized to HPRT and L32, ± standard error of mean. GraphPad Prism Software was used for statistical analysis. Results from day 0, 4, 14 and 21 were compared for each condition, (n=3). $P \leq .05$ was considered significant, $P \leq .01$ is represented as **, and $P \leq .001$ is represented as ***.

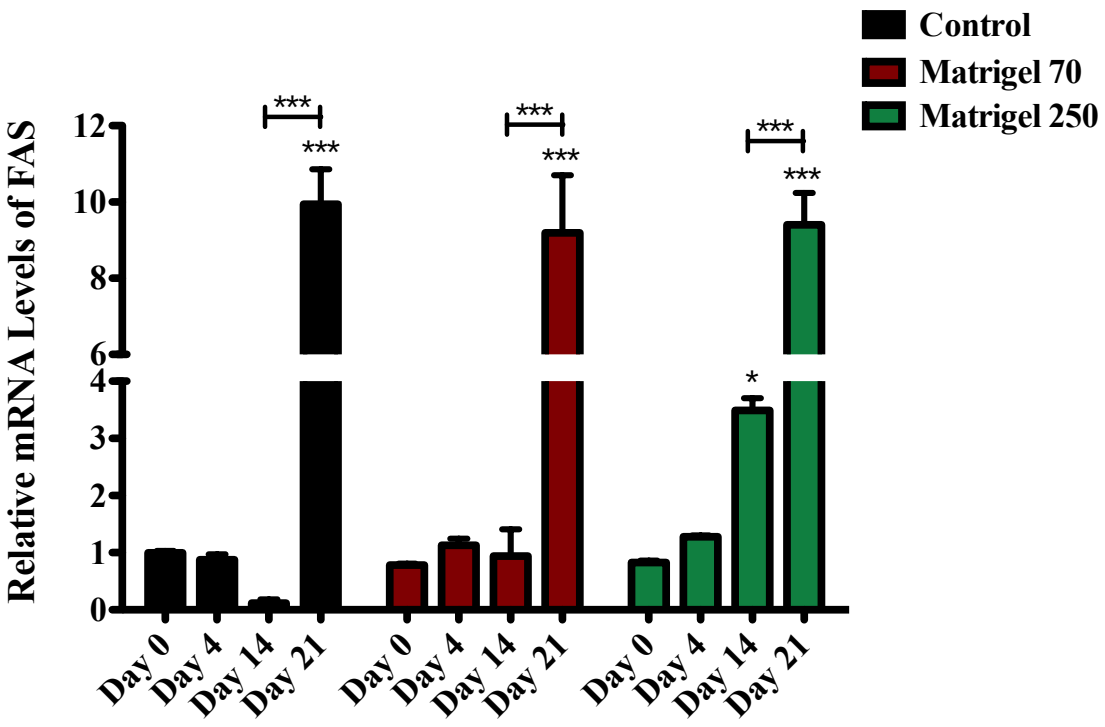

Supplementary Figure 9. Levels of FAS are up regulated following 21 days of differentiation in 3T3-L1 cells cultured under all conditions. 3T3-L1 cells were cultured and differentiated on the thin (70 µm) and thick (250 µm) layer on Matrigel, as well as tissue culture plates (control). Cells were harvested at days 0, 4, 14, and 21 for RT-qPCR. Day 0 represents undifferentiated 3T3-L1 cells. Results are expressed as the mean relative mRNA levels of FAS, normalized to HPRT and L32, ± standard error of mean. GraphPad Prism Software was used for statistical analysis. Results from day 0, 4, 14 and 21 were compared for each condition, (n=3). $P \leq .05$ was considered significant, $P \leq .01$ is represented as **, and $P \leq .001$ is represented as ***.

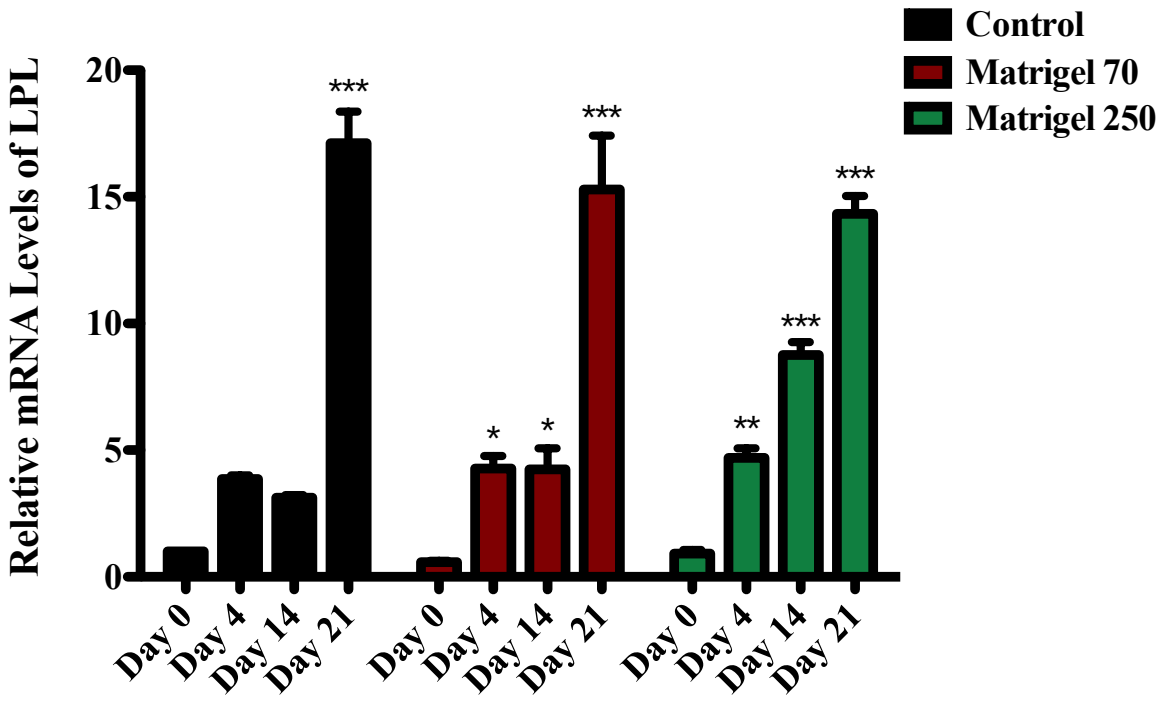

Supplementary Figure 10. LPL expression significantly increases after 21 days of differentiation in 3T3-L1 cells under all conditions. 3T3-L1 cells were cultured and differentiated on the thin (70 µm) and thick (250 µm) layer on Matrigel, as well as tissue culture plates (control). Cells were harvested at days 0, 4, 14, and 21 for RT-qPCR. Day 0 represents undifferentiated 3T3-L1 cells. Results are expressed as the mean relative mRNA levels of LPL, normalized to HPRT and L32, ± standard error of mean. GraphPad Prism Software was used for statistical analysis. Results from day 0, 4, 14 and 21 were compared for each condition, (n=3). $P \leq .05$ was considered significant, $P \leq .01$ is represented as **, and $P \leq .001$ is represented as ***.

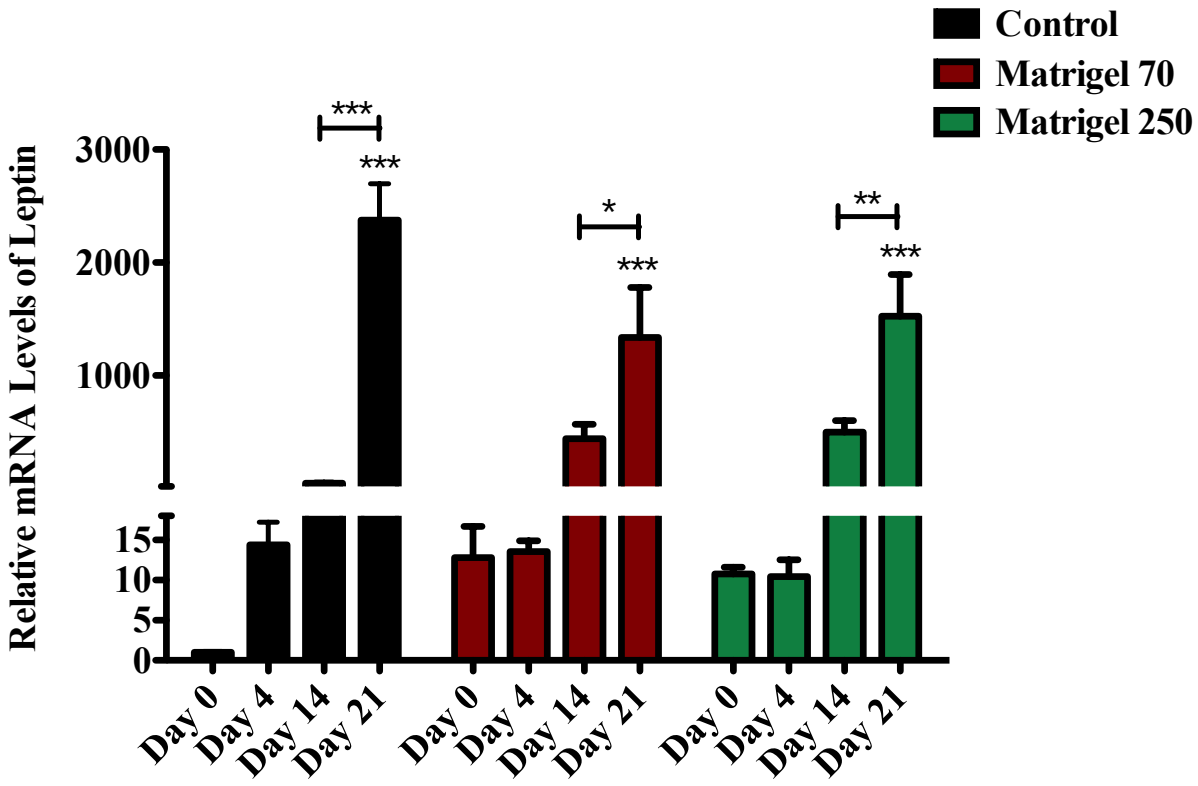

Supplementary Figure 11. Leptin expression is increased over 21 days of differentiation in 3T3-L1 cells cultured under all conditions. 3T3-L1 cells were cultured and differentiated on the thin (70 µm) and thick (250 µm) layer on Matrigel, as well as tissue culture plates (control). Cells were harvested at days 0, 4, 14, and 21 for RT-qPCR. Day 0 represents undifferentiated 3T3-L1 cells. Results are expressed as the mean relative mRNA levels of Leptin, normalized to HPRT and L32, ± standard error of mean. GraphPad Prism Software was used for statistical analysis. Results from day 0, 4, 14 and 21 were compared for each condition, (n=3). $P \leq .05$ was considered significant, $P \leq .01$ is represented as **, and $P \leq .001$ is represented as ***.

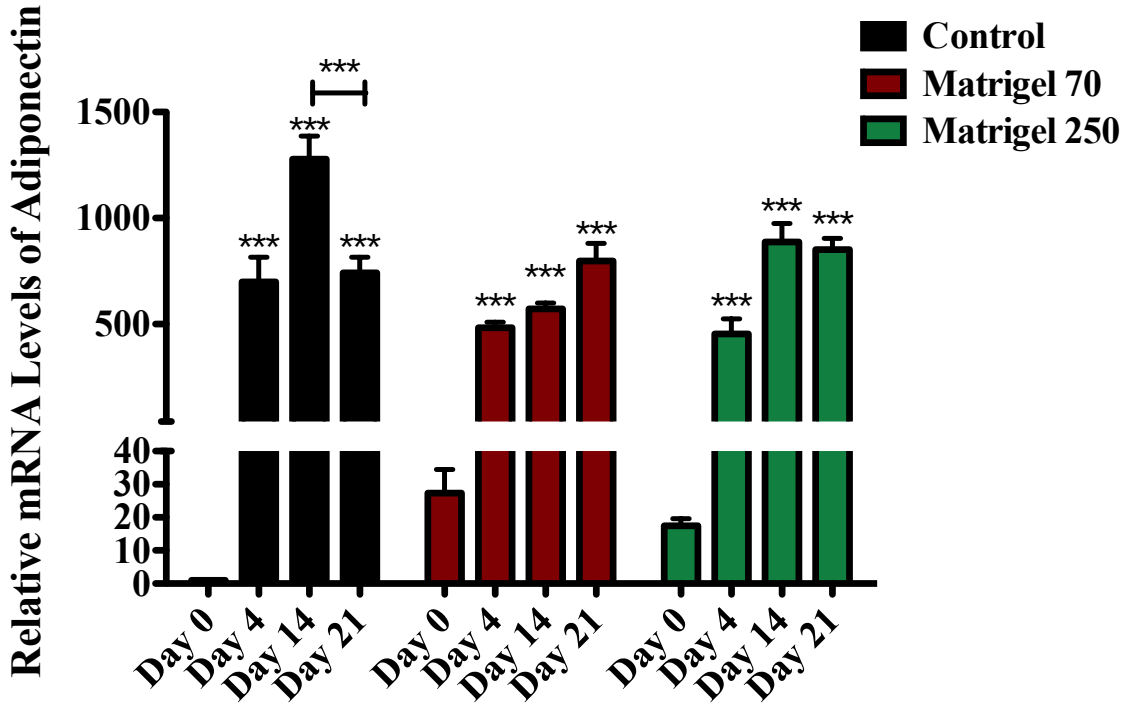

Supplementary Figure 12. Levels of Adiponectin are dramatically enhanced following differentiation of 3T3-L1 cells under all conditions. 3T3-L1 cells were cultured and differentiated on the thin (70 µm) and thick (250 µm) layer on Matrigel, as well as tissue culture plates (control). Cells were harvested at days 0, 4, 14, and 21 for RT-qPCR. Day 0 represents undifferentiated 3T3-L1 cells. Results are expressed as the mean relative mRNA levels of Adiponectin, normalized to HPRT and L32, ± standard error of mean. GraphPad Prism Software was used for statistical analysis. Results from day 0, 4, 14 and 21 were compared for each condition, (n=3). $P \leq .05$ was considered significant, $P \leq .01$ is represented as **, and $P \leq .001$ is represented as ***.

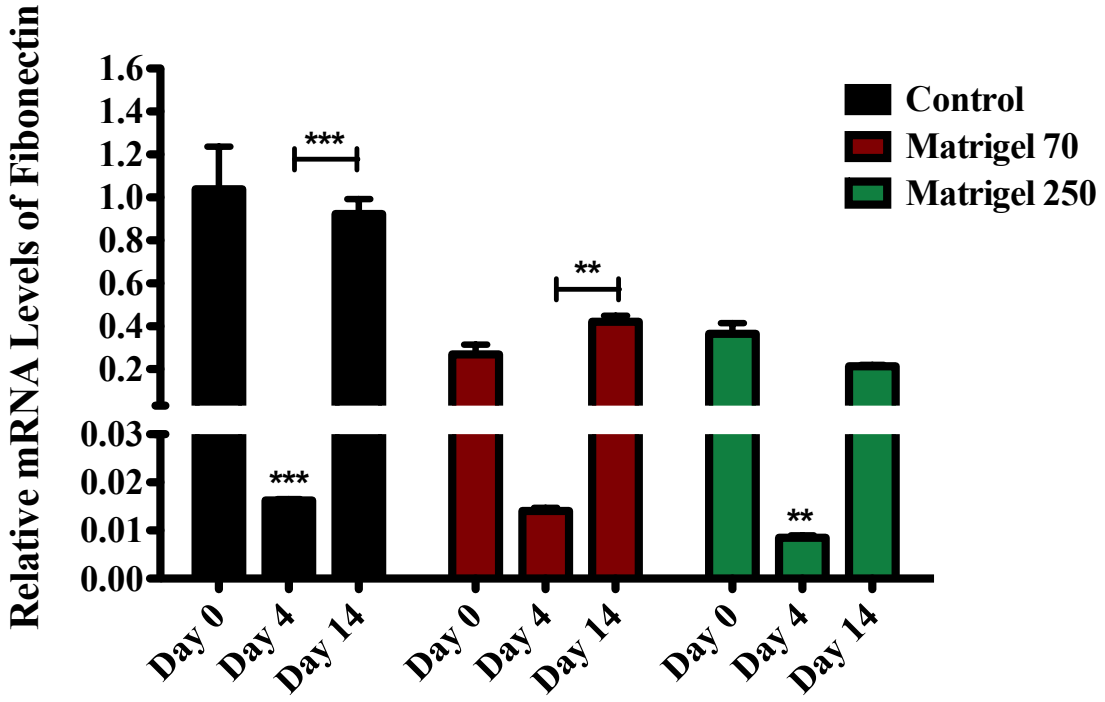

Supplementary Figure 13. Expression of Fibronectin significantly decreases immediately after differentiation in 3T3-L1 cells in all conditions. 3T3-L1 cells were cultured and differentiated on the thin (70 µm) and thick (250 µm) layer on Matrigel, as well as tissue culture plates (control). Cells were harvested at days 0, 4 and 14 for RT-qPCR. Day 0 represents undifferentiated 3T3-L1 cells. Results are expressed as the mean relative mRNA levels of Fibronectin, normalized to HPRT and L32, ± standard error of mean. GraphPad Prism Software was used for statistical analysis. Results from day 0, 4, 14 and 21 were compared for each condition, (n=3). $P \leq .05$ was considered significant, $P \leq .01$ is represented as **, and $P \leq .001$ is represented as ***.

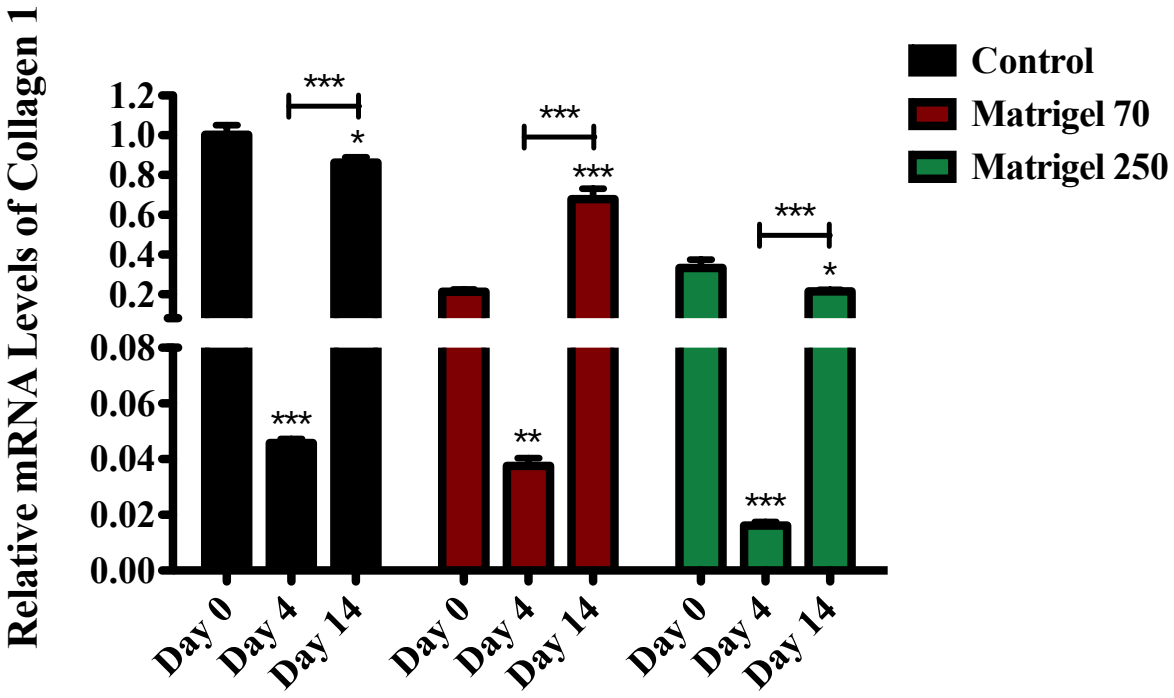

Supplementary Figure 14. Collagen 1 expression is down regulated following differentiation in 3T3-L1 cells in all conditions. 3T3-L1 cells were cultured and differentiated on the thin (70 µm) and thick (250 µm) layer on Matrigel, as well as tissue culture plates (control). Cells were harvested at days 0, 4 and 14 for RT-qPCR. Day 0 represents undifferentiated 3T3-L1 cells. Results are expressed as the mean relative mRNA levels of Collagen 1, normalized to HPRT and L32, ± standard error of mean. GraphPad Prism Software was used for statistical analysis. Results from day 0, 4, 14 and 21 were compared for each condition, (n=3). $P \leq .05$ was considered significant, $P \leq .01$ is represented as **, and $P \leq .001$ is represented as ***.

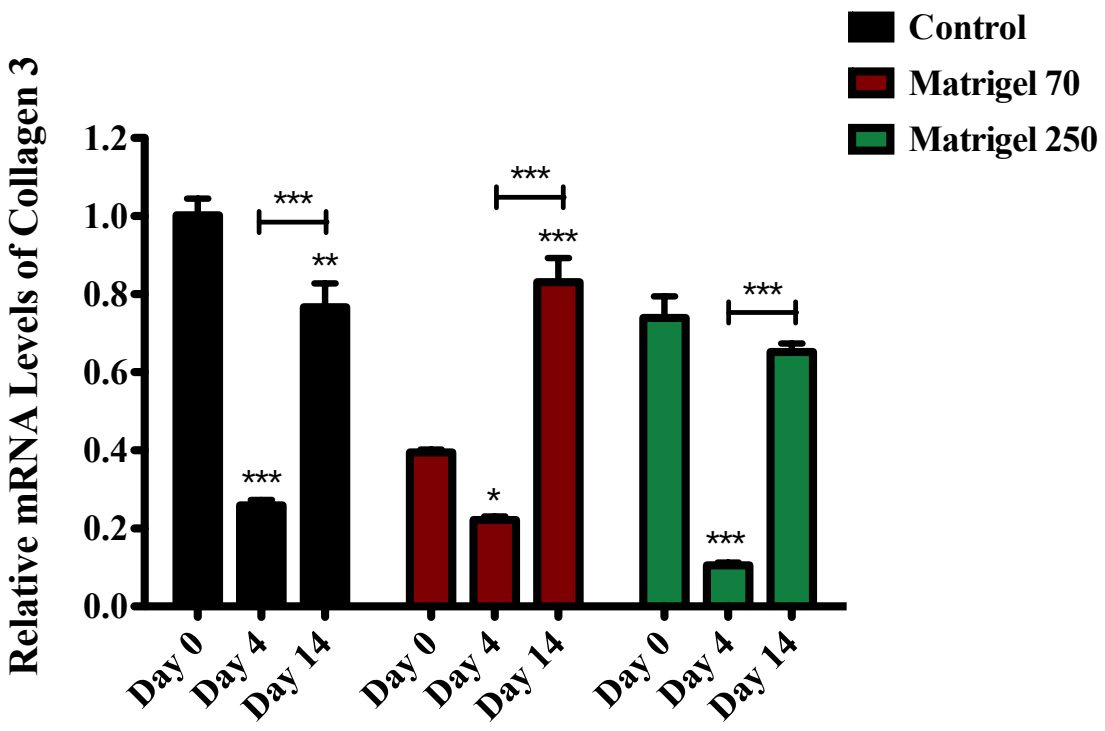

Supplementary Figure 15. Expression of Collagen 3 decreases following differentiation in 3T3-L1 cells under all conditions. 3T3-L1 cells were cultured and differentiated on the thin (70 µm) and thick (250 µm) layer on Matrigel, as well as tissue culture plates (control). Cells were harvested at days 0, 4 and 14 for RT-qPCR. Day 0 represents undifferentiated 3T3-L1 cells. Results are expressed as the mean relative mRNA levels of Collagen 3, normalized to HPRT and L32, ± standard error of mean. GraphPad Prism Software was used for statistical analysis. Results from day 0, 4, 14 and 21 were compared for each condition, (n=3). $P \leq .05$ was considered significant, $P \leq .01$ is represented as **, and $P \leq .001$ is represented as ***.

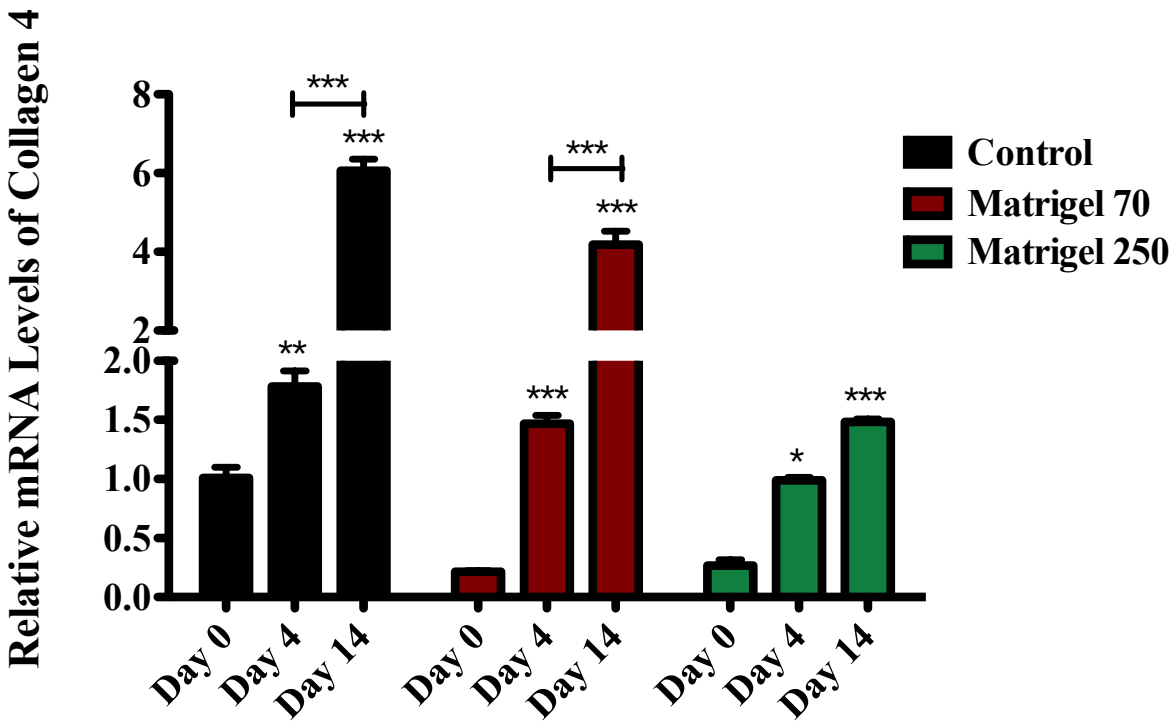

Supplementary Figure 16. Collagen 4 levels significantly increase following differentiation in 3T3-L1 cells cultured in all conditions. 3T3-L1 cells were cultured and differentiated on the thin (70 µm) and thick (250 µm) layer on Matrigel, as well as tissue culture plates (control). Cells were harvested at days 0, 4 and 14 for RT-qPCR. Day 0 represents undifferentiated 3T3-L1 cells. Results are expressed as the mean relative mRNA levels of Collagen 4, normalized to HPRT and L32, ± standard error of mean. GraphPad Prism Software was used for statistical analysis. Results from day 0, 4, 14 and 21 were compared for each condition, (n=3). $P \leq .05$ was considered significant, $P \leq .01$ is represented as **, and $P \leq .001$ is represented as ***.

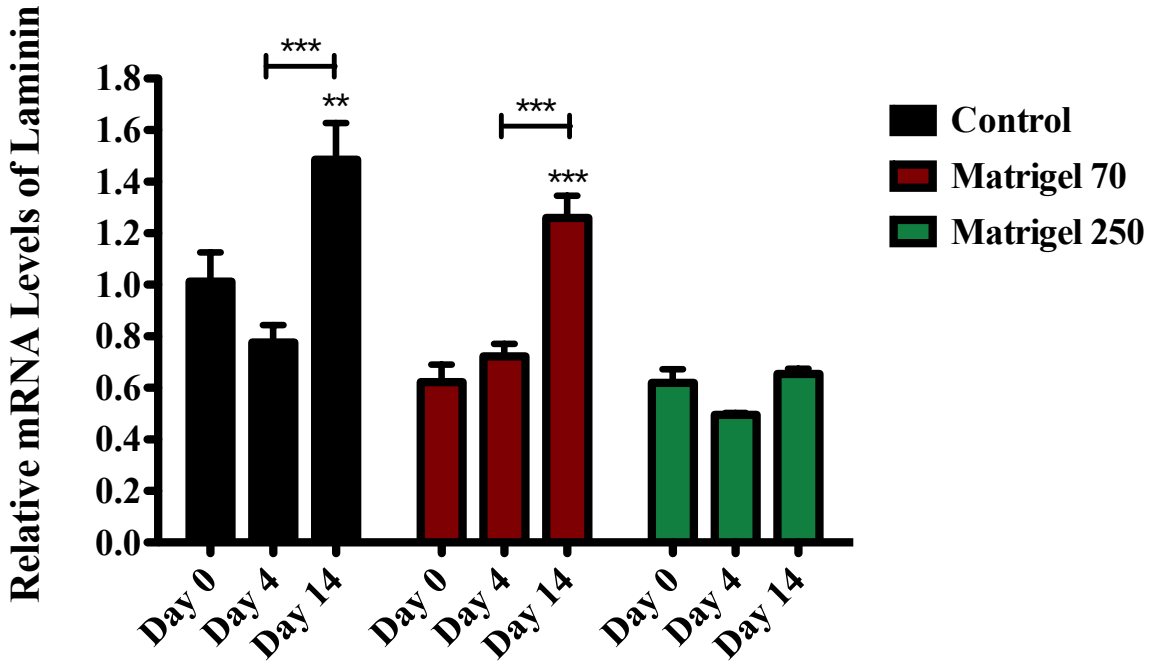

Supplementary Figure 17. The mRNA levels of Laminin increase following differentiation in 3T3-L1 cells cultured on plastic and the thick Matrigel. 3T3-L1 cells were cultured and differentiated on the thin (70 µm) and thick (250 µm) layer on Matrigel, as well as tissue culture plates (control). Cells were harvested at days 0, 4 and 14 for RT-qPCR. Day 0 represents undifferentiated 3T3-L1 cells. Results are expressed as the mean relative mRNA levels of Laminin, normalized to HPRT and L32, ± standard error of mean. GraphPad Prism Software was used for statistical analysis. Results from day 0, 4, 14 and 21 were compared for each condition, (n=3). $P \leq .05$ was considered significant, $P \leq .01$ is represented as **, and $P \leq .001$ is represented as ***.

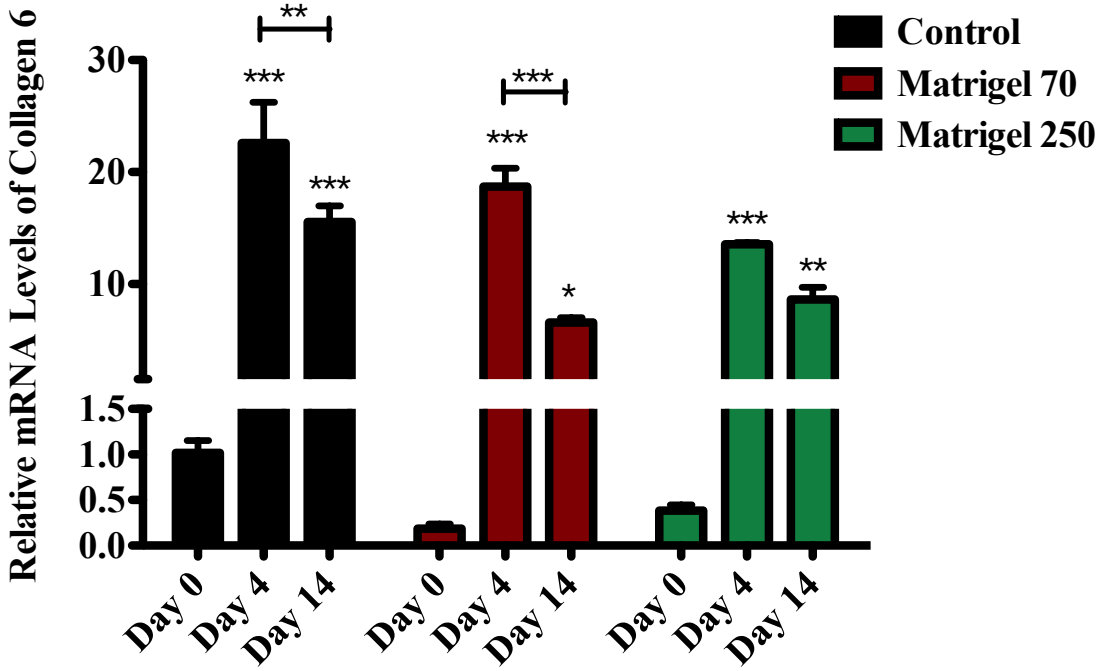

Supplementary Figure 18. Collagen 6 expression is up regulated following differentiation in 3T3-L1 cells under all conditions. 3T3-L1 cells were cultured and differentiated on the thin (70 µm) and thick (250 µm) layer on Matrigel, as well as tissue culture plates (control). Cells were harvested at days 0, 4 and 14 for RT-qPCR. Day 0 represents undifferentiated 3T3-L1 cells. Results are expressed as the mean relative mRNA levels of Collagen 6, normalized to HPRT and L32, ± standard error of mean. GraphPad Prism Software was used for statistical analysis. Results from day 0, 4, 14 and 21 were compared for each condition, (n=3). $P \leq .05$ was considered significant, $P \leq .01$ is represented as **, and $P \leq .001$ is represented as ***.

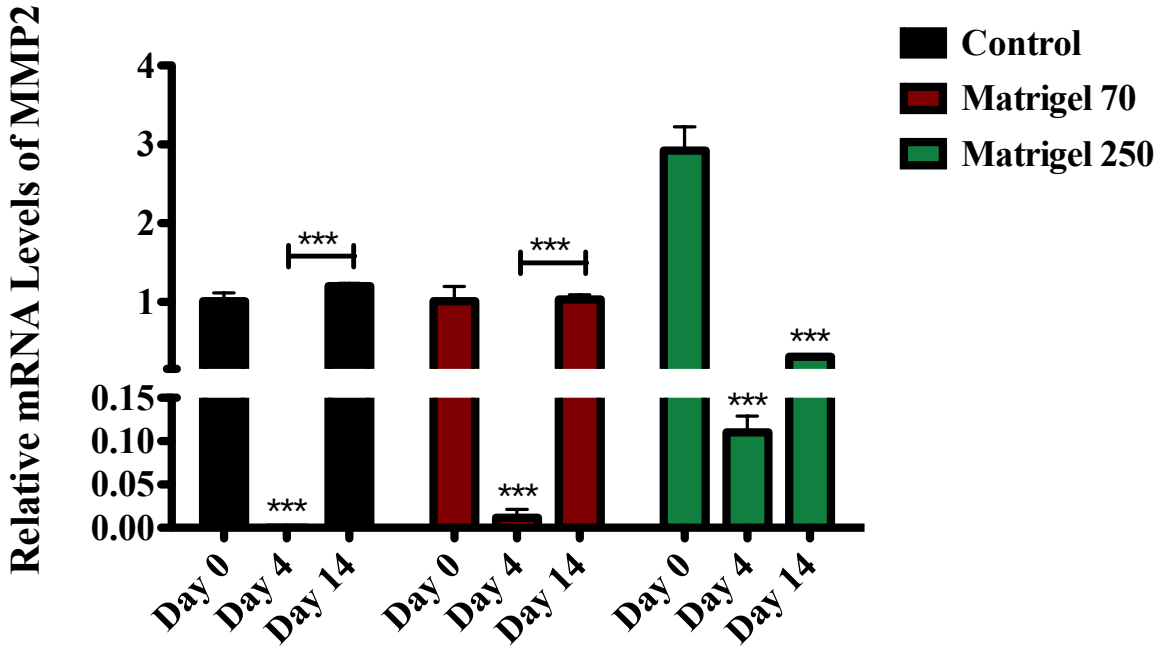

Supplementary Figure 19. MMP2 expression significantly decreases after differentiation in 3T3-L1 cells under all conditions. 3T3-L1 cells were cultured and differentiated on the thin (70 µm) and thick (250 µm) layer on Matrigel, as well as tissue culture plates (control). Cells were harvested at days 0, 4 and 14 for RT-qPCR. Day 0 represents undifferentiated 3T3-L1 cells. Results are expressed as the mean relative mRNA levels of MMP2, normalized to HPRT and L32, ± standard error of mean. GraphPad Prism Software was used for statistical analysis. Results from day 0, 4, 14 and 21 were compared for each condition, (n=3). $P \leq .05$ was considered significant, $P \leq .01$ is represented as **, and $P \leq .001$ is represented as ***.

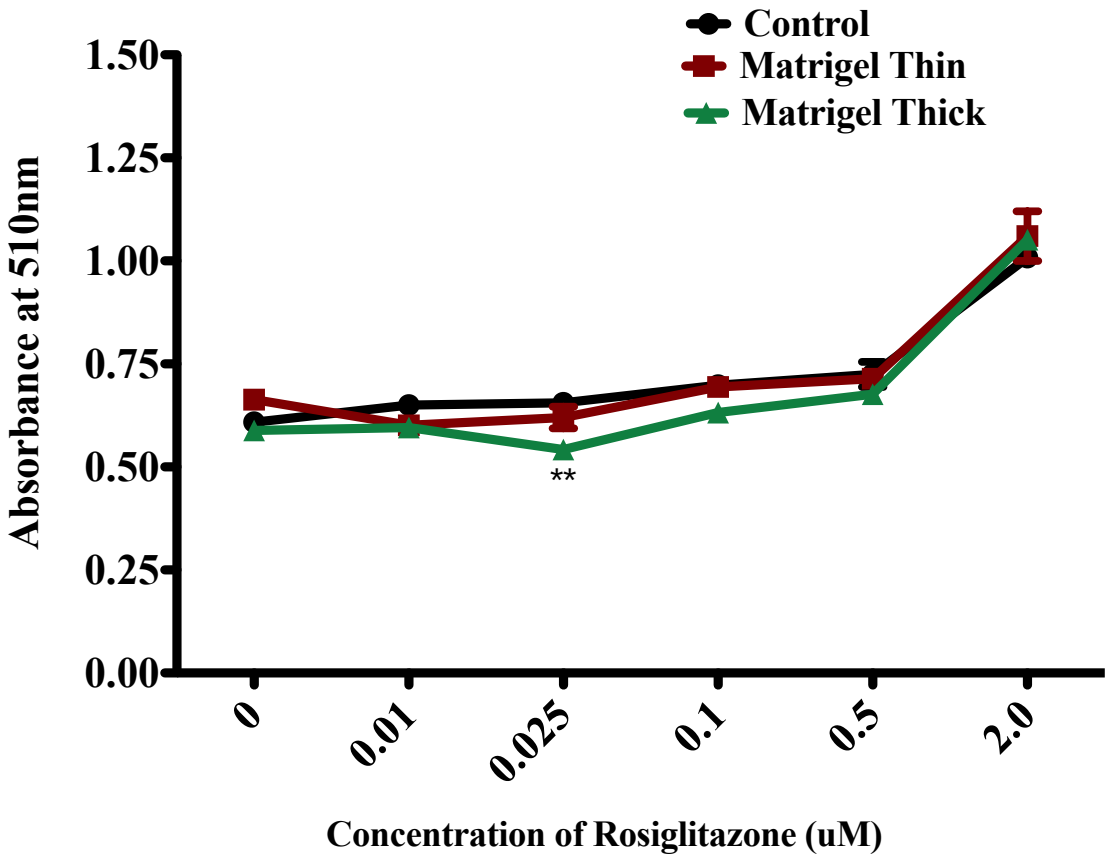

Supplementary Figure 20. Lipid accumulation in 3T3-L1 cells differentiated on Matrigel and tissue culture plastic at day 7, visualized by Oil Red O staining. 3T3-L1 cells cultured and differentiated on tissue culture plates, a thin (70 µm) and thick (250 µm) layer on Matrigel and treated with 0, 0.01, 0.025, 0.1, 0.5 or 2.0 µM of Rosiglitazone at differentiation, in addition to DEX, IBMX and Insulin. At day 7, Oil Red O was extracted for lipid quantification using a spectrophotometer at an absorbance of 510 nm. Data points were plotted in GraphPad Prism Software. To determine statistical significance, results from Control, Matrigel (70µm) and Matrigel (250µm) were compared at each concentration, (n=3). $P \leq .05$ was considered significant, $P \leq .01$ is represented as **, and $P \leq .001$ is represented as ***.